

Supporting Information

Highly branched bolapolyphilic liquid crystals with a cubic A15 network at the triangle-square transition

Christian Anders,^a Matthias Wagner,^a Mohamed Alaasar,^a Virginia-Marie Fischer,^b Rebecca Waldecker,^b Yangyang Zhao,^c Tianyi Tan,^c Yu Cao,^{*c} Feng Liu,^c and Carsten Tschierske ^{*a}

^a Institut of Chemistry, Martin-Luther University Halle-Wittenberg, Kurt-Mothes Str. 2, D-06120 Halle/Saale, German. E-mail: Carsten.tschierske@chemie.uni-halle.de

^b Institute of Mathematics, Martin Luther University Halle-Wittenberg, Theodor-Lieser-Str. 5, 06120 Halle, Germany

^b Shaanxi International Research Center for Soft Matter, State Key Laboratory for Mechanical Behavior of Materials, Xi'an Jiaotong University, Xi'an 710049, P. R. China. E-mail: yu.cao@xjtu.edu.cn

1. Experimental Section

Polarizing Optical Microscopy (POM)

Optical textures of all compounds were characterized by polarizing optical microscopy (Olympus BX51-P) with the combination of a heating stage (Linkam LTS420E) and controller (T95-HS). Optical investigations were carried out under equilibrium conditions between two glass slides that were used without further treatment. A full wavelength retardation plate was used to determine the sign of birefringence.

DSC measurements

Transition enthalpies were determined as obtained from differential scanning calorimetry (DSC) which were recorded on a TA DSC250 and DSC-8000 (Perkin Elmer) in sealed 30 μ L aluminum pans with heating and cooling rates of 10 K/min under an N₂ stream; peak temperatures are given in Tables 1a,b.

X-ray scattering

X-ray investigations were carried out with an Incoatec (Geesthacht, Germany) μ S microfocus source with a monochromator for CuK α radiation ($\lambda = 0.154$ nm), calibration with the powder pattern of Pb(NO₃)₂. A droplet of the sample was placed on a glass plate on a Linkam hot stage HFS-X350-GI (rate: 1 Kmin⁻¹ – 0.01 Kmin⁻¹). Exposure time was 5 min; the sample-detector distance was 9.00 cm for WAXS and 26.80 cm for SAXS. The diffraction patterns were recorded with a Vantec 500 area detector (Bruker AXS, Karlsruhe) and transformed to 1D plots using GADDS software.

Synchrotron-based X-ray scattering

High-resolution small-angle and wide-angle powder diffraction experiments were recorded on Beamline BL16B1 at Shanghai Synchrotron Radiation Facility (SSRF). Samples were held in evacuated 1 mm capillaries. A modified Linkam hot stage with thermal stability within 0.2 °C was used, with a hole for the capillary drilled through the silver heating block and mica windows attached to it on each side. A Pilatus 2M detector was used. q Calibration and linearization were verified using several orders of layer reflections from silver behenate and a series of n-alkanes. Experimental diffractograms are fitted using Gaussian-shaped peaks to determine the positions and intensities of the diffraction peaks. The diffraction peaks are indexed based on their peak positions, and the lattice parameters and the space groups are subsequently determined. Once the diffraction intensities are measured, and the corresponding plane group determined, 2D electron density maps can be reconstructed based on the general formula.

$$E(xy) = \sum_{hk} F(hk) e^{[i2\pi(hx+ky)]} \quad (1)$$

Here $F(hk)$ is the structure factor of a diffraction peak with index (hk) . It is normally a complex number, and the experimentally observed diffraction intensity is

$$I(xy) = K \cdot F(hk) = F^* (hk) = K \cdot |F(hk)|^2 \quad (2)$$

Here K is a constant related to the sample volume, incident beam intensity etc. If the constant is equal to 1, then the electron density is

$$E(xy) = \sum_{hk} \sqrt{I(hk)} e^{[i2\pi(hx+ky)+\Phi_{hk}]} \quad (3)$$

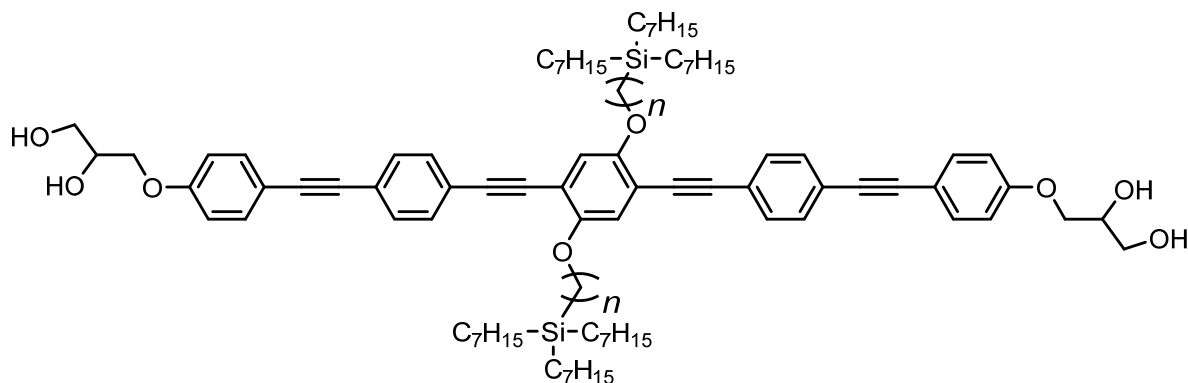
As the observed diffraction intensity $I(hk)$ is only related to the amplitude of the structure factor $|F(hk)|$, the information about the phase of $F(hk)$, Φ_{hk} , cannot be determined directly from experiment. However, the problem is much simplified when the structure of the ordered phase is centrosymmetric; hence, the structure factor $F(hk)$ is always real, and Φ_{hk} is either 0 or π . Case is essentially same for 3D centrosymmetric cubic phase.

This makes it possible for a trial-and-error approach, where candidate electron density maps are reconstructed for all possible phase combinations. The “correct” phase combination is then selected on the merit of the maps, helped by prior physical and chemical knowledge of the system. This is especially useful for the study of nanostructures, where typically only a limited number of diffraction peaks are observed.

2. Additional Data

2.1. Phase transitions, DSC traces and POM textures

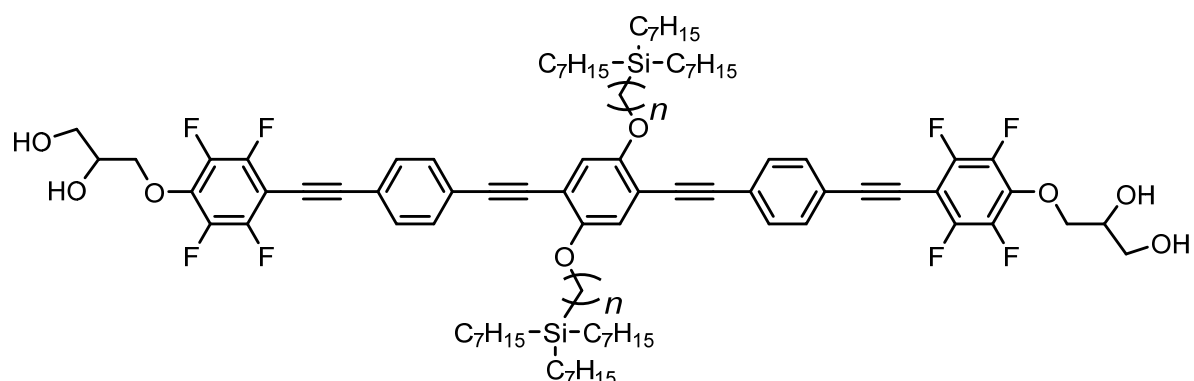
Table S1a. Phase transitions of the non-fluorinated compounds **Hn**.



Hn	Phase Transitions ($T/^\circ\text{C}$ [$\Delta H/\text{kJmol}^{-1}$] ^a)
H3	H: Cr 70 [13.6] Col _{hex} / <i>p6mm</i> 147 [3.5] Cub/ <i>Pm</i> $\bar{3}n$ 160 [1.5] Iso C: Iso 156 [-1.3] Cub/ <i>Pm</i> $\bar{3}n$ 143 [-3.8] Col _{hex} / <i>p6mm</i> 38 [-6.5] Cr
H4	H: Cr 91 [41.5] Cub/ <i>Pm</i> $\bar{3}n$ 159 [1.3] Iso C: Iso 155 [-1.4] Cub/ <i>Pm</i> $\bar{3}n$ 69 [-37.8] Cr
H5	H: Cr 50 [3.3] M 96 [2.2] Cub/ <i>Pm</i> $\bar{3}n$ 155 [1.3] Iso C: Iso 148 [-0.9] Cub/ <i>Pm</i> $\bar{3}n$ 86 [-2.9] M < 20 Cr
H6	H: Cr 54 [16.3] M 85 [1.1] Cub/ <i>Pm</i> $\bar{3}n$ 146 [0.5] Iso C: Iso 139 [-0.4] Cub/ <i>Pm</i> $\bar{3}n$ 59 [-0.7] M < 20 Cr
H7	H: Cr 77 [8.0] M 105 [2.9] Cub/ <i>Pm</i> $\bar{3}n$ 145 [0.8] Iso C: Iso 137 [-0.4] Cub/ <i>Pm</i> $\bar{3}n$ 89 [-2.6] M < 20 Cr
H8	H: 45 [1.5] Col _{squ} / <i>p4mm</i> 105 [3.0] Cub/ <i>Pm</i> $\bar{3}n$ 128 [0.4] Iso C: Iso 125 [-] Cub/ <i>Pm</i> $\bar{3}n$ 91 [-2.8] Col _{squ} / <i>p4mm</i> < 20 Cr
H9	H: Cr 80 [11.1] Col _{squ} / <i>p4mm</i> 127 [4.0] Iso C: Iso 119 [-3.8] Col _{squ} / <i>p4mm</i> < 20
H10	H: Cr 83 [15.3] Col _{squ} / <i>p4mm</i> 134 [5.4] Iso C: Iso 129 [-5.5] Col _{squ} / <i>p4mm</i> < 20 Cr
H11	H: Cr 78 [11.8] Col _{squ} / <i>p4mm</i> 142 [5.4] Iso C: Iso 136 [-5.2] Col _{squ} / <i>p4mm</i> < 20 Cr
H12	H: Cr 84 [16.5] Col _{squ} / <i>p4mm</i> 141 [5.9] Iso C: Iso 134 [-5.7] Col _{squ} / <i>p4mm</i> < 20 Cr

^a Data from first heating/cooling scan. Abbreviations: Cr = crystalline solid state; Iso = isotropic liquid; Col_{hex}/*p6mm* = hexagonal columnar phase representing a 2D triangular tiling; Col_{squ}/*p4mm* = square columnar phase representing a square tiling; Cub/*Pm* $\bar{3}n$ = cubic phase with space group *Pm* $\bar{3}n$ (A15 phase); M = unknown birefringent mesophases.

Table S1b. Phase transitions of the fluorinated compounds **Fn**.



Fn	Phase Transitions ($T/^\circ\text{C}$ [$\Delta H/\text{kJmol}^{-1}$]) ^a
F3	H: Cr 44 [2.8] Col _{hex} / <i>p6mm</i> 160 [6.3] Iso C: Iso 158 [-6.7] Col _{hex} / <i>p6mm</i> < 20 Cr
F4	H: Cr 50 [9.2] Col _{hex} / <i>p6mm</i> 134 [2.8] Iso C: Iso 129 [-2.9] Col _{hex} / <i>p6mm</i> 34 [-7.5] Cr
F5	H: Cr < 20 M 142 [1.6] Col _{hex} / <i>p6mm</i> 154 [5.4] Iso C: Iso 150 [-5.0] Col _{hex} / <i>p6mm</i> 136 [-1.9] M < 20 Cr
F6	H: Cr < 20 M 131 [0.3] Col _{hex} / <i>p6mm</i> 146 [5.4] Iso C: Iso 140 [-5.3] Col _{hex} / <i>p6mm</i> 117 [-0.7] M < 20 Cr
F7	H: Cr < 20 M 150 [5.7] Iso C: Iso 144 [-5.7] M < 20 Cr
F8	H: Cr < 20 Col _{rec} / <i>p2mg</i> 73 [-] Col _{rec} / <i>c2mm</i> 81 [0.3] Col _{squ} / <i>p4mm</i> 143 [5.4] Iso C: Iso 137 [-5.4] Col _{squ} / <i>p4mm</i> 79 [-0.5] Col _{rec} / <i>c2mm</i> 68 [-] Col _{rec} / <i>p2mg</i> < 20 Cr
F9	H: Cr 59 [8.2] Col _{rec} / <i>c2mm</i> 115 [-] Col _{squ} / <i>p4mm</i> 148 [8.8] Iso C: Iso 144 [-8.3] Col _{squ} / <i>p4mm</i> 112 [-] Col _{rec} / <i>c2mm</i> < 20 Cr
F10	H: Cr 94 [22.0] Col _{squ} / <i>p4mm</i> 150 [4.8] Iso C: Iso 144 [-5.2] Col _{squ} / <i>p4mm</i> < 20 Cr
F11	H: Cr 67 [10.2] Col _{rec} / <i>c2mm</i> 80 [-] Col _{squ} / <i>p4mm</i> 158 [9.1] Iso C: Iso 154 [-8.9] Col _{squ} / <i>p4mm</i> 78 [-] Col _{rec} / <i>c2mm</i> < 20 Cr
F12	H: Cr 94 [18.5] Col _{squ} / <i>p4mm</i> 159 [10.8] Iso C: Iso 154 [-10.4] Col _{squ} / <i>p4mm</i> < 20 Cr

^a Data from the first heating/cooling scan. For abbreviations: Col_{rec}/*c2mm* = rectangular columnar phase representing a rhomb tiling; Col_{rec}/*p2mg* = rectangular columnar phase representing a tiling by triangular cells; for other abbreviations, see Table S1a.

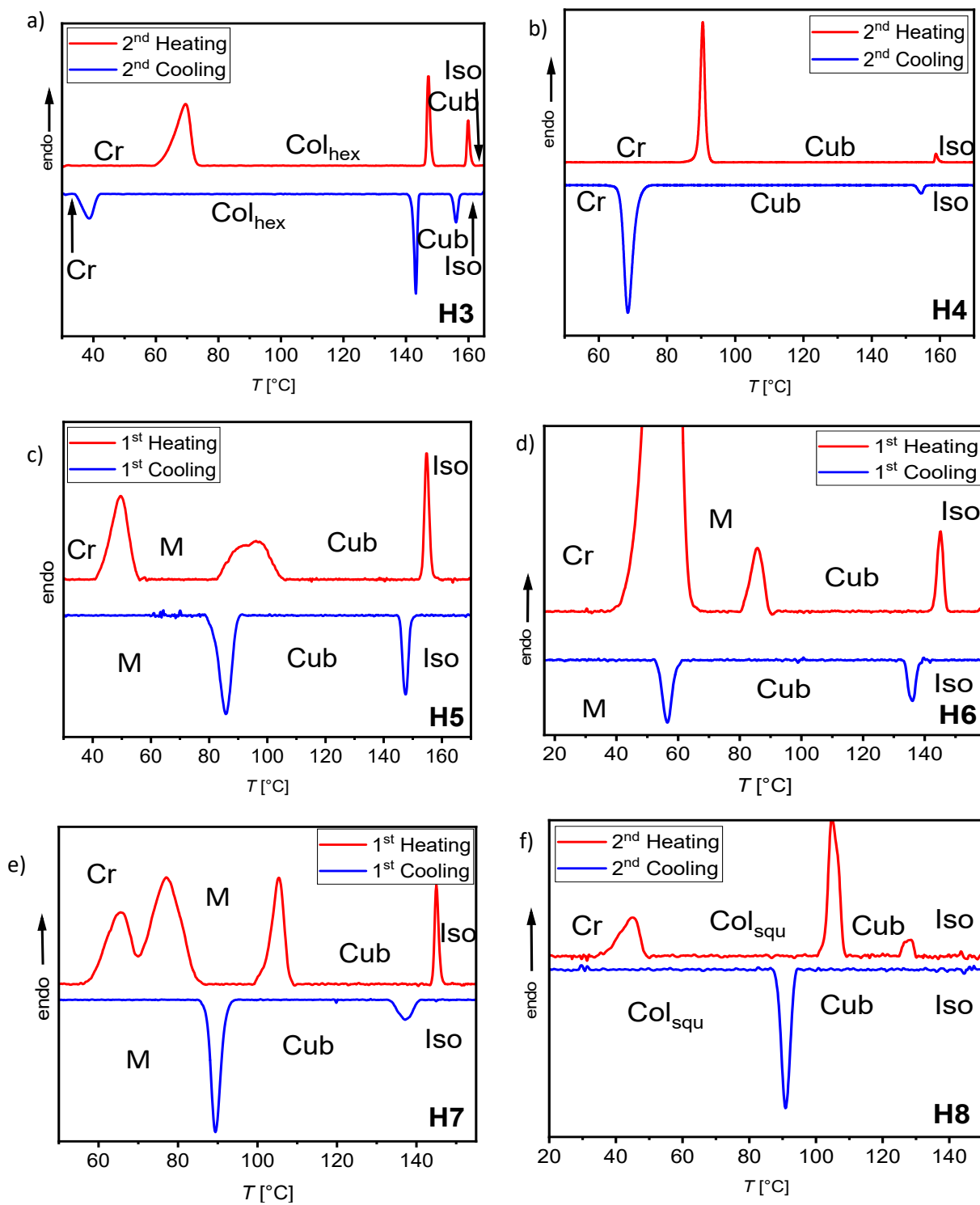


Figure S1. DSC heating and cooling traces of compounds **H_n**, recorded at 10 K min⁻¹.

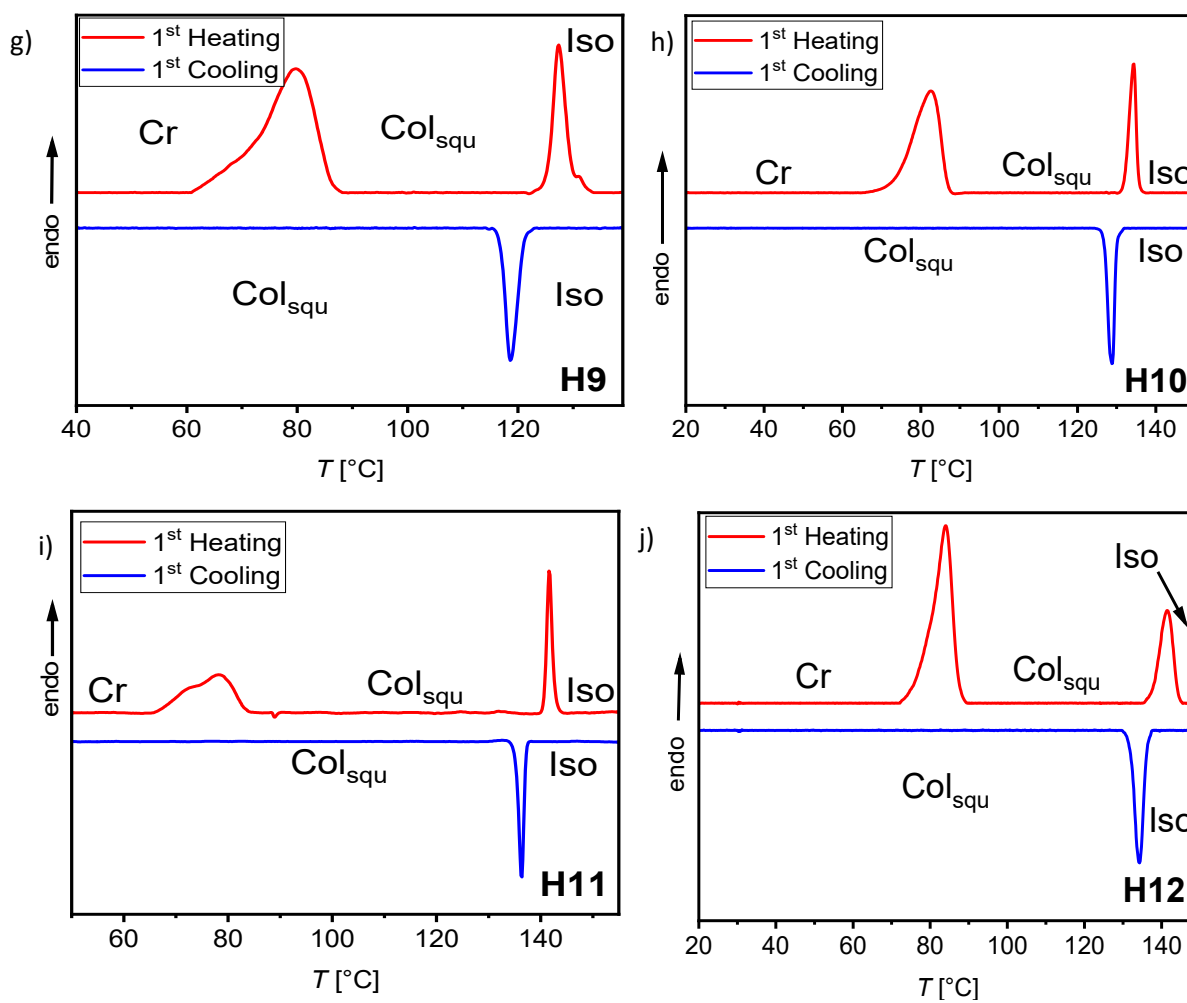


Figure S1 (cont.). DSC heating and cooling traces of compounds **Hn**, recorded at 10 K min^{-1} .

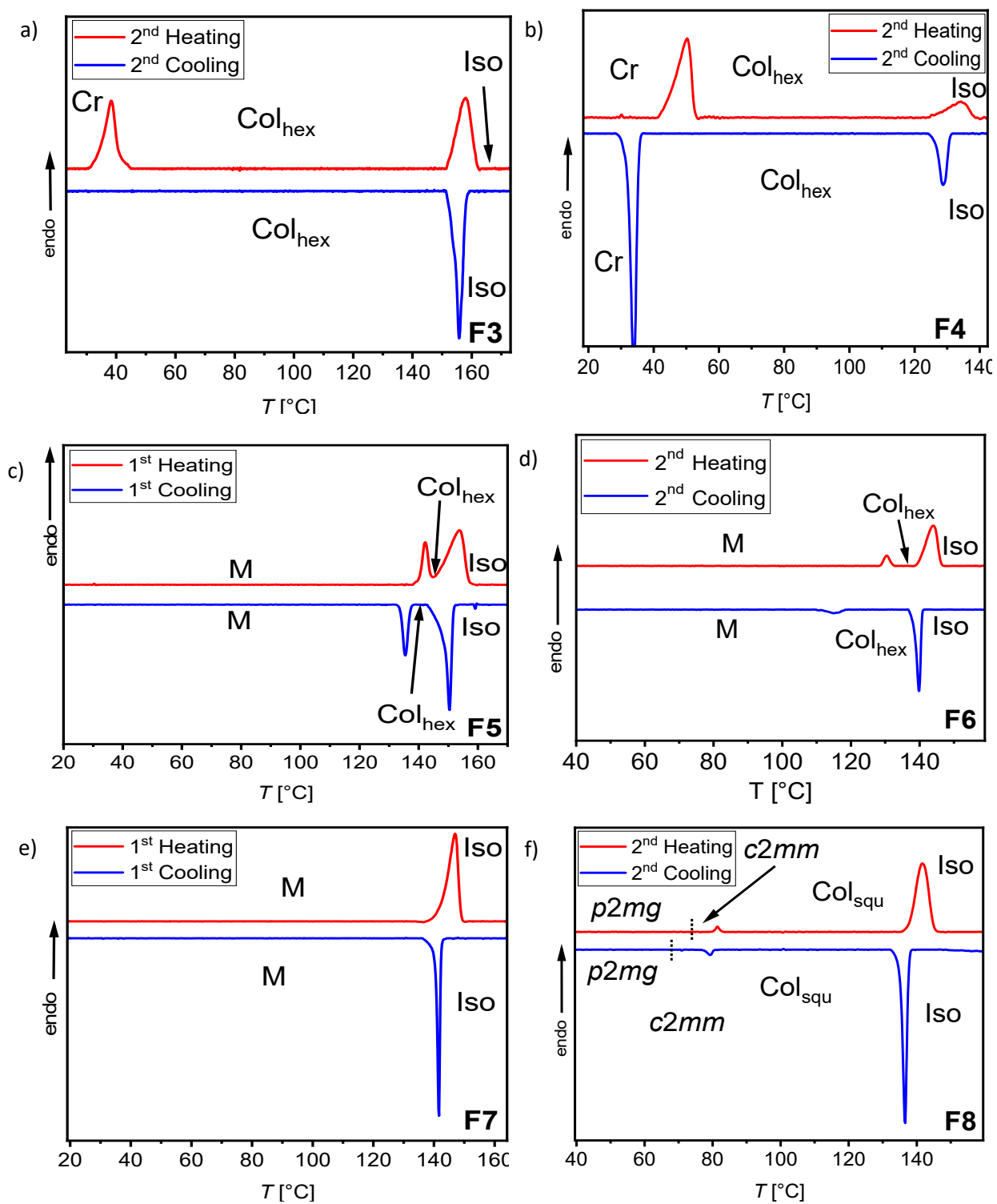


Figure S2. DSC heating and cooling traces of compounds **F_n**, recorded at 10 K min⁻¹.

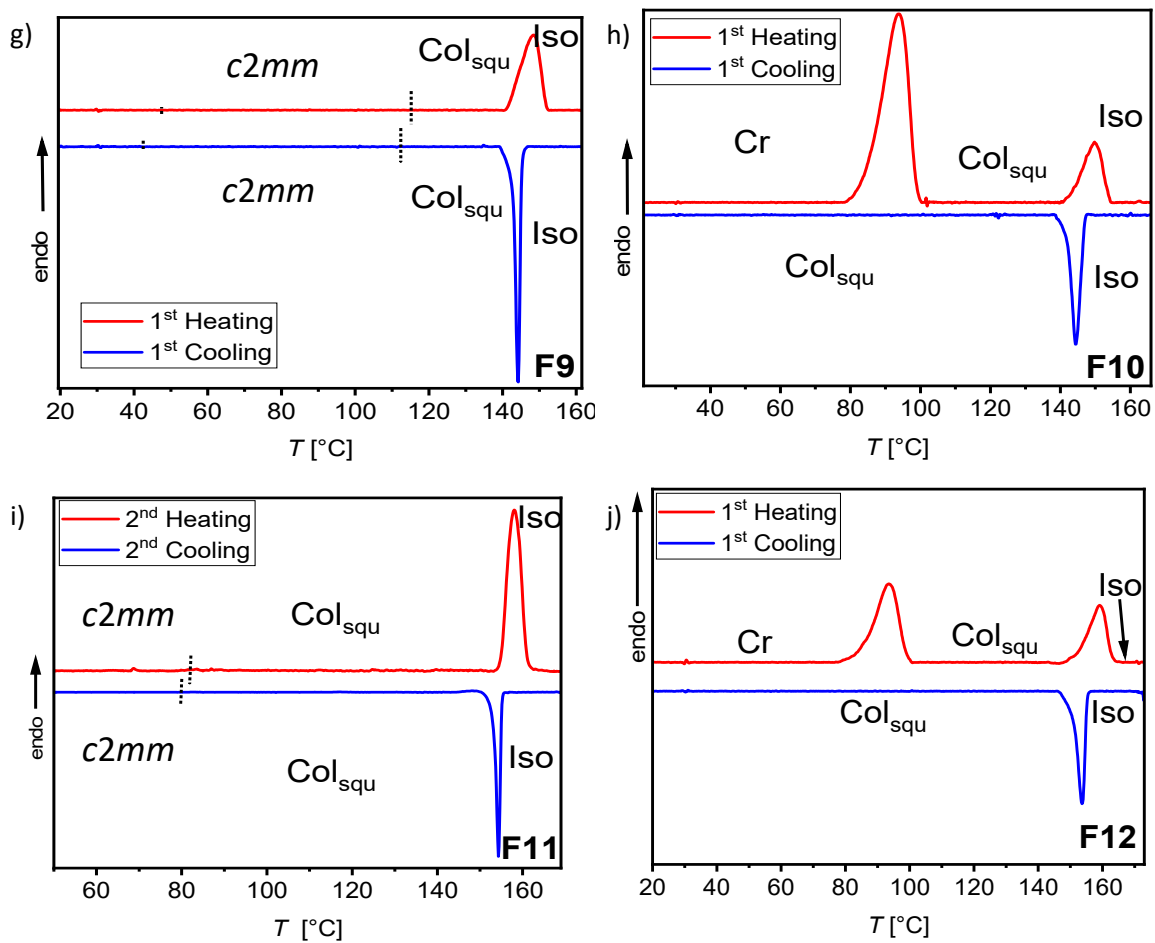


Figure S2 (cont.). DSC heating and cooling traces of compounds **F_n**, recorded at 10 K min^{-1} .

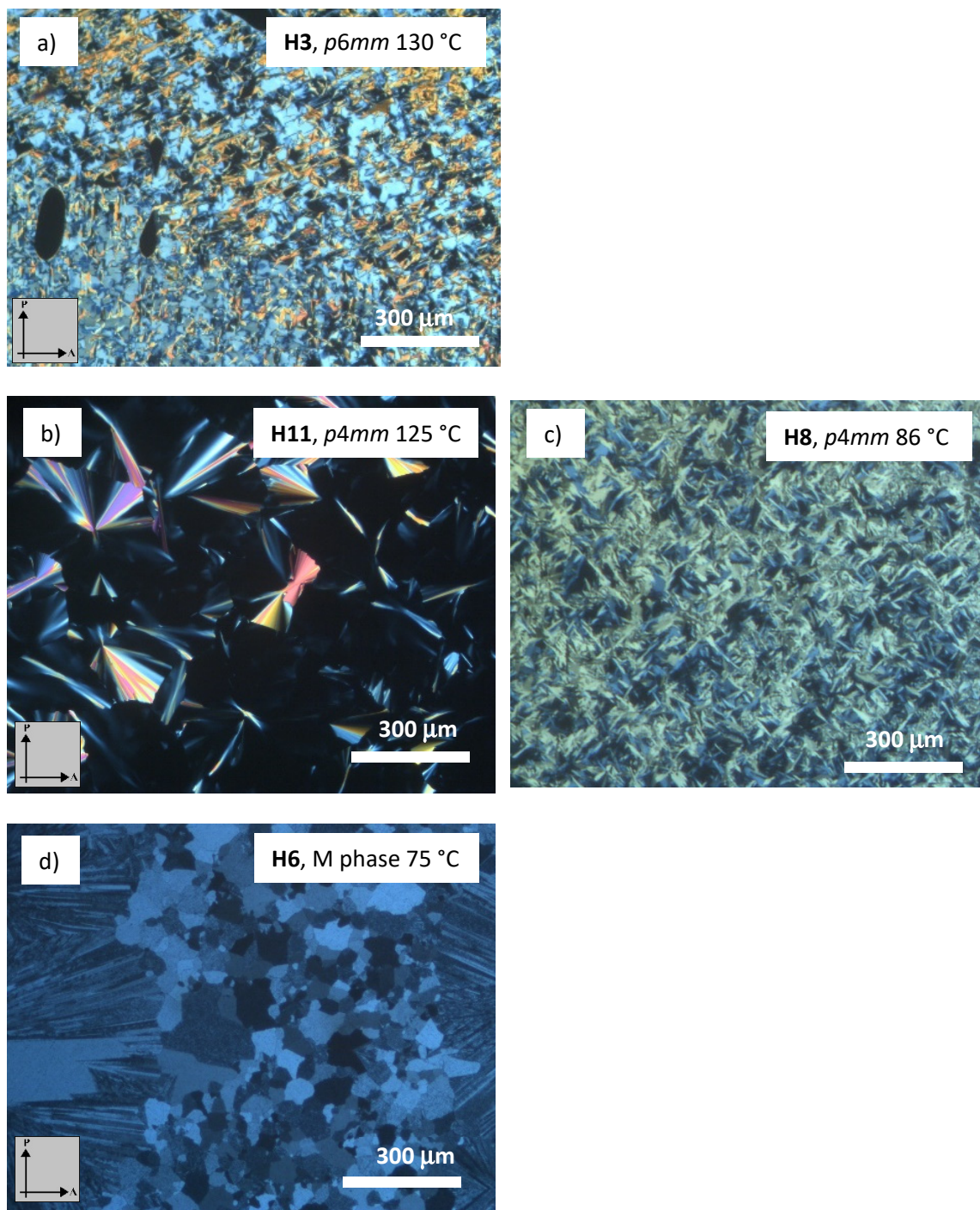


Figure S3. Selected textures of compounds **H_n**. a) Paramorphotic texture of the $Col_{hex}/p6mm$ phase of **H3** (from Cub); b) natural texture of the $Col_{hex}/p6mm$ phase of **H11**; c) paramorphotic texture of the $Col_{sq}/p4mm$ phase of **H8** (from Cub); paramorphotic texture of the M phase of **H6** (from Cub) as observed upon cooling between crossed polarizers

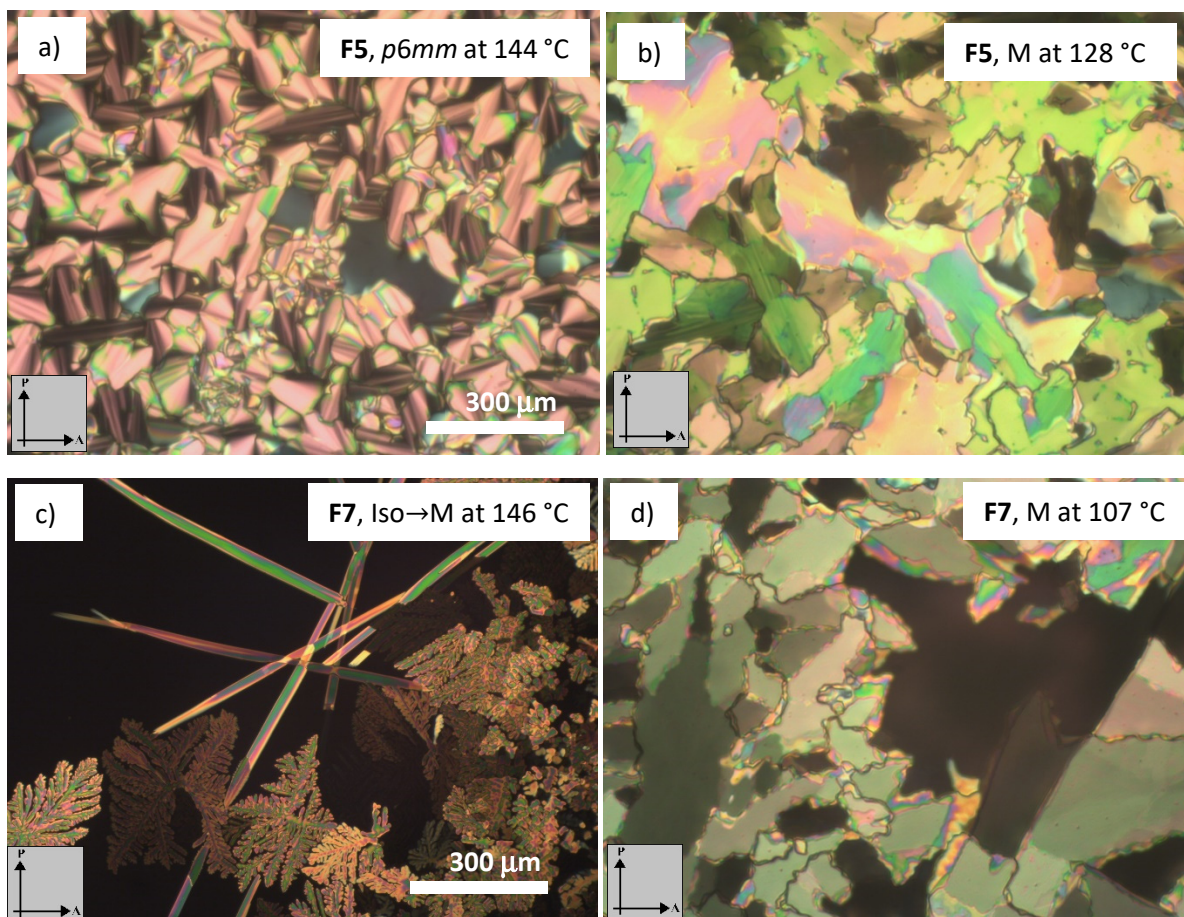


Figure S4. Textures of compounds **F_n**. a) $Col_{hex}/p6mm$ phase (dark areas are homeotropic aligned) and b) the paramorphotic texture of the M phase of compound **F5**; c, d) original texture of the M phase of compounds **F7** as observed upon cooling at the indicated temperatures between crossed polarizers; dark areas in c) are residues of the isotropic liquid whereas the dark areas in the M phase become birefringent after rotation of the sample between the crossed polarizers.

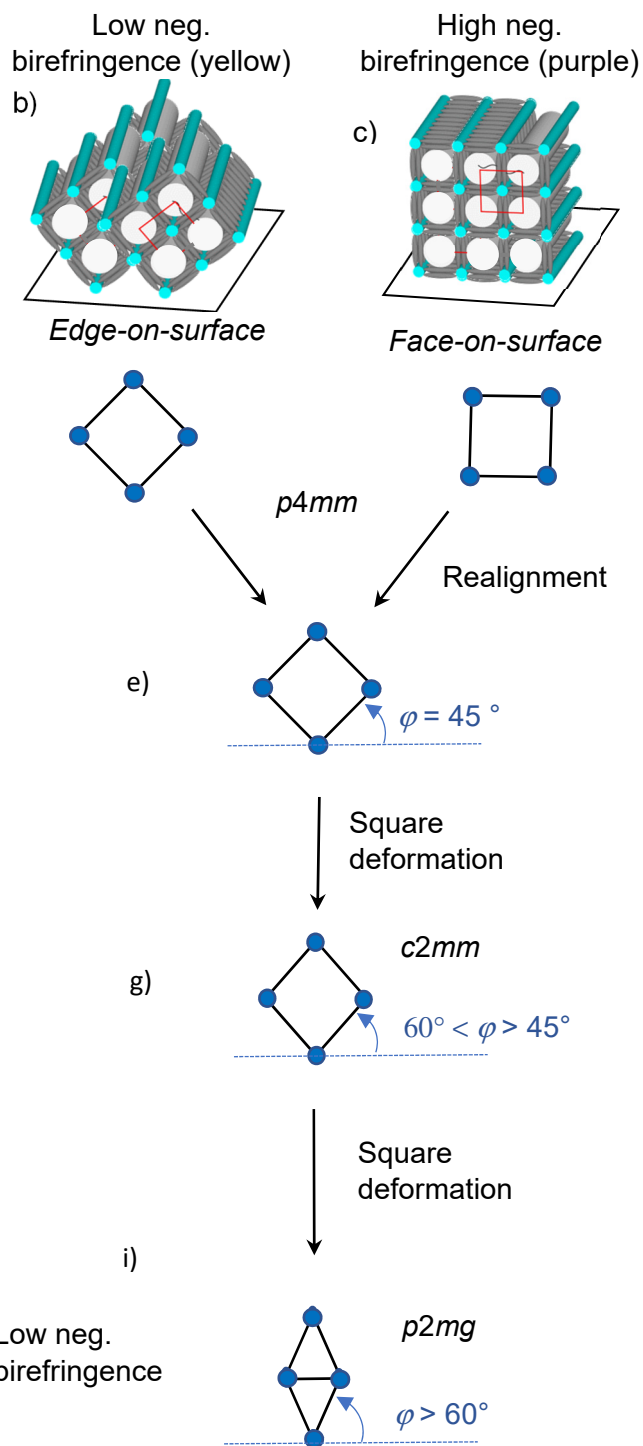
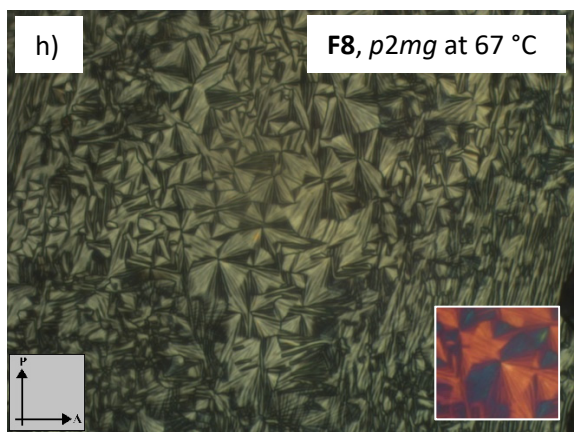
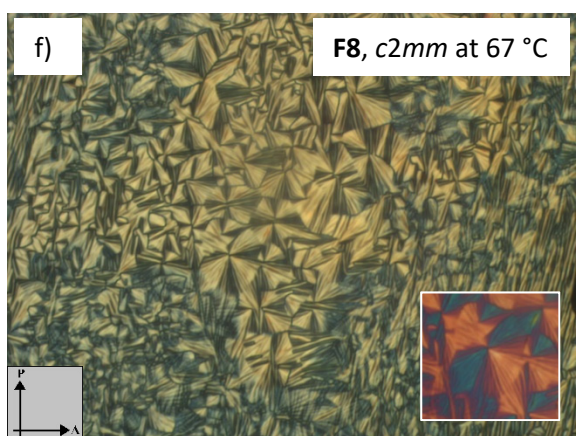
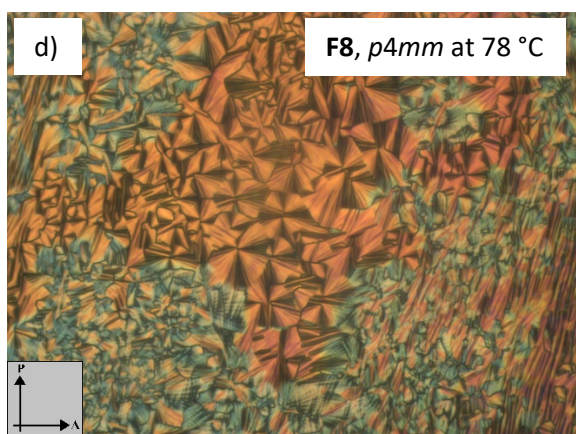
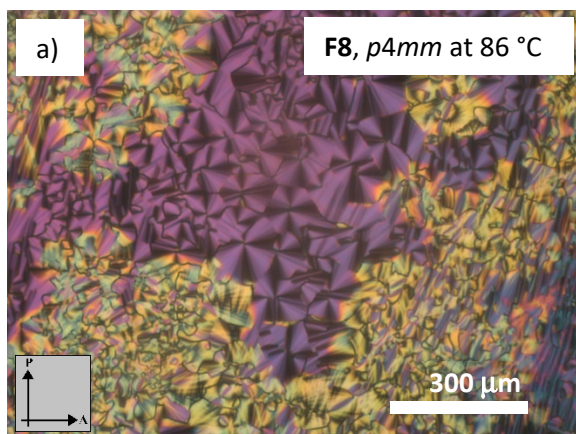


Figure S5. Textures of **F8** depending on temperature. a-c) in the $p4mm$ phase the honeycomb assume two alignments; d, e) realignment leads to uniform edge-on-surface orientation with low birefringence, f, g) the birefringence decreases at the $p4mm \rightarrow c2mm$ transition because the angle φ increases, thus decreasing the contribution of the conjugation pathway parallel to the rod-long axis and retaining that perpendicular to the core direction (with organization of the π -planes of the benzenes preferentially parallel to the honeycomb main axis. h, i) In $p2gm$ φ exceeds 60° ; the additional terphenyls

separating the triangles parallel to the surface contribute to retaining the negative birefringence despite of this strong tilt with respect to the substrate surface. The insets in f, h) were taken with additional λ -retarder plate and confirm negative birefringence by NE-SW orientation of the blue shifted brushes (parallel to the slow axis). The decreasing birefringence supports the indexation of the low temperature phase to $p2mg$, while the alternative $p2mm$ phase (see Fig. S12) is expected to lead to increased birefringence.

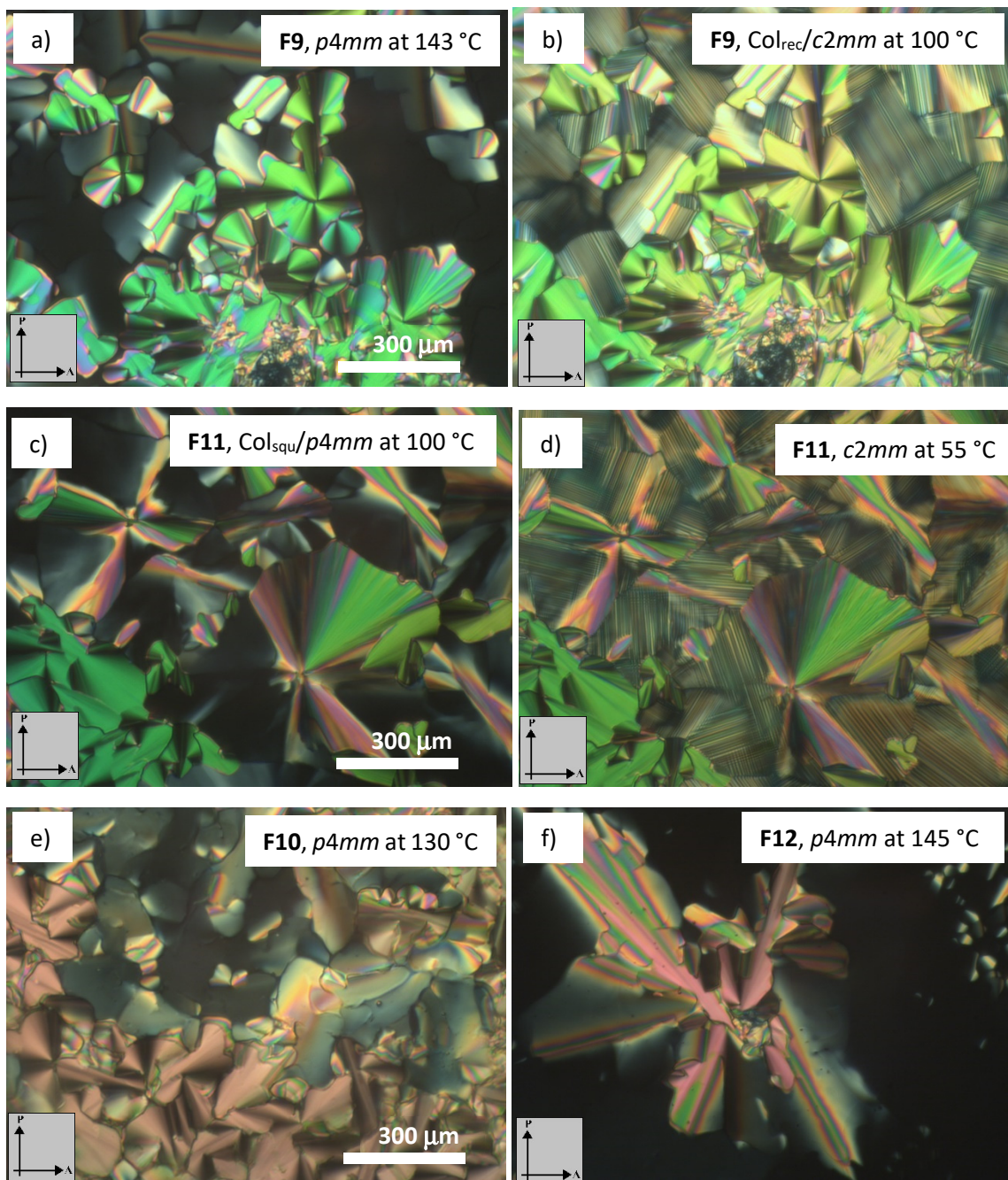


Figure S6. Textures of compounds **F9-F12** at the given temperatures in the $Col_{squ}/p4mm$ and $Col_{rec}/c2mm$ phases.

2.2. XRD data

2.2.1. WAXS patterns

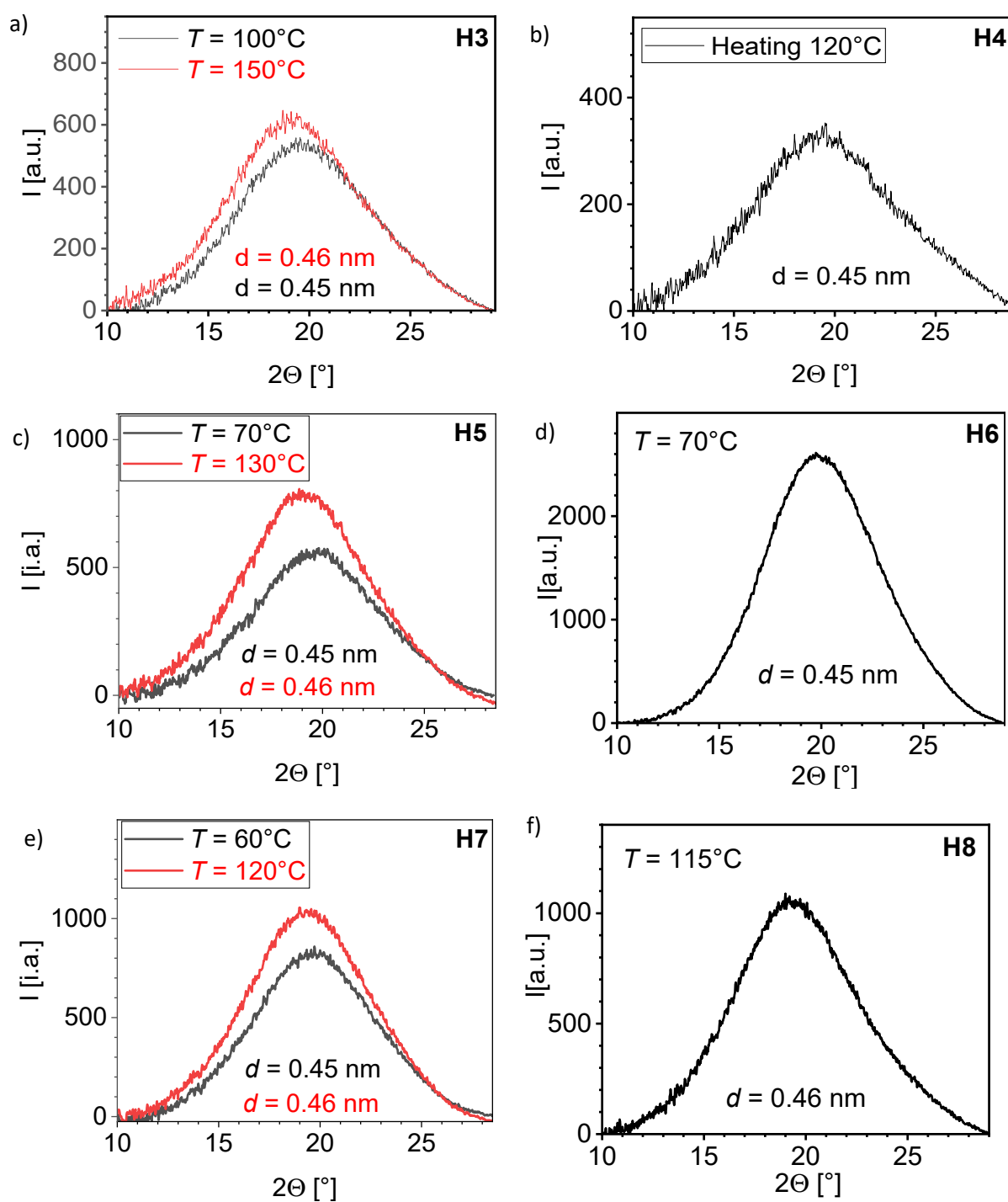


Figure S7. WAXS diffractograms of compounds Hn.

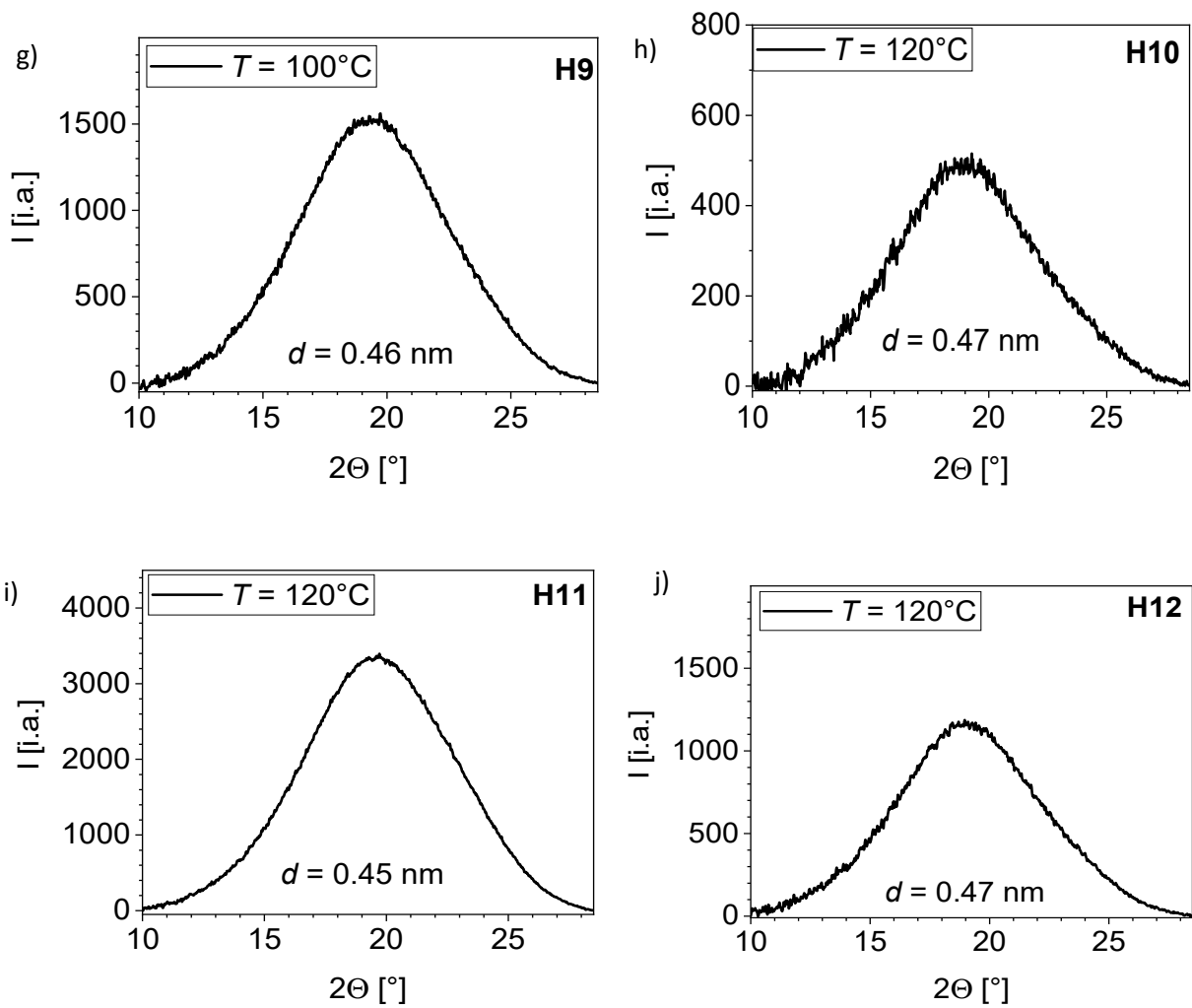


Figure S7 (cont.). WAXS diffractograms of compounds **Hn**.

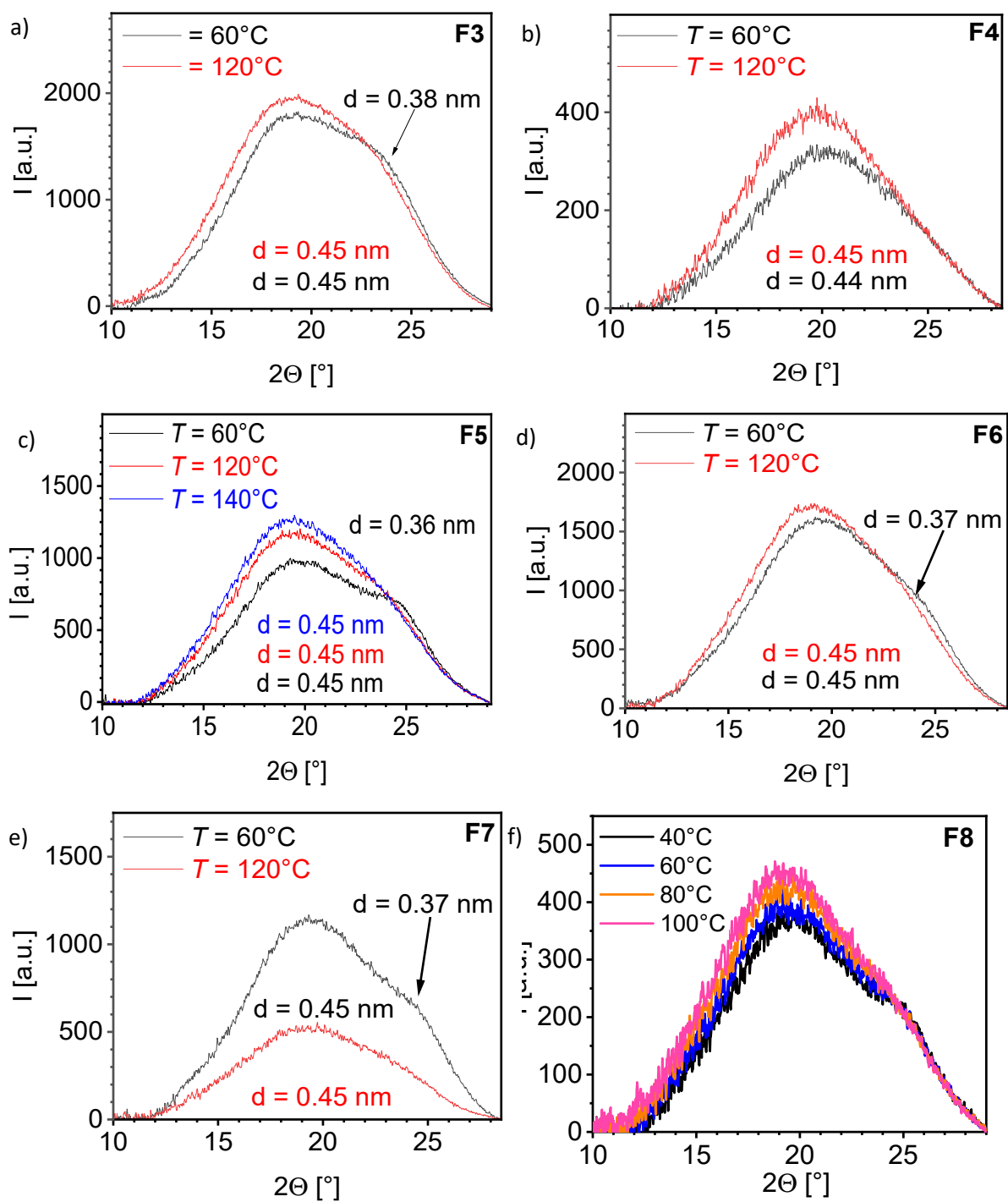


Figure S8. WAXS diffractograms of compounds F_n .

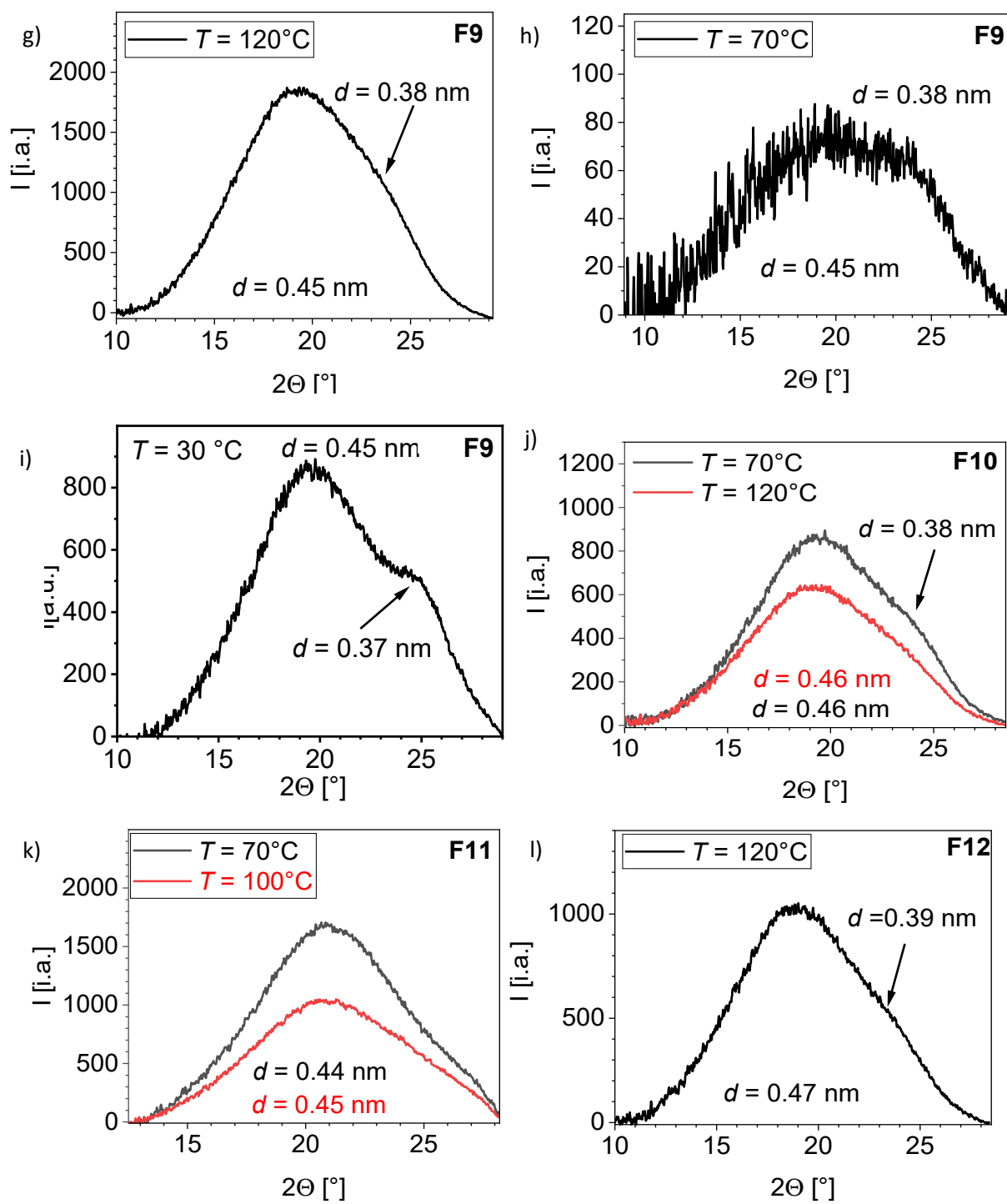


Figure S8 (cont.). WAXS diffractograms of compounds **F_n**.

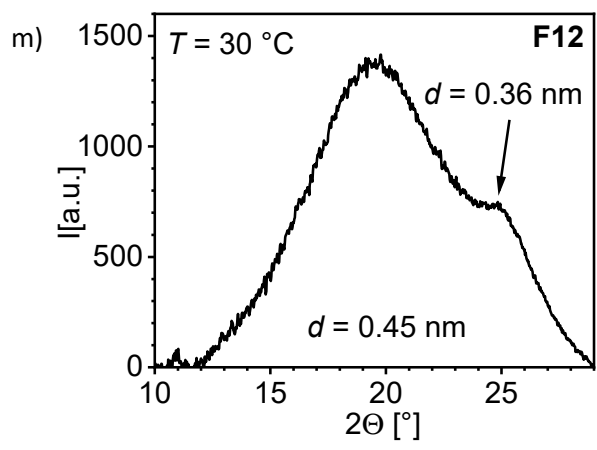


Figure S8 (cont.). WAXS diffractograms of compounds **F n** .

2.2.2. Additional SAXS patterns

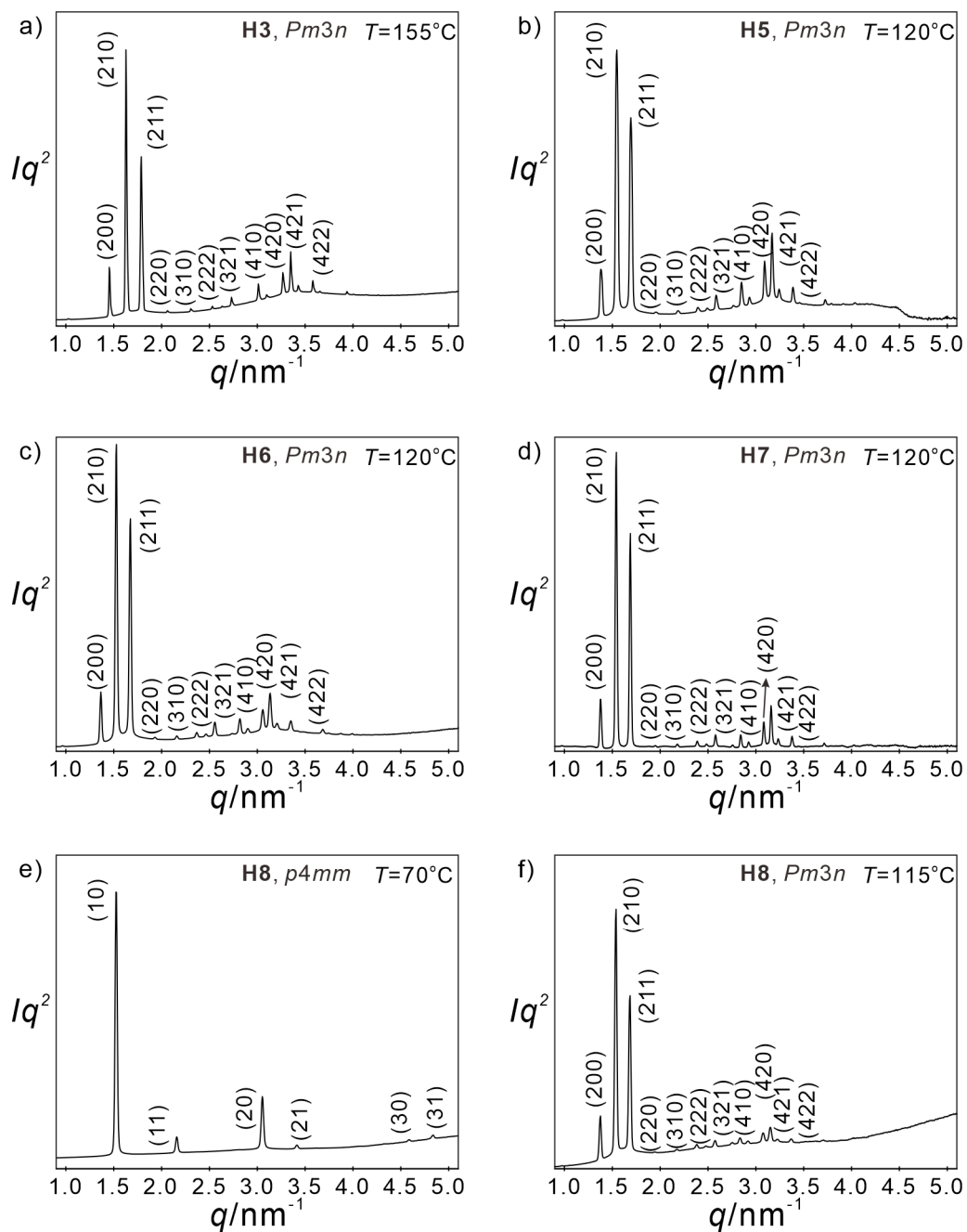


Figure S9. SAXS diffractograms of compounds **Hn**. at the indicated temperatures.

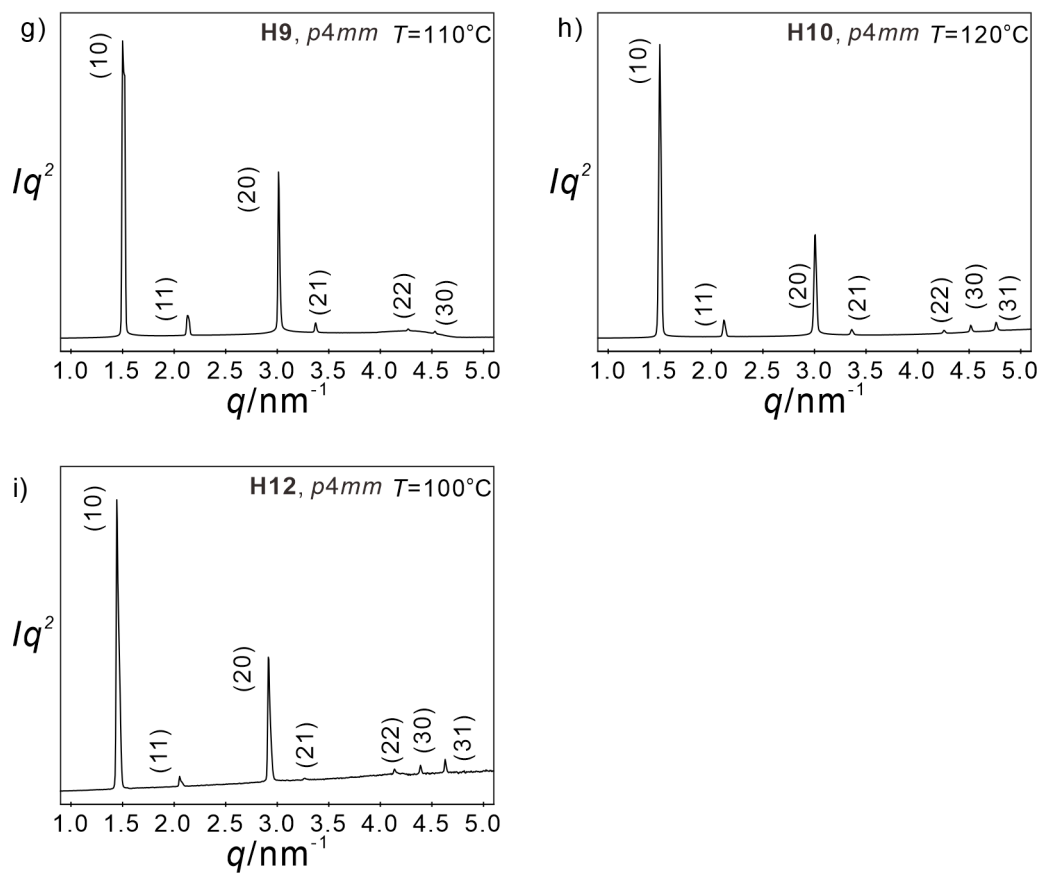


Figure S9 (cont.). SAXS diffractograms of compounds **H n** . at the indicated temperatures.

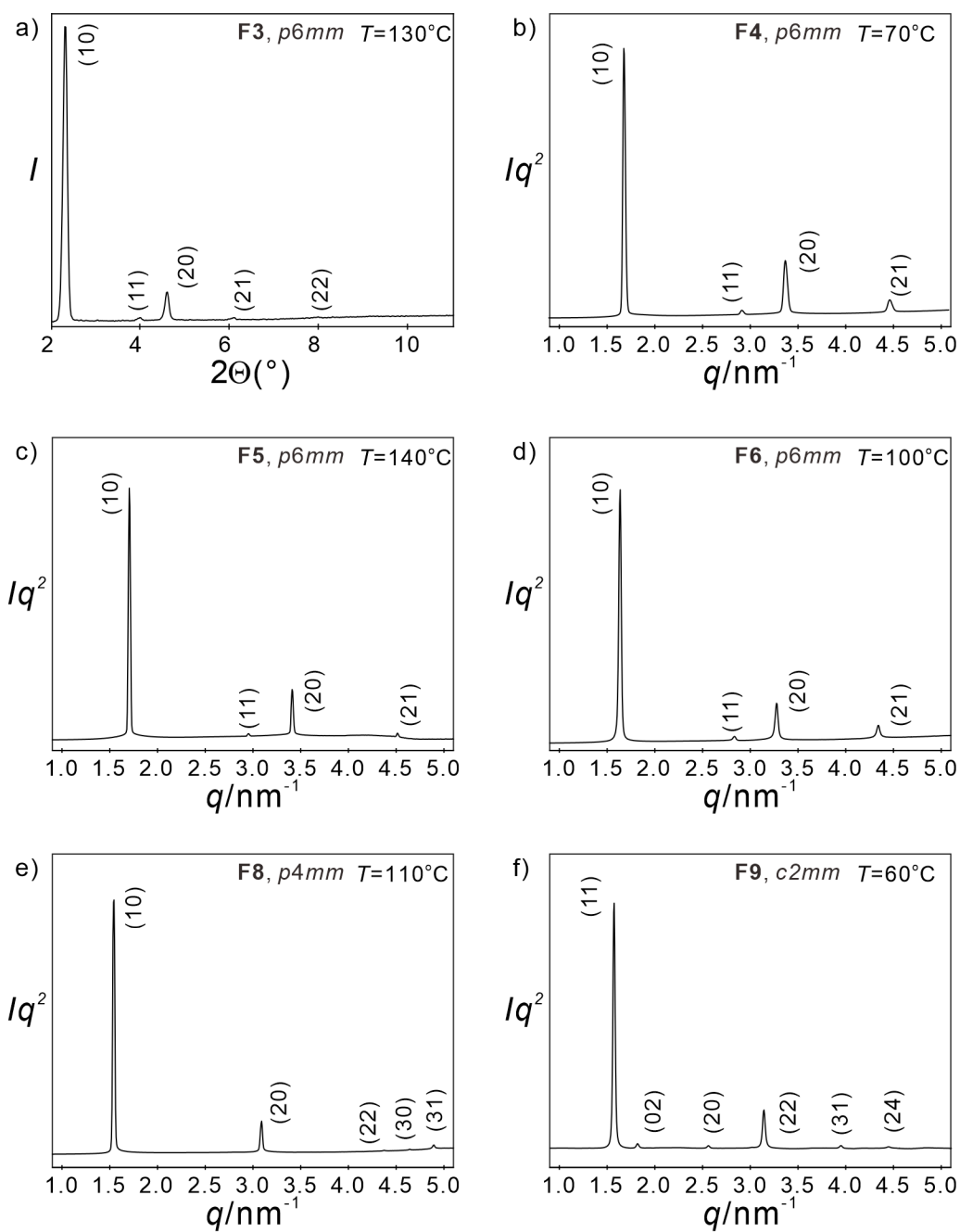


Figure S10. SAXS diffractograms of compounds **F_n** at the indicated temperatures.

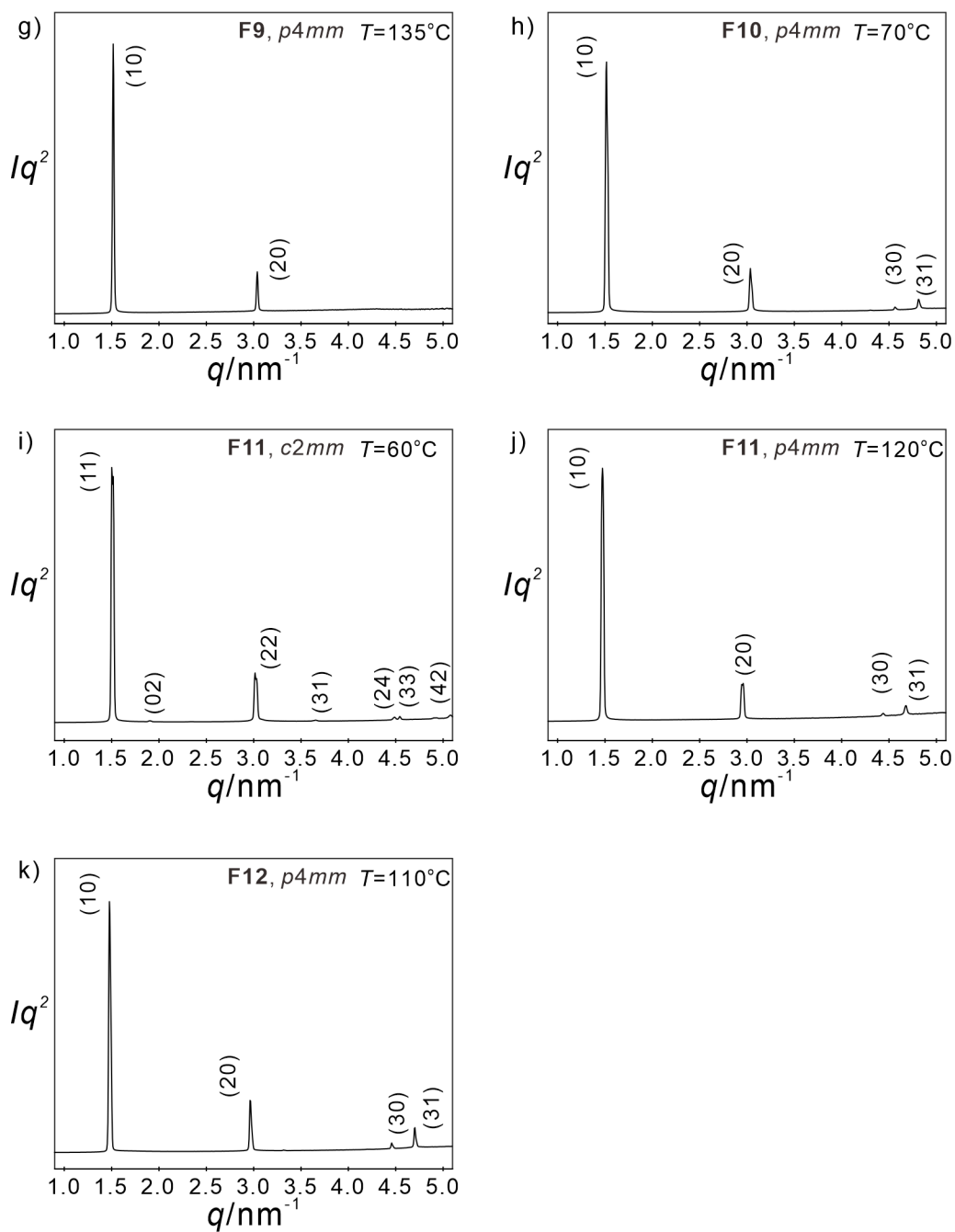


Figure S10 (cont.). SAXS diffractograms of compounds **F_n** at the indicated temperatures.

2.2.3. Numerical SAXS data

Table S2. Experimental and calculated d -spacing for the observed SAXS reflections of the $\text{Col}_{\text{hex}}/p6mm$ phase of compound **H3** at $T = 100$ °C. All intensity values are Lorentz and multiplicity corrected.

(hk)	$d_{\text{obs.}}$ –spacing (nm)	$d_{\text{cal.}}$ –spacing (nm)	<i>intensity</i>	<i>phase</i>
(10)	3.80	3.80	35.5	0
(11)	2.19	2.20	6.6	π
(20)	1.90	1.90	100.0	0
(21)	1.43	1.44	0.3	0
(30)	1.26	1.27	2.1	0
$a_{\text{hex}} = 4.39$ nm				

Table S3. Experimental and calculated d -spacing for the observed SAXS reflections of the $\text{Cub}/Pm\bar{3}n$ phase of compound **H3** at $T = 120$ °C. All intensity values are Lorentz and multiplicity corrected.

(hkl)	$d_{\text{obs.}}$ –spacing (nm)	$d_{\text{cal.}}$ –spacing (nm)	<i>intensity</i>	<i>phase</i>
(110)	6.10	6.10	0.6	π
(200)	4.31	4.31	55.3	0
(210)	3.85	3.85	100.0	0
(211)	3.51	3.52	77.0	0
(220)	3.04	3.05	1.1	π
(310)	2.72	2.73	0.9	0
(222)	2.48	2.49	2.3	π
(320)	2.39	2.39	0.3	π
(321)	2.30	2.30	1.4	π
(410)	2.09	2.09	5.8	0
(330)	2.03	2.03	11.5	π
(411)	2.03	2.03	5.7	π
(420)	1.92	1.93	10.1	0
(421)	1.87	1.88	8.4	0
(332)	1.83	1.84	3.6	0
(422)	1.75	1.76	4.1	0
(430)	1.72	1.72	0.4	0
$a_{\text{cub}} = 8.62$ nm				

Table S4. Experimental and calculated d -spacing for the observed SAXS reflections of the $\text{Cub}/Pm\bar{3}n$ phase of compound **H4** at $T = 120$ °C. All intensity values are Lorentz and multiplicity corrected.

(hkl)	$d_{\text{obs.}}$ -spacing (nm)	$d_{\text{cal.}}$ -spacing (nm)	<i>intensity</i>	<i>phase</i>
(110)	6.28	6.28	0.6	π
(200)	4.44	4.44	63.7	0
(210)	3.98	3.97	100.0	0
(211)	3.63	3.63	76.8	0
(220)	3.14	3.14	1.4	π
(310)	2.81	2.81	1.3	0
(222)	2.57	2.56	3.7	π
(320)	2.46	2.46	0.9	π
(321)	2.38	2.37	2.8	π
(410)	2.15	2.15	3.7	0
(330)	2.15	2.15	15.4	π
(411)	2.09	2.09	7.7	π
(420)	1.99	1.99	9.5	0
(421)	1.94	1.94	8.1	0
(332)	1.89	1.89	2.8	0
(422)	1.81	1.81	3.8	0
(430)	1.77	1.78	1.2	0
$a_{\text{cub}} = 8.88$ nm				

Table S5. Experimental and calculated d -spacing for the observed SAXS reflections of the $\text{Cub}/Pm\bar{3}n$ phase of compound **H5** at $T = 120$ °C. All intensity values are Lorentz and multiplicity corrected.

(hkl)	$d_{\text{obs.}}$ -spacing (nm)	$d_{\text{cal.}}$ -spacing (nm)	<i>intensity</i>	<i>phase</i>
(110)	6.40	6.41	1.0	π
(200)	4.54	4.54	64.4	0
(210)	4.06	4.06	100.0	0
(211)	3.71	3.70	75.5	0
(220)	3.21	3.21	1.2	π
(310)	2.87	2.87	1.8	0
(222)	2.62	2.62	7.1	π
(320)	2.52	2.52	1.3	π
(321)	2.42	2.42	3.3	π
(410)	2.20	2.20	2.4	0
(330)	2.14	2.14	17.2	π
(411)	2.14	2.14	8.6	π
(420)	2.03	2.03	7.2	0
(421)	1.98	1.98	9.4	0
(332)	1.93	1.93	6.8	0
(422)	1.85	1.85	6.0	0
(430)	1.81	1.80	0.2	0
$a_{\text{cub}} = 9.07$ nm				

Table S6. Experimental and calculated d -spacing for the observed SAXS reflections of the $\text{Cub}/Pm\bar{3}n$ phase of compound **H6** at $T = 120$ °C. All intensity values are Lorentz and multiplicity corrected.

(hkl)	$d_{\text{obs.}}$ -spacing (nm)	$d_{\text{cal.}}$ -spacing (nm)	<i>intensity</i>	<i>phase</i>
(110)	6.51	6.51	0.6	π
(200)	4.60	4.60	52.1	0
(210)	4.11	4.11	100.0	0
(211)	3.75	3.76	78.5	0
(220)	3.25	3.25	1.2	π
(310)	2.91	2.91	0.9	0
(222)	2.66	2.66	2.4	π
(320)	2.55	2.55	0.3	π
(321)	2.46	2.46	1.5	π
(410)	2.23	2.23	6.1	0
(330)	2.17	2.17	12.2	π
(411)	2.17	2.17	6.1	π
(420)	2.06	2.06	10.8	0
(421)	2.01	2.01	8.9	0
(332)	1.96	1.96	3.8	0
(422)	1.88	1.88	4.4	0
(430)	1.84	1.84	0.4	0
$a_{\text{cub}} = 9.20$ nm				

Table S7. Experimental and calculated d -spacing for the observed SAXS reflections of the $\text{Cub}/Pm\bar{3}n$ phase of compound **H7** at $T = 120$ °C. All intensity values are Lorentz and multiplicity corrected.

(hkl)	$d_{\text{obs.}}$ -spacing (nm)	$d_{\text{cal.}}$ -spacing (nm)	<i>intensity</i>	<i>phase</i>
(110)	6.45	6.45	1.8	π
(200)	4.56	4.56	62.3	0
(210)	4.08	4.08	100.0	0
(211)	3.72	3.72	71.4	0
(220)	3.22	3.22	3.5	π
(310)	2.88	2.88	2.7	0
(222)	2.63	2.63	1.5	π
(320)	2.53	2.53	0.9	π
(321)	2.44	2.44	1.0	π
(410)	2.21	2.21	1.0	0
(330)	2.15	2.15	7.1	π
(411)	2.15	2.15	3.5	π
(420)	2.04	2.04	8.1	0
(421)	1.99	1.99	5.9	0
(332)	1.94	1.94	2.1	0
(422)	1.86	1.86	2.4	0
(430)	1.82	1.82	0.4	0
$a_{\text{cub}} = 9.12$ nm				

Table S8. Experimental and calculated d -spacing for the observed SAXS reflections of the $Cub/Pm\bar{3}n$ phase of compound **H8** at $T = 115$ °C. All intensity values are Lorentz and multiplicity corrected.

(hkl)	$d_{obs.}$ –spacing (nm)	$d_{cal.}$ –spacing (nm)	<i>intensity</i>	<i>phase</i>
(110)	6.46	6.46	0.8	π
(200)	4.57	4.57	54.4	0
(210)	4.09	4.09	100.0	0
(211)	3.73	3.73	70.3	0
(220)	3.23	3.23	1.6	π
(310)	2.89	2.89	1.3	0
(222)	2.64	2.64	3.4	π
(320)	2.53	2.53	0.5	π
(321)	2.44	2.44	1.9	π
(410)	2.22	2.22	1.4	0
(330)	2.15	2.15	16.4	π
(411)	2.15	2.15	8.2	π
(420)	2.04	2.04	12.2	0
(421)	1.99	1.99	9.8	0
(332)	1.94	1.95	4.2	0
(422)	1.86	1.87	4.8	0
(430)	1.82	1.83	0.4	0
$a_{cub} = 9.14$ nm				

Table S9. Experimental and calculated d -spacing for the observed SAXS reflections of the $Col_{squ}/p4mm$ phase of compound **H8** at $T = 70$ °C. All intensity values are Lorentz and multiplicity corrected.

(hk)	$d_{obs.}$ –spacing (nm)	$d_{cal.}$ –spacing (nm)	<i>intensity</i>	<i>phase</i>
(10)	4.12	4.12	100	π
(11)	2.91	2.91	6.6	π
(20)	2.06	2.06	22.2	0
(21)	1.84	1.84	0.6	0
(30)	1.37	1.37	0.7	π
(31)	1.30	1.30	0.9	π
$a_{squ} = 4.12$ nm				

Table S10. Experimental and calculated d -spacing for the observed SAXS reflections of the $\text{Col}_{\text{squ}}/p4mm$ phase of compound **H9** at $T = 110$ °C. All intensity values are Lorentz and multiplicity corrected.

(hk)	$d_{\text{obs.}}$ –spacing (nm)	$d_{\text{cal.}}$ –spacing (nm)	<i>intensity</i>	<i>phase</i>
(10)	4.16	4.16	100	π
(11)	2.94	2.94	6.2	π
(20)	2.08	2.08	35.0	0
(21)	1.86	1.86	0.1	0
(22)	1.47	1.47	0.3	0
(30)	1.39	1.39	2.8	π
$a_{\text{squ}} = 4.16$ nm				

Table S11. Experimental and calculated d -spacing for the observed SAXS reflections of the $\text{Col}_{\text{squ}}/p4mm$ phase of compound **H10** at $T = 120$ °C. All intensity values are Lorentz and multiplicity corrected.

(hk)	$d_{\text{obs.}}$ –spacing (nm)	$d_{\text{cal.}}$ –spacing (nm)	<i>intensity</i>	<i>phase</i>
(10)	4.18	4.18	100	π
(11)	2.96	2.96	5.7	π
(20)	2.09	2.09	42.9	0
(21)	1.87	1.87	0.3	0
(30)	1.39	1.39	2.8	π
(31)	1.32	1.32	3.7	π
$a_{\text{squ}} = 4.18$ nm				

Table S12. Experimental and calculated d -spacing for the observed SAXS reflections of the $\text{Col}_{\text{squ}}/p4mm$ phase of compound **H11** at $T = 100$ °C. All intensity values are Lorentz and multiplicity corrected.

(hk)	$d_{\text{obs.}}$ –spacing (nm)	$d_{\text{cal.}}$ –spacing (nm)	<i>intensity</i>	<i>phase</i>
(10)	4.25	4.25	100	π
(11)	3.00	3.00	4.7	π
(20)	2.12	2.13	42.1	0
(21)	1.90	1.90	0.9	0
(22)	1.50	1.50	2.0	0
(30)	1.41	1.41	2.9	π
(31)	1.34	1.34	2.1	π
$a_{\text{squ}} = 4.25$ nm				

Table S13. Experimental and calculated d -spacing for the observed SAXS reflections of the $\text{Col}_{\text{squ}}/p4mm$ phase of compound **H12** at $T = 100$ °C. All intensity values are Lorentz and multiplicity corrected.

(hk)	$d_{\text{obs.}} - \text{spacing (nm)}$	$d_{\text{cal.}} - \text{spacing (nm)}$	<i>intensity</i>	<i>phase</i>
(10)	4.32	4.32	100	π
(11)	3.05	3.05	4.4	π
(20)	2.16	2.16	44.8	0
(21)	1.93	1.93	0.1	0
(22)	1.53	1.53	0.2	0
(30)	1.44	1.44	3.3	π
(31)	1.37	1.37	3.9	π
$a_{\text{squ}} = 4.32$ nm				

Table S14. Experimental and calculated d -spacing for the observed SAXS reflections of the $\text{Col}_{\text{hex}}/p6mm$ phase of compound **F3** at $T = 120$ °C.

(hk)	$d_{\text{obs.}} - \text{spacing (nm)}$	$d_{\text{cal.}} - \text{spacing (nm)}$	Δ
(10)	3.797	3.796	0.00
(11)	2.211	2.191	0.02
(20)	1.917	1.898	0.02
(21)	1.450	1.435	0.01
(22)	1.102	1.096	0.01
$a_{\text{hex}} = 4.38$ nm			

Table S15. Experimental and calculated d -spacing for the observed SAXS reflections of the $\text{Col}_{\text{hex}}/p6mm$ phase of compound **F4** at $T = 70$ °C. All intensity values are Lorentz and multiplicity corrected.

(hk)	$d_{\text{obs.}} - \text{spacing (nm)}$	$d_{\text{cal.}} - \text{spacing (nm)}$	<i>intensity</i>	<i>phase</i>
(10)	3.72	3.72	100.0	0
(11)	2.14	2.15	2.0	0
(20)	1.86	1.86	30.0	0
(21)	1.40	1.40	5.0	π
$a_{\text{hex}} = 4.29$ nm				

Table S16. Experimental and calculated d -spacing for the observed SAXS reflections of the $\text{Col}_{\text{hex}}/p6mm$ phase of compound **F5** at $T = 140\text{ }^\circ\text{C}$. All intensity values are Lorentz and multiplicity corrected.

(hk)	$d_{\text{obs.}}$ –spacing (nm)	$d_{\text{cal.}}$ –spacing (nm)	<i>intensity</i>	<i>phase</i>
(10)	3.68	3.68	100.0	0
(11)	2.13	2.13	2.0	0
(20)	1.84	1.84	18.9	0
(21)	1.39	1.39	0.7	π
$a_{\text{hex}} = 4.25\text{ nm}$				

Table S17. Experimental and calculated d -spacing for the observed SAXS reflections of the $\text{Col}_{\text{hex}}/p6mm$ phase of compound **F6** at $T = 100\text{ }^\circ\text{C}$. All intensity values are Lorentz and multiplicity corrected.

(hk)	$d_{\text{obs.}}$ –spacing (nm)	$d_{\text{cal.}}$ –spacing (nm)	<i>intensity</i>	<i>phase</i>
(10)	3.84	3.84	100.0	0
(11)	2.22	2.22	1.4	0
(20)	1.92	1.92	18.9	0
(21)	1.45	1.45	6.2	π
$a_{\text{hex}} = 4.43\text{ nm}$				

Table S18. Experimental and calculated d -spacing of the observed SAXS reflection of the $p4mm$ phase in **F8** at heating $110\text{ }^\circ\text{C}$. All intensity values are Lorentz and multiplicity corrected.

(hkl)	$d_{\text{obs.}}$ –spacing (nm)	$d_{\text{cal.}}$ –spacing (nm)	<i>intensity</i>	<i>phase</i>
(10)	4.07	4.07	100	π
(20)	2.03	2.03	13.5	0
(22)	1.43	1.44	0.3	π
(30)	1.35	1.36	0.2	π
(31)	1.28	1.29	0.8	0
$a_{\text{squ}} = 4.07\text{ nm}$				

Table S19. Experimental and calculated d -spacing of the observed SAXS reflection of the $c2mm$ phase in **F8** at heating 74 °C. All intensity values are Lorentz and multiplicity corrected.

(hkl)	$d_{\text{obs.}}$ –spacing (nm)	$d_{\text{cal.}}$ –spacing (nm)	$intensity$	$phase$
(11)	4.02	4.04	100	π
(02)	3.40	3.40	1.7	0
(20)	2.51	2.51	1.1	0
(22)	2.01	2.02	14.6	0
(31)	1.62	1.62	0.5	0
(24)	1.40	1.41	0.3	0
(33)	1.34	1.34	0.6	π
$a_{\text{rec}} = 4.95 \text{ nm}; b_{\text{rec}} = 6.96 \text{ nm}$				

Table S20. Experimental and calculated d -spacing of the observed SAXS reflection of the $p2mg$ phase in **F8** at cooling 64 °C. All intensity values are Lorentz and multiplicity corrected.

(hkl)	$d_{\text{obs.}}$ –spacing (nm)	$d_{\text{cal.}}$ –spacing (nm)	$intensity$	$phase$
(02)	4.05	4.05	100	π
(11)	3.60	3.60	53.4	π
(03)	2.69	2.70	0.06	-
(13)	2.25	2.24	0.06	-
(04)	2.02	2.03	20.0	0
(22)	1.80	1.80	6.0	0
(06)	1.35	1.35	1.7	π
(25)	1.26	1.26	3.2	0
$a_{\text{rec}} = 4.02 \text{ nm}; b_{\text{rec}} = 8.11 \text{ nm}$				

Table S21. Experimental and calculated d -spacing for the observed SAXS reflections of the $Col_{\text{rec}}/c2mm$ phase of compound **F9** at $T = 60$ °C. All intensity values are Lorentz and multiplicity corrected.

(hkl)	$d_{\text{obs.}}$ –spacing (nm)	$d_{\text{cal.}}$ –spacing (nm)	$intensity$	$phase$
(11)	4.01	4.01	100	π
(02)	3.46	3.46	2.0	0
(20)	2.46	2.46	2.2	0
(22)	2.00	2.00	18.8	0
(31)	1.59	1.60	1.4	0
(24)	1.42	1.42	1.0	0
$a_{\text{rec}} = 4.92 \text{ nm}; b_{\text{rec}} = 6.92 \text{ nm}$				

Table S22. Experimental and calculated d -spacing for the observed SAXS reflections of the $\text{Col}_{\text{squ}}/p4mm$ phase of compound **F9** at $T = 135$ °C. All intensity values are Lorentz and multiplicity corrected.

(hk)	$d_{\text{obs.}}$ –spacing (nm)	$d_{\text{cal.}}$ –spacing (nm)	<i>intensity</i>	<i>phase</i>
(10)	4.14	4.14	100	π
(20)	2.07	2.07	15.2	0
$a_{\text{squ}} = 4.14$ nm				

Table S23. Experimental and calculated d -spacing for the observed SAXS reflections of the $\text{Col}_{\text{squ}}/p4mm$ phase of compound **F10** at $T = 70$ °C. All intensity values are Lorentz and multiplicity corrected.

(hkl)	$d_{\text{obs.}}$ –spacing (nm)	$d_{\text{cal.}}$ –spacing (nm)	<i>intensity</i>	<i>phase</i>
(10)	4.14	4.14	100	π
(20)	2.07	2.07	16.1	0
(30)	1.38	1.38	1.2	π
(31)	1.30	1.31	2.5	0
$a_{\text{squ}} = 4.14$ nm				

Table S24. Experimental and calculated d -spacing for the observed SAXS reflections of the $\text{Col}_{\text{rec}}/c2mm$ phase of compound **F11** at $T = 60$ °C. All intensity values are Lorentz and multiplicity corrected.

(hkl)	$d_{\text{obs.}}$ –spacing (nm)	$d_{\text{cal.}}$ –spacing (nm)	<i>intensity</i>	<i>phase</i>
(11)	4.13	4.12	100	π
(02)	3.32	3.32	1.1	0
(20)	2.63	2.63	0.2	-
(22)	2.06	2.06	16.7	0
(31)	1.69	1.69	0.5	-
(24)	1.40	1.40	1.3	π
(33)	1.37	1.37	1.2	π
(15)	1.28	1.29	0.4	-
(42)	1.22	1.22	1.9	0
$a_{\text{rec}} = 5.25$ nm; $b_{\text{rec}} = 6.64$ nm				

Table S25. Experimental and calculated d -spacing for the observed SAXS reflections of the $\text{Col}_{\text{squ}}/p4mm$ phase of compound **F11** at $T = 120$ °C. All intensity values are Lorentz and multiplicity corrected.

(hkl)	$d_{\text{obs.}}$ -spacing (nm)	$d_{\text{cal.}}$ -spacing (nm)	<i>intensity</i>	<i>phase</i>
(10)	4.26	4.26	100	π
(20)	2.13	2.13	17.7	0
(30)	1.42	1.42	0.9	π
(31)	1.34	1.35	1.9	0
$a_{\text{squ}} = 4.26$ nm				

Table S26. Experimental and calculated d -spacing for the observed SAXS reflections of the $\text{Col}_{\text{squ}}/p4mm$ phase of compound **F12** at $T = 110$ °C. All intensity values are Lorentz and multiplicity corrected.

(hkl)	$d_{\text{obs.}}$ -spacing (nm)	$d_{\text{cal.}}$ -spacing (nm)	<i>intensity</i>	<i>phase</i>
(10)	4.23	4.23	100	π
(20)	2.12	2.12	18.7	0
(30)	1.41	1.41	1.7	π
(31)	1.33	1.34	6.7	0
$a_{\text{squ}} = 4.23$ nm				

2.2.4. Electron density maps

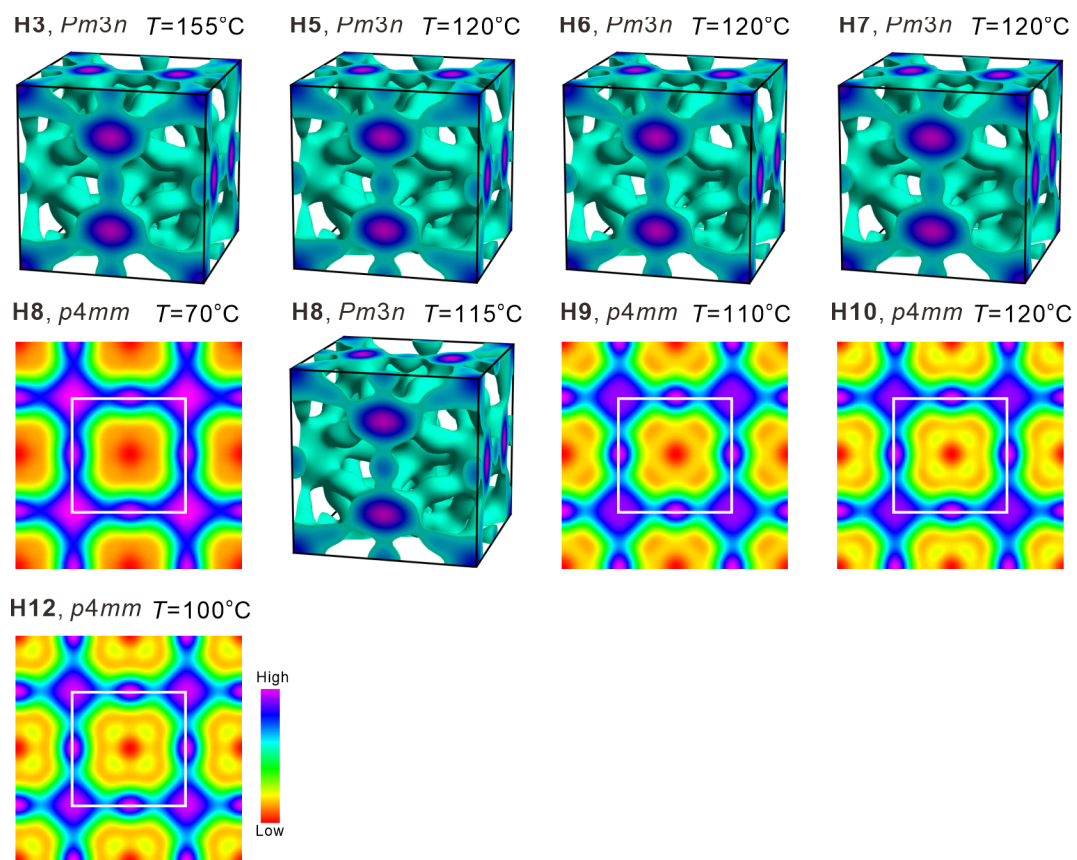


Figure S11. ED map of H_n at indicated temperatures.

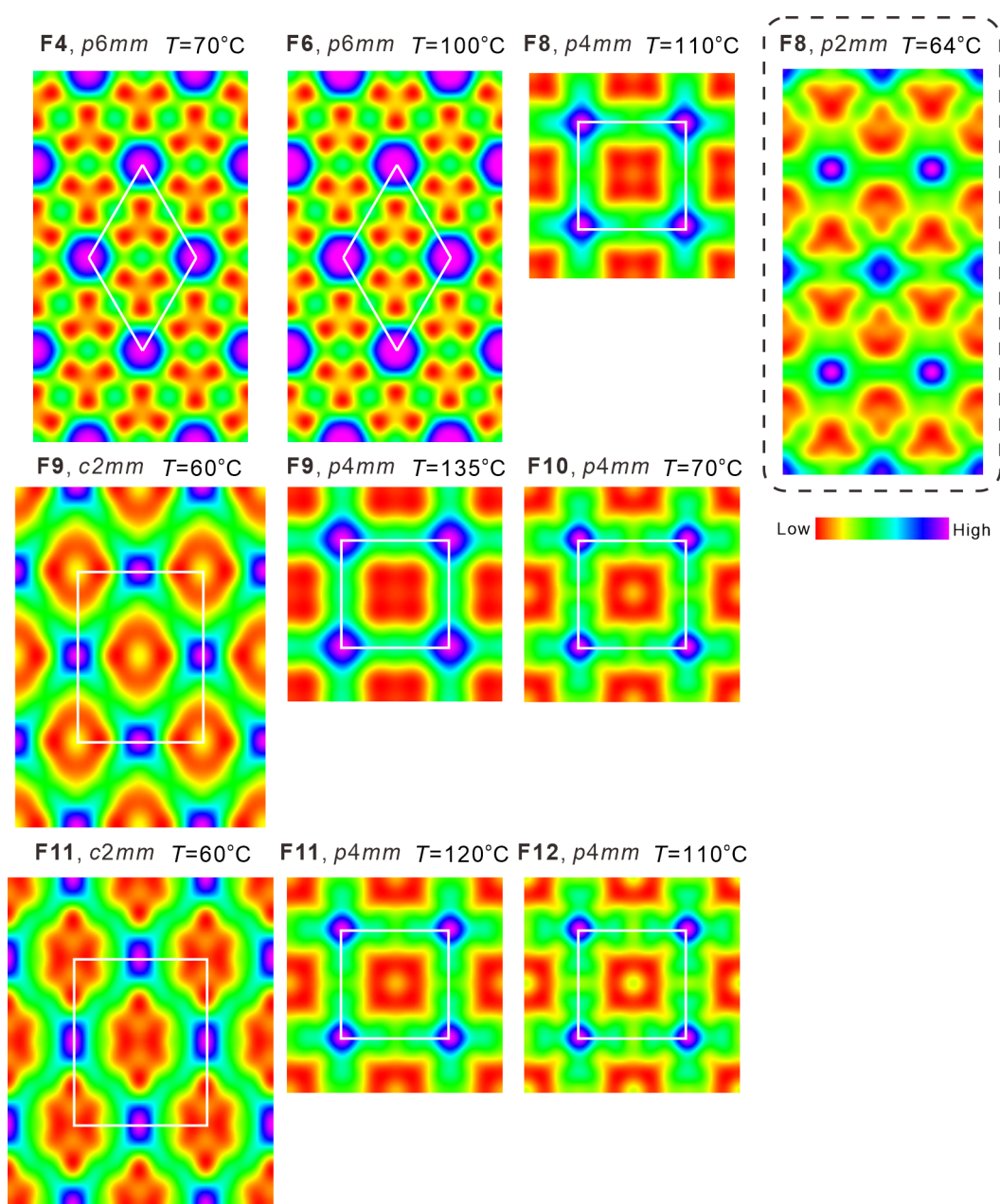


Figure S12. ED map of F_n at indicated temperatures. The low temperature phase of **F8**, obtained after indexation to plane group $p2mm$ (same as Table S20) is shown in dashed square. The stronger distortion of the triangles in the alternative $p2mg$ lattice supports the POM observation of decreasing birefringence in the low temperature LC phase (see Fig. S5). Therefore, the alternative indexation to $p2mg$ is preferred.

2.2.5. Structural data

Table S27. Structural data for Col_{hex}/*p6mm* phase of compounds **Hn** and **Fn**.^a

Comp.	<i>T</i> /°C	<i>a</i> _{hex} /nm	<i>V</i> _{mol;cr.} /nm ³	<i>V</i> _{cell} /nm ³	<i>n</i> _{cell;cr}	<i>n</i> _{cell;liq}	<i>n</i> _{cell;LC}	<i>n</i> _{wall}	<i>L</i> _{wall} /nm
H3	100	4.39	2.06	7.51	3.58	2.81	3.19	1.1	4.4
F3	120	4.38	2.10	7.48	3.63	2.85	3.24	1.1	4.4
F4	70	4.29	2.15	7.17	3.34	2.62	2.98	1.0	4.3
F5	140	4.25	2.20	7.04	3.20	2.51	2.86	1.0	4.3
F6	100	4.43	2.25	7.64	3.40	2.67	3.04	1.0	4.4

^a $V_{\text{cell}} = \frac{\sqrt{3}}{2} a_{\text{hex}}^2 h$ where *h* represents the height of the unit cell and is assumed to be 0.45 nm. *V*_{mol} = volume of the molecule as determined by the crystal volume increments.^{S1} *n*_{cell,cr} = number of molecules per unit cell in the crystalline state, calculated according to $n_{\text{cell,cr}} = V_{\text{cell}}/V_{\text{mol}}$ (average packing coefficient in the crystal is *k* = 0.7). *n*_{cell,liq} = the number of molecules in the unit cell of an isotropic liquid with an average packing coefficient *k* = 0.55, calculated according to $n_{\text{cell,liq}} = 0.55/0.7$. *n*_{cell,LC} = number of molecules in the unit cell in the LC state as estimated from the average of *n*_{cell,cr} and *n*_{cell,liq}.^{S2} *n*_{wall} = the number of molecules in the cross-section of the honeycomb walls, calculated as $n_{\text{wall}} = \frac{n_{\text{cell,LC}}}{3}$.

Table S28. Structural data for the Cub/*Pm* $\bar{3}$ *n* phases of compounds **Hn**.^a

Comp.	<i>T</i> /°C	<i>a</i> _{cub} /nm	<i>V</i> _{mol;cr.} /nm ³	<i>V</i> _{cell} /nm ³	<i>n</i> _{cell;cr}	<i>n</i> _{cell;liq}	<i>n</i> _{cell;LC}	<i>n</i> _{bundle}
H3	120	8.62	2.06	641	312	245	278	5.2
H4	120	8.88	2.10	700	335	263	299	5.5
H5	120	9.07	2.15	746	347	273	311	5.8
H6	120	9.20	2.20	779	353	277	315	5.8
H7	120	9.12	2.25	759	337	265	301	5.6
H8	115	9.14	2.30	764	331	260	296	5.5

^a *V*_{cell} = volume of the unit cell, calculated according to $V_{\text{cell}} = a_{\text{cub}}^3$. *n*_{bundle} = number of molecules per bundle in the cubic organization as $n_{\text{bundle}} = n_{\text{cell,LC}}/54$. For other explanations see Table S27.

Table S29. Structural data for $\text{Col}_{\text{squ}}/p4mm$ and $\text{Col}_{\text{rec}}/p2mm$ and $p2gg$ phase of compounds **Hn** and **Fn**.^a

Comp.	T/°C (Phase)	a, b/nm	$V_{\text{mol};\text{cr.}}$ /nm ³	V_{cell} /nm ³	$n_{\text{cell};\text{cr}}$	$n_{\text{cell};\text{liq}}$	$n_{\text{cell};\text{LC}}$	n_{wall}	L_{wall} /nm
H8	70 ($\text{Col}_{\text{squ}}/p4mm$)	4.12	2.30	7.64	3.32	2.61	3.0	1.5	4.1
H9	110 ($\text{Col}_{\text{squ}}/p4mm$)	4.16	2.35	7.79	3.32	2.60	2.9	1.5	4.2
H10	120 ($\text{Col}_{\text{squ}}/p4mm$)	4.18	2.40	7.86	3.28	2.57	2.9	1.5	4.2
H11	100 ($\text{Col}_{\text{squ}}/p4mm$)	4.25	2.45	8.13	3.32	2.61	3.0	1.5	4.3
H12	100 ($\text{Col}_{\text{squ}}/p4mm$)	4.32	2.50	8.40	3.36	2.64	3.0	1.5	4.3
F8	110 ($\text{Col}_{\text{squ}}/p4mm$)	$a_{\text{squ}} = 4.07$	2.35	7.45	3.17	2.49	2.8	1.4	4.1
	74 ($\text{Col}_{\text{rec}}/c2mm$)	$a_{\text{rec}} = 4.95$ $b_{\text{rec}} = 6.96$		14.90	6.34	4.98	5.7	1.4	4.3
	64 ($\text{Col}_{\text{rec}}/p2mg$)	$a_{\text{rec}} = 4.02$ $b_{\text{rec}} = 8.11$		14.67	6.24	4.91	5.6	0.9	4.5/4.0
F9	135 ($\text{Col}_{\text{squ}}/p4mm$)	$a_{\text{squ}} = 4.14$	2.40	7.71	3.22	2.52	2.9	1.5	4.1
	60 ($\text{Col}_{\text{rec}}/c2mm$)	$a_{\text{rec}} = 4.92$ $b_{\text{rec}} = 6.92$		15.32	6.46	5.08	5.80	1.4	4.2
F10	70 ($\text{Col}_{\text{squ}}/p4mm$)	4.14	2.45	7.71	3.15	2.47	2.8	1.4	4.1
F11	120 ($\text{Col}_{\text{squ}}/p4mm$)	$a_{\text{squ}} = 4.26$	2.50	8.17	3.27	2.57	2.9	1.5	4.3
	60 ($\text{Col}_{\text{rec}}/p2gg$)	$a_{\text{rec}} = 5.25$ $b_{\text{rec}} = 6.64$		15.69	6.27	4.93	5.6	1.4	4.2
F12	110 ($\text{Col}_{\text{squ}}/p4mm$)	4.23	2.55	8.05	3.15	2.49	2.8	1.4	4.2

^a V_{cell} was determined according to $V_{\text{cell}} = a_{\text{squ}}^2 \cdot h$ for the square and $a_{\text{rec}} \cdot b_{\text{rec}} \cdot h$ for the rectangular, where h represents the height of the unit cell which was assumed to be 0.45 nm. n_{wall} = the number of molecules in the cross-section of the honeycomb walls, calculated as $n_{\text{wall}} = \frac{n_{\text{cell},\text{LC}}}{2}$ for $p4mm$ cells, $n_{\text{wall}} = \frac{n_{\text{cell},\text{LC}}}{4}$ for $c2mm$ cells and $n_{\text{wall}} = \frac{n_{\text{cell},\text{LC}}}{6}$ for $p2mg$ cells, L_{wall} is the side length of the polygonal cells. For other explanations see Table S27.

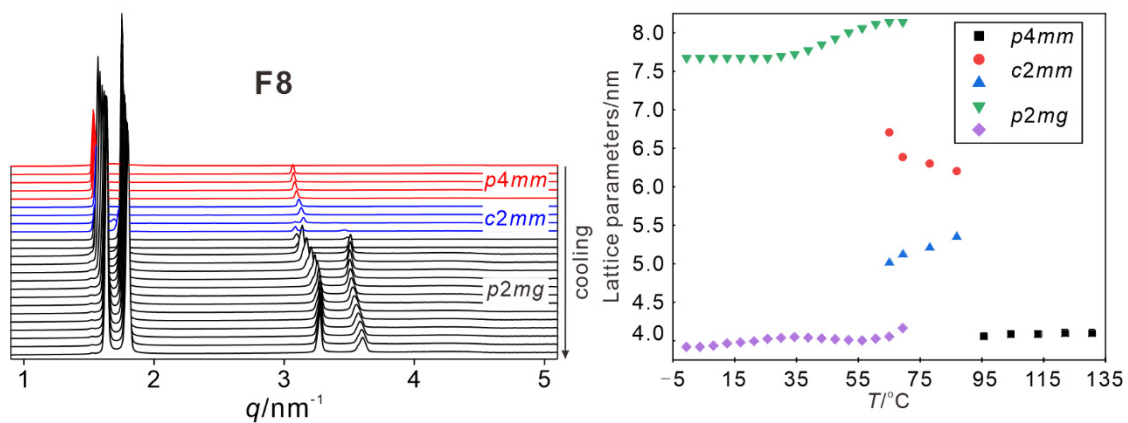


Figure S13. Lattice parameter-temperature dependence of compound **F8**; in the $p2mg$ phase the lattice parameters remain almost constant.

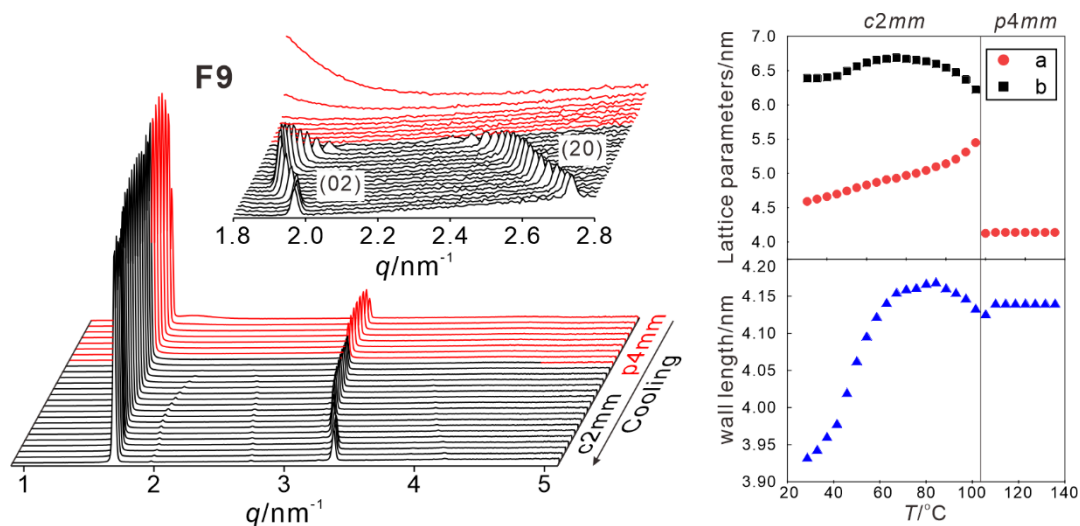


Figure S14. Lattice parameter-temperature dependence of compound **F9**. In the $c2mm$ phase the aromatic wall length decreases almost continuously upon cooling below ~ 60 – 70 °C.

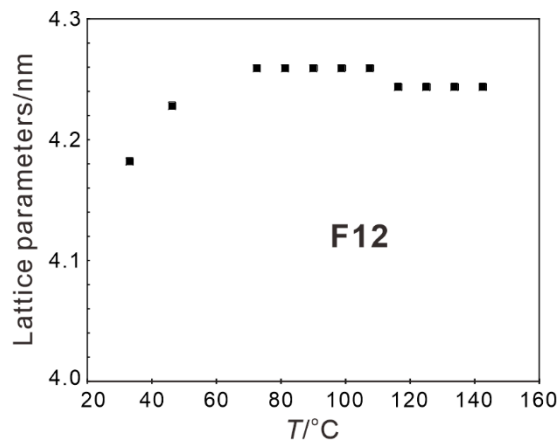


Figure S15. Lattice parameter-temperature dependence of compound **F12**. Only a marginal decrease is observed below 60 – 70 °C compared with **F9**.

3. Additional discussions

3.1 Discussion of intermolecular forces and development of the self-assembled structure at the molecular level

At first place it is noted that all discussed self-assembled LC phase structures represent highly dynamic thermodynamic equilibrium structures, i.e. all discussed structural models represent idealized time-averaged structures with long-range periodicity (sharp SAXS), but without fixed positions of the individual molecules (diffuse WAXS). The self-assembly of the bolapolyphiles under discussion is affected by at least 3 types of intermolecular interactions, as well as by nano-segregation effects leading to compartmentalization, and by the degree of curvature of the interfaces between these compartments.

Intermolecular interactions:

(1) Cooperative hydrogen bonding between the glycerol units (sigma-bond cooperativity)^{S3} provides the main source of cohesive intermolecular forces, leading to structure formation of the compounds under consideration in the fluid LC phases. This leads to the development of large dynamic H-bonding networks, increasing in stability with the number of OH groups (i.e. number of molecules) involved in these networks, meaning that quasi infinite columns in the honeycombs are preferred over spheres with limited size. It is noted, that due to the almost free rotations around the C-C bonds in the LC state there is a decoupling of the OH groups in the glycerol units and of the glycerol units from the OPE cores, and no long-range directionality is provided by these H-bondings.

2) The London dispersion forces provide the main attraction between the carbosilane based aliphatic side chains.

3) The π -stacking interactions between the aromatic cores contribute to the packing of the OPE core-units either in the ribbons of parallel arranged OPEs in the honeycomb wall or in the rod-bundles forming the networks ($Pm\bar{3}n$). While an edge-to-face stacking dominates for the electron rich π -systems of compounds **Hn** (Fig. S17a), there is a contribution of face-to-face

π -stacking for compounds **F_n** (additional scattering around 0.36-0.38 nm) including electron deficit perfluorinated phenylenes (Fig, S17b-e).

Nano-segregation and interface curvature:

The combination of three very distinct molecular segments in compounds **H_n** and **F_n** leads to multiple incompatibilities (polyphilic self-assembly), giving rise to nano-scale segregation of the distinct segments into separate nano-scale domains. One kind of incompatibility is based on the different types of intermolecular interactions, the “hard” electrostatic hydrogen bonding interactions between the glycerol groups, and the “soft” dispersion forces based on polarization of the electron clouds of the aliphatic and aromatic units. According to the HSAB (hard and soft acids and bases) concept, the like interactions (soft-soft and hard-hard) are energetically preferred over unlike (soft-hard) interactions, thus causing a “chemical incompatibility” and segregation into distinct separate nano-domains.

A second segregation force has a significant entropic component, which is the separation of rigid from flexible units. In our case the rigid-rod-like OPE cores from the flexible aliphatic side chains and, to some extent, also from the flexible polar glycerols. However, some π -HO hydrogen bonding interactions might partially reduce this incompatibility between OPE core and glycerols and might be important for the formation of the relatively large spheroids in the $Pm\bar{3}n$ phase (see below).

Finally, nematic ordering, i.e. the parallel alignment of rod-like rigid segments needs to be considered, which mainly occurs between the OPE cores, but also between *all-anti* segments of linear alkyl chain segments, especially at lower temperature. This is responsible for the parallel alignment of the OPE cores in the ribbons forming the honeycomb walls and the rod-bundles forming the $Pm\bar{3}n$ network phase.

As a result of nano-scale segregation, interfaces are formed between the incompatible nano-domains, the so-called inter-materials dividing surfaces (IMDS). As the volume of the different incompatible units is different, different volume is enclosed by the IMDSs and a curvature arises. It can be zero in layers or non-zero for networks, columns, and spheres and increasing in this sequence. The sign of the curvature can be positive if the nano-domains with the lower cohesive energy density are smaller and enclosed by the higher cohesive energy density domain (normal phases), and negative if it is the other way around (reversed phases).

For the honeycombs the curvature is negative for the major polar-apolar incompatibility as the hydrogen bonded glycerol columns or spheres with highest cohesive energy density are enclosed in the “less polar environment” involving the side chains and the OPE cores. The absolute amount of curvature of the glycerol domains increases from honeycombs (columns) to $Pm\bar{3}n$ (spheres), i.e. the curvature becomes more negative.

However, due to the polyphilic molecular structure, the “less polar environment” can be further subdivided into the semipolar and rigid aromatic and the non-polar and flexible aliphatic subdomains. Here, the IMDS curvature is additionally affected and restricted by the parallel alignment of the rods, and the amount of curvature increases from honeycombs (ribbons of parallel arranged OPE cores) to $Pm\bar{3}n$ (columns of rod-bundles). The overall phase sequence on increasing V_R would therefore be $p6mm - p4mm - Pm\bar{3}n$. Because the effective chain volume increases with temperature (thermal chain expansion) $Pm\bar{3}n$ is the high temperature phase either above $p4mm$ (triangular) or $p6mm$ (square) honeycombs.

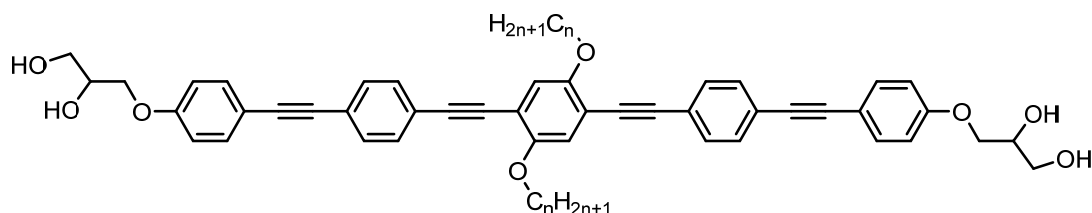
These fundamental principles determine the self-assembly of the bolapolyphiles **Hn** and **Fn**. These basic concepts of polyphilic self-assembly in low molecular mass soft matter systems were summarized in several reviews, collated in ref S4 and will be applied in Section 3.2 more specifically to the case of compounds **Hn** in comparison with related bolapolyphiles having less branched hydrocarbon side-chains, shown in Scheme. S1b.

3.2 Comparison with the self-assembly of related bolapolyphiles with non-silylated side chains

As noted above, the relative volume of the incompatible units determines the structures developing by LC self-assembly. However, also the mode of side-chain branching has a large impact as shown in Scheme S1 for compounds **A26**, **B26** and **C26** with identical side-chain volume. The total chain volume required for $Pm\bar{3}n$ phase formation (as evaluated by the number of CH_2/CH_3 units + silicons in both side-chains = N_R) is $N_R = 52-64$ for the branched compounds **C** with very different length of the branches ($n \neq m$, ref. S16). It is close to N_R required for the transition from triangular ($N_R < 60$) to square honeycombs ($N_R > 76$) in the case of symmetrically branched compounds **B** ($n = m$, ref. S5) which do not form $Pm\bar{3}n$. In contrast,

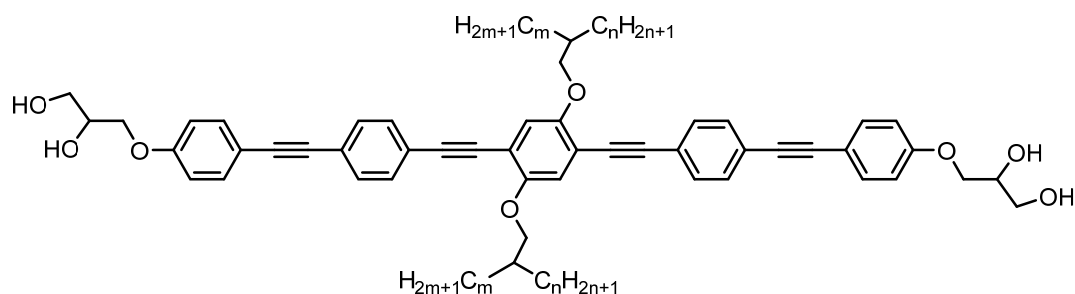
compound **A26** with linear side-chains forms rhombic cells with a volume intermediate between triangular and square cells. In the case of compounds **Hn** the $Pm\bar{3}n$ phase is formed for $N_R = 50-60$ in almost the same range as observed for the compounds **C**.

(a)



A26: $n = 26$: Cr 115 $Col_{rec}/c2mm$ 112 Iso ($^{\circ}C$)

(b)



B26: $m = n = 12$: Cr 97 $Col_{hex}/p6mm$ 175 Iso ($^{\circ}C$)

C26: $m = 4, n = 20$: Cr 76 $Col_{hex}/p6mm$ 121 Cub/ $Pm\bar{3}n$ 131 Iso ($^{\circ}C$)

Scheme S1. Structures and LC phases of representative examples of OPE-based X-shaped bolapolyphiles (a) with linear or (b) branched hydrocarbon side-chains having the same total side-chain volume ($N_R = 52$); $Col_{rec}/c2mm$ is rhombic honeycomb and $Col_{hex}/p6mm$ is a regular hexagonal honeycomb.^{S5,S6,S7,S8}

This means that besides the total chain volume also the effective chain length i.e., the distance between core and the most distant CH_3 group is important for filling the space at larger distances to the core units. From the investigations with compounds **C** in ref. S16 it can be deduced that the chain length (L_R) required for $Pm\bar{3}n$ formation is >20 C-equivalent units for bolapolyphiles based on the OPE core unit. However, for compounds **Hn** due to the higher degree of chain branching, L_R it is only 11-16 (C+Si), i. e. it is outside the range of $Pm\bar{3}n$ formation, though the chain volume would fulfill the conditions for $Pm\bar{3}n$ formation.

Another important difference to the previously reported branched compounds is that the branching point is for compounds **Hn** at a larger distance to the rod-like core (spacer $n = 3-12C$ compared to only one CH_2 in **B** and **C**). This leads to a reduced aliphatic crowding close to the cores (Fig. S16) and allows more rods to be packed side-by-side in the rod-bundles of the $Pm\bar{3}n$ network phase. Indeed, the number of molecules in the cross-section of the rod-bundles changes from 4-5 in the $Pm\bar{3}n$ phases of compounds **B** (ref. S16) to 5-6 for compounds **Hn** (Table S28). Because expansion of the bundles simultaneously increases the number of glycerols involved in the junctions, also the glycerol spheroids grow and contribute more to the space filling. This means that a shortfall in space filling by the limited length of the highly branched lateral chains of **Hn** is compensated by expansion of the rod-bundle and sphere diameter, and this allows even larger lattice parameters for the $Pm\bar{3}n$ phases of compounds **Hn** ($a_{\text{cub}} = 8.6-9.2$ nm, larger glycerol spheres) with short L_R compared to the weakly branched compounds **C** with larger L_R ($a_{\text{cub}} = 8.6-8.7$ nm, smaller glycerol spheres). So, overall, there are complex coupled molecular structural variables with feed-back loops forming regulatory networks which determine the observed phase structure.

Besides, there is a competition with alternative structures which in this case are the honeycomb networks, having the advantage of forming larger cooperative hydrogen bonding networks along the columns than possible in the restricted spaces of spheres of $Pm\bar{3}n$. Also, the formation of the honeycombs depends on L_{core} , V_R , L_R , and n , but the presence of only 2D instead of 3D boundaries provides different conditions. Here, the tight vertices in triangular and rhombic cells might provide additional difficulty for accommodation of the bulky carbosilane end groups of compounds **Hn** and provide a destabilizing effect on honeycombs involving such prismatic cells. Though the amount of (negative) curvature of the inter-materials dividing surfaces (IMDS) between polar domains and non-polar regions should be very similar in triangular and square honeycombs and should change only slightly at the transition between them, in fact it first increases at the transition from $p6mm$ to $Pm\bar{3}n$ and then decreases at the next transition from $Pm\bar{3}n$ to $p4mm$. This leads to our hypothesis, saying that $Pm\bar{3}n$ formation "...is not preliminary caused by the changing interface curvature (IMDS, determined mainly by V_R), but by the destabilization of the competing honeycombs due to a steric and geometric frustration arising at the triangle-square transition.

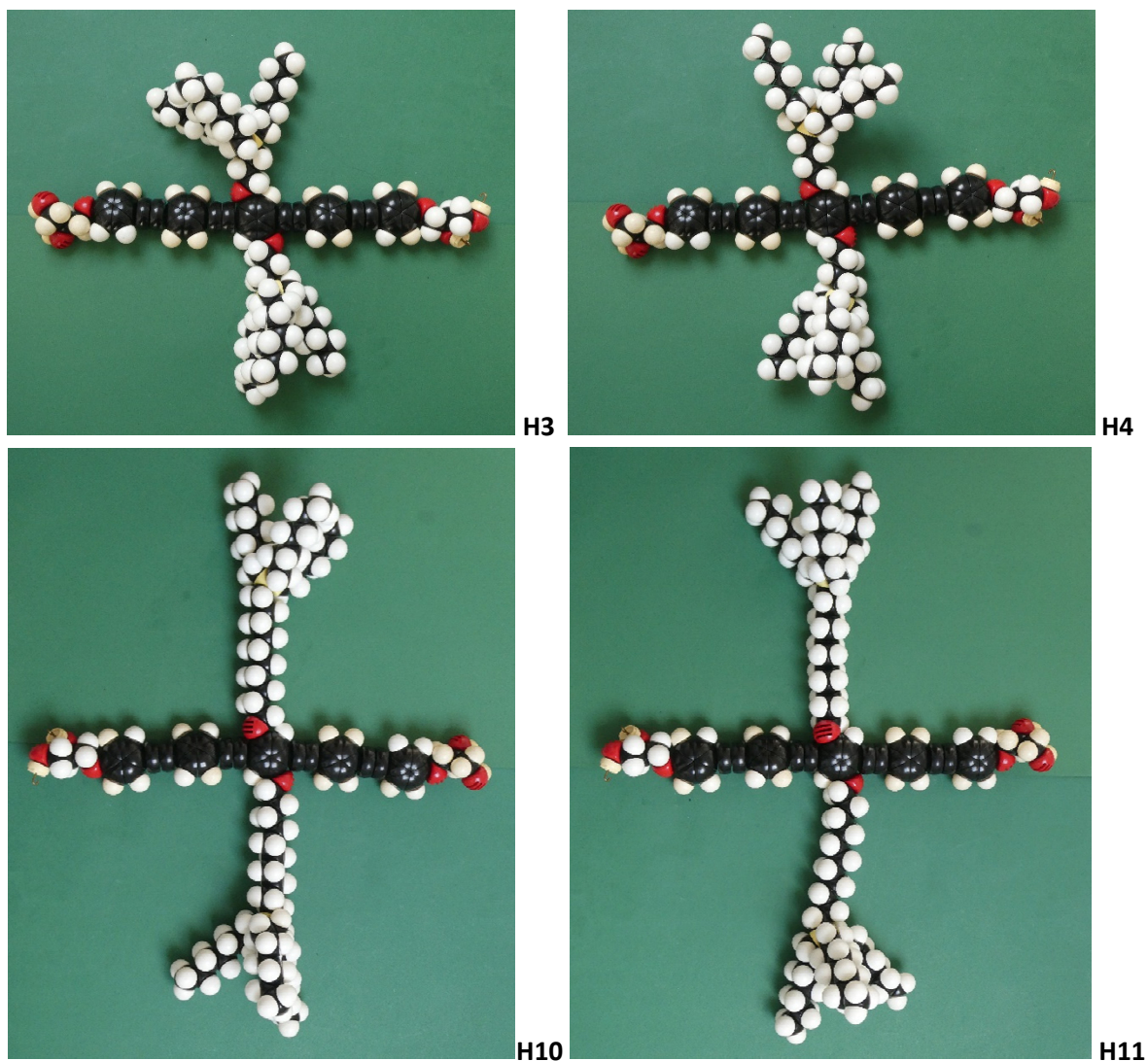


Figure S16. CPK models of selected compounds H_n with odd and even numbered n , there is a small difference in the preferred side-chain conformation (**H3/H4**), which decreases with elongation of n (**H10/H11**). There is a larger effect of these differences for the fluorinated compounds F_n with fluorinated outer benzene rings, due to the presence of π -stacking interactions, magnifying these small effects.

The effects of core fluorination are explained in the main text and their effect on OPE packing is illustrated in Fig. S17.

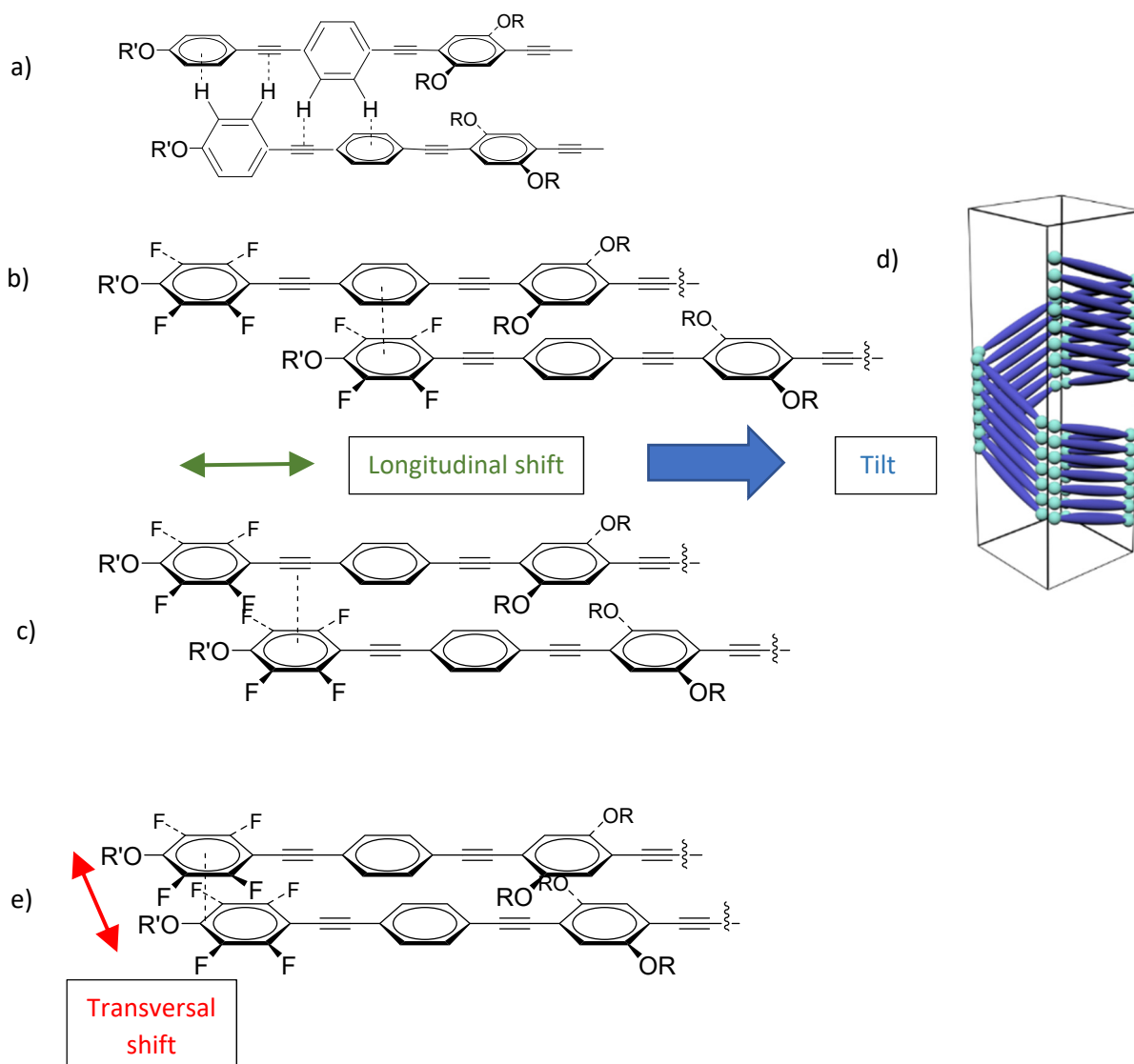
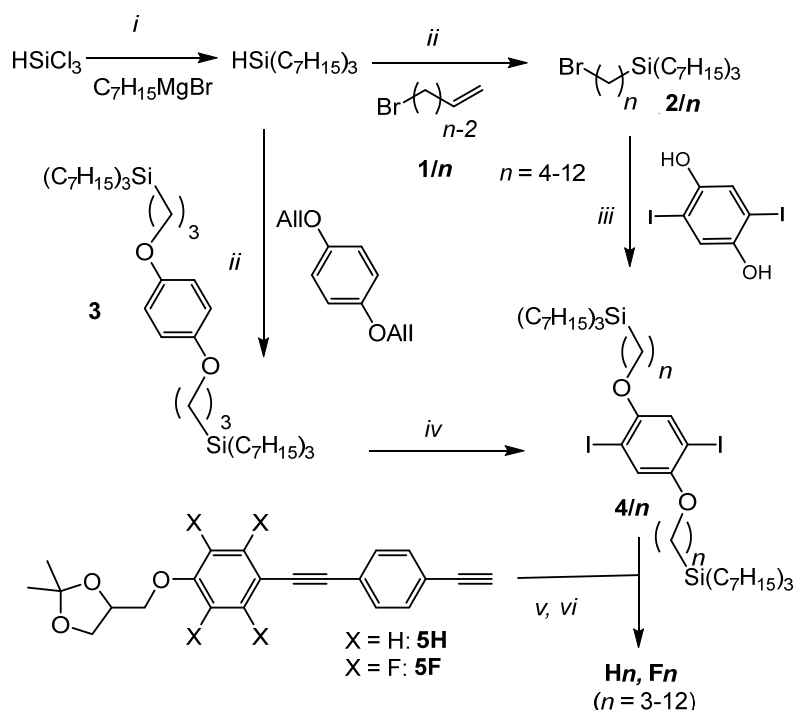


Figure S17. Different stacking modes for the packing of the OPE cores in the honeycomb walls^{S8} a) edge-to-face stacking as dominating for compounds **Hn**, b-d) possible stacking modes of compounds **Fn** with decreasing shift between adjacent OPE cores. b) Stacking of hydrogenated and fluorinated benzenes; c) staking of the fluorinated benzenes and acetylene, leading to d) a tilted organization of the rods in the cylinder walls, and e) slightly staggered face-to-face organization between two electron deficit fluorinated benzenes; the shift can take place longitudinal (green, parallel to the OPE long axis) leading to a tilt of the molecules in the walls or transversal (red), i.e. perpendicular to the OPE long axis, avoiding any tilt and leading to the organization of the OPEs as shown in Fig. 5b, c; R = side-chains, R' = glycerol groups.

4. Synthesis and analytical data

4.1. General

As displayed in Scheme S2 the synthesis of all compounds with $n > 3$ was conducted by hydrosilylation^{S9} of ω -bromo- n -alkenes **1/n** with tri- n -heptylsilane^{S10} to yield the branched alkyl bromides **2/n** which were used for the alkylation of 2,6-diiodohydroquinone, yielding the diiodobenzenes **4/n**. In the final steps compounds **4/n** were coupled in Sonogashira reactions^{S11} with two equivalents of the tolane based building blocks **5H** or **5F**,^{S5,S12} followed by deprotection of the glycerol groups yielding the target compounds **Hn** and **Fn**, respectively. For the synthesis of the homologue with $n = 3$ the diiodobenzene **4/3** was prepared in a different way from 1,4-diallyloxybenzene by hydrosilylation with tri- n -heptylsilane, providing the hydroquinone diether **3** which was selectively iodinated in the 2,6-positions with the hypervalent iodination reagent $\text{PhI}(\text{OCOCF}_3)_2/\text{I}_2$.^{S13}



Scheme S2. Synthesis of compounds **Hn** and **Fn**. *Reagents and conditions:* i: THF, LiCl, 20 °C, 24 h; ii: CH_2Cl_2 , Karstedts cat., 20 °C, 1d,^{S9} iii: K_2CO_3 , Bu_4NI , DMF, 80 °C, 3d;^{S14} iv: $\text{PhI}(\text{OCOCF}_3)_2$, I_2 , DCM, 60 °C, 1d;^{S15} v: $\text{Pd}(\text{PPh}_3)_4$, CuI, Et_3N , 80 °C, 1d;^{S11} vi: PPTS, MeOH / THF, 50 °C.^{S16}

2,6-Diiodohydroquinone, hydroquinone, 1-bromoheptane, 3-bromo-1-propene, 5-bromo-1-pentene, 9-bromo-1-nonene, 10-bromo-1-decene, trichlorosilane and dichloromethylsilane were obtained from Sigma-Aldrich; 4-bromo-1-butene, 6-bromo-1-hexene, 7-bromo-1-heptene and 8-bromo-1-octene were received from ABCR; 11-bromo-1-undecene was provided by SYNTHON Chemicals GmbH & Co. KG and 12-bromo-1-dodecene was available from BLDpharm. All compounds were used as received. Triethylamine was distilled from CaH_2 and stored over the molecular sieve. The synthesis of the isopropylidene functionalized bistolane derivatives **5H** and **5F**^{S12} was reported previously. All compounds were synthesized from racemic *rac*-1,2-*O*-isopropylidene glycerol and therefore **Hn** and **Fn** represent racemic mixtures of diastereomers.

Column chromatography was performed with silica gel 60 (0.063-0.2, Merck), and flash-chromatography with silica gel 60 (0.040-0.063, Merck). The purity of all compounds was checked by thin-layer chromatography (TLC, silica gel 60 F254, Merck).

^1H -, ^{13}C -NMR spectra (Varian Unity 500 and Varian Unity 400 spectrometers) were recorded in CDCl_3 or pyridine- d_5 solutions, with tetramethylsilane as the internal standard). All measurements were operated at 27 °C.

Elemental analyses were performed using a Leco CHNS-932 elemental analyzer. Mass spectra were recorded with a Bruker HR-ESI-TOF. The measurements were performed in THF (1 mg/mL) with 0.1 mg/mL LiCl.

4.2. Synthesis of Intermediates

4.2.1. Synthesis of the branched alkyl bromides 2/n

Triheptylsilane^{S10}: Heptylmagnesium bromide solution in THF was cooled with stirring to 0 °C. LiCl (1.0 g, 23.6 mmol) was added followed by trichlorosilane (3.5 g, 2.6 ml, 26.0 mmol) by adding with a syringe. The reaction is heated up to room temperature and stirred for 24h. Afterward, the reaction is quenched with water (1 ml / 1 ml THF) and the aqueous layers were extracted with Et_2O (3x50 ml) The combined organic layers were washed with water and brine. After drying over anhydrous Na_2SO_4 , filtration, and evaporation of the solvent (850 mbar, 60°C), the crude product was purified by column chromatography (eluent: *n*-hexane), colorless liquid, $\text{C}_{21}\text{H}_{46}\text{Si}$ M = 326.68 g/mol, yield: 7.35 g (87 %), R_f = 0.88, $^1\text{H-NMR}$ (CDCl_3 , 400 MHz): δ / ppm = 3.73 – 3.61 (1H, m, -SiH), 1.41 – 1.20 (30H, m, - CH_2), 0.89 (9H, t, $^3J_{\text{H,H}}$ = 6.8 Hz, - CH_3), 0.62 – 0.53 (6H, m, - SiCH_2). $^{29}\text{Si-NMR}$ (CDCl_3 , 79 MHz): δ / ppm = -6.38 (Si).

(ω -Bromoalkyl)triheptylsilanes 2/n^{S9}: Triheptylsilane (1 equ.), the appropriate ω -bromoalk-1-ene (1.5 equ), and Karstedt-cat. (3 mol%) were added to anhydrous CH_2Cl_2 (20 mL/mmol) and stirred at RT for 3 days. Afterward, the solvent was evaporated and the crude product was purified by column chromatography.

(4-Bromobutyl)triheptylsilane 2/4: Synthesized from triheptylsilane (3.0 g, 9.2 mmol), 4-Bromobut-1-ene (1.8 g, 1.4 ml, 13.8 mmol), Karstedt-Cat (0.11 g, 0.12 ml, 0.28 mmol) in anhydrous CH_2Cl_2 (20 ml); purification by column chromatography (eluent: *n*-hexane), colorless liquid, $\text{C}_{25}\text{H}_{53}\text{SiBr}$ M = 461.69 g/mol, yield: 1.5 g (50 %), $^1\text{H-NMR}$ (CDCl_3 , 400 MHz): δ / ppm = 3.42 (2H, t, $^3J_{\text{H,H}}$ = 6.8 Hz, BrCH_2 -), 1.86 (2H, p, $^3J_{\text{H,H}}$ = 7.0 Hz, BrCH_2CH_2 -), 1.47 – 1.38 (2H, m, $\text{BrCH}_2\text{CH}_2\text{CH}_2$ -), 1.36 – 1.20 (30H, m, - CH_2 -), 0.89 (9H, t, $^3J_{\text{H,H}}$ = 6.8 Hz, - CH_3), 0.63 – 0.44 (8H, m, - SiCH_2 -). $^{29}\text{Si-NMR}$ (CDCl_3 , 79 MHz): δ / ppm = 3.10 (Si).

(5-Bromopentyl)triheptylsilane 2/5: Synthesized from triheptylsilane (2.3 g; 7.0 mmol), 5-Bromopent-1-ene (1.57 g, 1.3 ml, 10.6 mmol), Karstedt-Cat (80.1 mg, 0.09 ml, 0.21 mmol) in anhydrous CH_2Cl_2 (20 ml); purification by column chromatography (eluent: *n*-hexane), colorless liquid, $\text{C}_{26}\text{H}_{55}\text{SiBr}$ M = 475.72 g/mol, yield: 2.01 g (60 %), $^1\text{H-NMR}$ (CDCl_3 , 500 MHz): δ / ppm = 3.40 (2H, t, $^3J_{\text{H,H}}$ = 6.9 Hz, BrCH_2 -), 1.87 (2H, p, $^3J_{\text{H,H}}$ = 7.0 Hz, BrCH_2CH_2 -), 1.47 – 1.40 (2H, m, $\text{BrCH}_2\text{CH}_2\text{CH}_2$ -), 1.41 – 1.20 (32H, m, - CH_2 -), 0.88 (9H, t, $^3J_{\text{H,H}}$ = 7.3 Hz, - CH_3), 0.63 – 0.45 (8H, m, - SiCH_2 -). $^{29}\text{Si-NMR}$ (CDCl_3 , 79 MHz): δ / ppm = 2.94 (Si).

(6-Bromohexyl)triheptylsilane 2/6: Synthesized from triheptylsilane (1.3 g, 3.8 mmol), 6-Bromohex-1-ene (0.9 g, 0.8 ml, 5.7 mmol), Karstedt-Cat (43.3 mg, 0.05 ml, 0.12 mmol) in anhydrous CH_2Cl_2 (20 ml); purification by column chromatography (eluent: *n*-hexane), colorless liquid, $\text{C}_{27}\text{H}_{57}\text{SiBr}$ $M = 489.94$ g/mol, yield: 0.73 g (39 %), $^1\text{H-NMR}$ (CDCl_3 , 400 MHz): δ / ppm = 3.40 (2H, t, $^3J_{\text{H,H}} = 7.7$ Hz, BrCH_2 -), 1.85 (2H, p, $^3J_{\text{H,H}} = 7.7$ Hz, BrCH_2CH_2 -), 1.48 – 1.38 (2H, m, $\text{BrCH}_2\text{CH}_2\text{CH}_2$ -), 1.37 – 1.20 (34H, m, $-\text{CH}_2$ -), 0.89 (9H, t, $^3J_{\text{H,H}} = 6.8$ Hz, $-\text{CH}_3$), 0.52 – 0.44 (8H, m, $-\text{SiCH}_2$ -). $^{29}\text{Si-NMR}$ (CDCl_3 , 79 MHz): δ / ppm = 2.92 (Si).

(7-Bromoheptyl)triheptylsilane 2/7: Synthesized from triheptylsilane (2.3 g, 7.0 mmol), 7-Bromohept-1-ene (1.9 g, 1.6 ml, 10.6 mmol), Karstedt-Cat (80.1 mg, 0.09 ml, 0.21 mmol) in anhydrous CH_2Cl_2 (20 ml); purification by column chromatography (eluent: *n*-hexane), colorless liquid, $\text{C}_{28}\text{H}_{59}\text{SiBr}$ $M = 503.77$ g/mol, yield: 1.43 g (40.3 %), $^1\text{H-NMR}$ (CDCl_3 , 500 MHz): δ / ppm = 3.41 (2H, t, $^3J_{\text{H,H}} = 6.9$ Hz, BrCH_2 -), 1.86 (2H, p, $^3J_{\text{H,H}} = 7.0$ Hz, BrCH_2CH_2 -), 1.47 – 1.37 (2H, m, $\text{BrCH}_2\text{CH}_2\text{CH}_2$ -), 1.37 – 1.23 (36H, m, $-\text{CH}_2$ -), 0.89 (9H, t, $^3J_{\text{H,H}} = 6.9$ Hz, $-\text{CH}_3$), 0.62 – 0.43 (8H, m, $-\text{SiCH}_2$ -). $^{29}\text{Si-NMR}$ (CDCl_3 , 99 MHz): δ / ppm = 2.92 (Si).

(8-Bromooctyl)triheptylsilane 2/8: Synthesized from triheptylsilane (2.2 g, 6.7 mmol), 8-Bromooct-1-ene (1.9 g, 2.0 ml, 10.1 mmol), Karstedt-Cat (72.6 mg, 0.08 ml, 0.20 mmol) in anhydrous CH_2Cl_2 (20 ml); purification by column chromatography (eluent: *n*-hexane), colorless liquid, $\text{C}_{29}\text{H}_{61}\text{SiBr}$ $M = 517.80$ g/mol, yield: 1.89 g (54 %), $^1\text{H-NMR}$ (CDCl_3 , 400 MHz): δ / ppm = 3.40 (2H, t, $^3J_{\text{H,H}} = 6.9$ Hz, BrCH_2 -), 1.86 (2H, p, $^3J_{\text{H,H}} = 7.0$ Hz, BrCH_2CH_2 -), 1.38 – 1.17 (40H, m, $-\text{CH}_2$ -), 0.88 (9H, t, $^3J_{\text{H,H}} = 6.7$ Hz, $-\text{CH}_3$), 0.64 – 0.41 (8H, m, $-\text{SiCH}_2$ -). $^{29}\text{Si-NMR}$ (CDCl_3 , 79 MHz): δ / ppm = 2.91 (Si).

(9-Bromononyl)triheptylsilane 2/9: Synthesized from triheptylsilane (2.2 g, 6.7 mmol), 9-Bromonon-1-ene (2.1 g, 1.9 ml, 10.1 mmol), Karstedt-Cat (76.7 mg, 0.09 ml, 0.20 mmol) in anhydrous CH_2Cl_2 (20 ml); purification by column chromatography (eluent: *n*-hexane), colorless liquid, $\text{C}_{30}\text{H}_{63}\text{SiBr}$ $M = 531.82$ g/mol, yield: 1.29 g (36 %), $^1\text{H-NMR}$ (CDCl_3 , 400 MHz): δ / ppm = 3.40 (2H, t, $^3J_{\text{H,H}} = 6.9$ Hz, BrCH_2 -), 1.85 (2H, p, $^3J_{\text{H,H}} = 7.0$ Hz, BrCH_2CH_2 -), 1.46 – 1.37 (2H, m, $\text{BrCH}_2\text{CH}_2\text{CH}_2$ -), 1.37 – 1.19 (40H, m, $-\text{CH}_2$ -), 0.88 (9H, t, $^3J_{\text{H,H}} = 6.9$ Hz, $-\text{CH}_3$), 0.64 – 0.41 (8H, m, $-\text{SiCH}_2$ -). $^{29}\text{Si-NMR}$ (CDCl_3 , 79 MHz): δ / ppm = 2.91 (Si).

(10-Bromodecyl)triheptylsilane 2/10: Synthesized from triheptylsilane (2.2 g, 6.7 mmol), 10-Bromodec-1-ene (2.2 g, 2.0 ml, 10.1 mmol), Karstedt-Cat (76.7 mg, 0.09 ml, 0.20 mmol) in anhydrous CH_2Cl_2 (20 ml); purification by column chromatography (eluent: *n*-hexane), colorless liquid, $\text{C}_{31}\text{H}_{65}\text{SiBr}$ $M = 545.85$ g/mol, yield: 1.19 g (32 %), $^1\text{H-NMR}$ (CDCl_3 , 400 MHz): δ / ppm = 3.40 (2H, t, $^3J_{\text{H,H}} = 6.9$ Hz, BrCH_2 -), 1.85 (2H, p, $^3J_{\text{H,H}} = 7.6$ Hz, BrCH_2CH_2 -), 1.46 – 1.38 (2H, m, $\text{BrCH}_2\text{CH}_2\text{CH}_2$ -), 1.36 – 1.18 (42H, m, $-\text{CH}_2$ -), 0.88 (9H, t, $^3J_{\text{H,H}} = 7.0$ Hz, $-\text{CH}_3$), 0.50 – 0.44 (8H, m, $-\text{SiCH}_2$ -). $^{29}\text{Si-NMR}$ (CDCl_3 , 79 MHz): δ / ppm = 2.91 (Si).

(11-Bromoundecyl)triheptylsilane 2/11: Synthesized from triheptylsilane (2.0 g, 6.1 mmol), 11-Bromoundec-1-ene (2.1 g, 2.0 ml, 9.2 mmol), Karstedt-Cat (70 mg, 0.08 ml, 0.18 mmol) in anhydrous CH_2Cl_2 (20 ml); purification by column chromatography (eluent: *n*-hexane), colorless liquid, $\text{C}_{32}\text{H}_{67}\text{SiBr}$ $M = 559.88$ g/mol, yield: 1.17 g (34 %), $^1\text{H-NMR}$ (CDCl_3 , 400 MHz): δ / ppm = 3.40 (2H, t, $^3J_{\text{H,H}} = 6.9$ Hz, BrCH_2 -), 1.85 (2H, p, $^3J_{\text{H,H}} = 7.0$ Hz, BrCH_2CH_2 -), 1.48 – 1.37 (2H, m, $\text{BrCH}_2\text{CH}_2\text{CH}_2$ -), 1.37 – 1.19 (44H, m, $-\text{CH}_2$ -), 0.88 (9H, t, $^3J_{\text{H,H}} = 6.8$ Hz, $-\text{CH}_3$), 0.61 – 0.43 (8H, m, $-\text{SiCH}_2$ -). $^{29}\text{Si-NMR}$ (CDCl_3 , 79 MHz): δ / ppm = 2.91 (Si).

(12-Bromododecyl)triheptylsilane 2/12: Synthesized from triheptylsilane (2.2 g, 6.7 mmol), 12-Bromododec-1-ene (2.5 g, 2.3 ml, 10.1 mmol), Karstedt-Cat (76.7 mg, 0.09 ml, 0.20 mmol) in anhydrous CH_2Cl_2 (20 ml); purification by column chromatography (eluent: *n*-hexane), colorless liquid, $\text{C}_{33}\text{H}_{69}\text{SiBr}$ $M = 573.90$ g/mol, yield: 1.27 g (33 %), $^1\text{H-NMR}$ (CDCl_3 , 400 MHz): δ / ppm = 3.40 (2H, t, $^3J_{\text{H,H}} = 6.9$ Hz, BrCH_2 -), 1.85 (2H, p, $^3J_{\text{H,H}} = 7.1$ Hz, BrCH_2CH_2 -), 1.48 – 1.36 (2H, m, $\text{BrCH}_2\text{CH}_2\text{CH}_2$ -), 1.36 – 1.16 (46H, m,

-CH₂), 0.88 (9H, t, ³J_{H,H} = 6.8 Hz, -CH₃), 0.52 – 0.43 (8H, m, -SiCH₂-). ²⁹Si-NMR (CDCl₃, 79 MHz): δ / ppm = 2.91 (Si).

2.2.2 Synthesis of the 1,4-bis[ω-(triheptylsilyl)alkoxy]-2,5-diiodobenzenes 4/n

4.2.2.1 1,4-Bis[3-(triheptylsilyl)propoxy]-2,5-diiodobenzene 4/3

1,4-Bis(allyloxy)benzene(3)^{S15}: Hydroquinone (1 equ., 5.0 g; 0.45 mol) and ally bromide (2.5 equ., 13.7 g; 9.8 ml, 1.14 mol) and KOH (5 equ., 12.7 g, 2.27 mol) were added to CH₂Cl₂ (50 mL) and stirred for 24 h at 25 °C. Afterward, the solvent was evaporated and the crude product was purified by column chromatography (eluent: *n*-hexane/EE = 7:3), colorless solid, mp: 36 °C, C₁₂H₁₄O₂ M = 190.24 g/mol, yield: 7.91 g (91.6 %), ¹H-NMR (CDCl₃, 400 MHz): δ / ppm = 6.85 (4H, s, Aryl-H), 6.11 – 6.00 (2H, m, -CH=CH₂), 5.43 – 5.36 (2H, m, -CH=CH₂), 5.30 – 5.25 (2H, m, -CH=CH₂), 4.50 – 4.47 (4H, m, -OCH₂-).

1,4-Bis[3-(triheptylsilyl)propoxy]benzene: Synthesized by hydrosilylation of **3** (0.5 g, 2.6 mmol), with triheptylsilane (1.9 g, 5.8 mmol), Karstedt-cat (6 mol%, 0.13 mg, 0.15 ml, 0.4 mmol) in anhydrous CH₂Cl₂; purified by column chromatography (eluent: *n*-hexane), colorless liquid, C₅₄H₁₀₆O₂Si₂ M = 843.61 g/mol, yield: 1.35 g (61 %), ¹H-NMR (CDCl₃, 400 MHz): δ / ppm = 6.83 (4H, s, Aryl-H), 3.87 (4H, t, ³J_{H,H} = 6.9 Hz, -OCH₂-), 1.80 – 1.72 (4H, m, -OCH₂CH₂-), 1.36 – 1.23 (60H, m, -CH₂-), 0.91 (18H, t, ³J_{H,H} = 6.9 Hz, -CH₃), 0.63 – 0.50 (18H, m, -SiCH₂-). ²⁹Si-NMR (CDCl₃, 79 MHz): δ / ppm = 3.51 (Si).

1,4-Bis[3-(triheptylsilyl)propoxy]-2,5-diiodobenzene 4/3: A mixture of **3.1/3** (1.4 g, 1.60 mmol), PhI(OCOCF₃)₂ (1.1 equ, 0.8 mg, 1.8 mmol) and I₂ (1.1 equ, 0.5 mg, 1.8 mmol) in CH₂Cl₂ was refluxed for 1d. After cooling to RT the reaction was quenched with saturated Na₂S₂O₄ solution. The aqueous layer was extracted with Et₂O (3x50 ml) The combined organic layers were washed with water, and brine, and dried over Na₂SO₄. The solvent was evaporated (850 mbar, 60 °C) and the crude product was purified by column chromatography (eluent: *n*-hexane), colorless liquid, C₅₄H₁₀₄I₂O₂Si₂ M = 1095.40 g/mol, yield: 300 mg (17 %), ¹H-NMR (CDCl₃, 400 MHz): δ / ppm = 7.16 (2H, s, Aryl-H), 3.88 (4H, t, ³J_{H,H} = 6.5 Hz, -OCH₂-), 1.82 – 1.72 (4H, m, -OCH₂CH₂-), 1.36 – 1.20 (60H, m, -CH₂-), 0.88 (1H, t, ³J_{H,H} = 6.8 Hz, -CH₃), 0.70 – 0.47 (18H, m, -SiCH₂-). ²⁹Si-NMR (CDCl₃, 79 MHz): δ / ppm = 3.52 (Si).

4.2.2.2 1,4-Bis[3-(triheptylsilyl)alkoxy]-2,5-diiodobenzenes 4/n (n > 3)

A mixture of 2,6-diiodohydroquinone (1 equ.), (*n*-bromoalkyl)triheptylsilane (2.2 equ.), K₂CO₃ (10 equ.), and Bu₄Ni (tip of a spatula) in anhydrous DMF (10 ml/ 1 mmol 2,6-diiodohydroquinone) was stirred at 80 °C for 3 days.^{S14} After cooling to room temperature, the reaction was quenched with water (10 ml / 10 ml DMF), and the aqueous layer was extracted with Et₂O (3x50 ml). The combined organic layers were washed with saturated aq. LiCl, water, and brine. After drying over anhydrous Na₂SO₄, filtration, and evaporation of the solvent, the crude product was purified by column chromatography.

1,4-Bis[4-(triheptylsilyl)butoxy]-2,5-diiodobenzene 4/4: Synthesized from 2,6-diiodohydroquinone (0.5 g, 1.5 mmol), **2/4** (1.50 g, 3.3 mmol), K₂CO₃ (2.05 g, 14.8 mmol), Bu₄Ni (0.3 g, 0.8 mmol) in DMF (15 ml); purification by column chromatography (eluent: *n*-hexane); colorless liquid, C₅₆H₁₀₈I₂O₂Si₂ M = 1123.46 g/mol, yield: 550 mg (33 %), ¹H-NMR (CDCl₃, 400 MHz): δ / ppm = 7.18 (2H, s, Aryl-H), 3.94 (4H, t, ³J_{H,H} = 6.2 Hz, -OCH₂-), 1.81 (4H, p, ³J_{H,H} = 6.6 Hz, -OCH₂CH₂-), 1.57 – 1.49 (4H, m, -OCH₂CH₂CH₂-), 1.35 – 1.22 (60H, m, -CH₂-), 0.89 (18H, t, ³J_{H,H} = 6.9 Hz, -CH₃), 0.59 – 0.48 (16H, m, -SiCH₂-). ²⁹Si-NMR (CDCl₃, 79 MHz): δ / ppm = 3.07 (Si).

1,4-Bis[5-(triheptylsilyl)pentoxy]-2,5-diiodobenzene 4/5: Synthesized from 2,6-diiodohydroquinone (0.7 g, 1.9 mmol), **2/5** (2.0 g, 4.2 mmol), K₂CO₃ (2.7 g, 19.2 mmol), Bu₄Ni (0.4 g, 1.0 mmol) in DMF (19

ml); purification by column chromatography (eluent: *n*-hexane); colorless liquid, C₅₈H₁₁₂I₂O₂Si₂ M = 1151.51 g/mol, yield: 270 mg (12 %), ¹H-NMR (CDCl₃, 400 MHz): δ / ppm = 7.17 (2H, s, Aryl-H), 3.91 (4H, t, ³J_{H,H} = 6.4 Hz, -OCH₂-), 1.80 (4H, p, ³J_{H,H} = 6.8 Hz, -OCH₂CH₂-), 1.57 – 1.45 (4H, m, -OCH₂CH₂CH₂-), 1.34 – 1.20 (64H, m, -CH₂-), 0.88 (18H, t, ³J_{H,H} = 6.8 Hz, -CH₃), 0.58 – 0.44 (16H, m, -SiCH₂-). ²⁹Si-NMR (CDCl₃, 79 MHz): δ / ppm = 2.94 (Si).

1,4-Bis[6-(triheptylsilyl)hexoxy]-2,5-diiodobenzene 4/6: Synthesized from 2,6-diiodohydroquinon (0.3 g, 0.7 mmol), **2/6** (0.7 g, 1.4 mmol), K₂CO₃ (0.9 g, 6.7 mmol), Bu₄NI (0.2 g, 0.5 mmol) in DMF (10 ml); purification by column chromatography (eluent: *n*-hexane); colorless liquid, C₆₀H₁₁₆I₂O₂Si₂ M = 1179.66 g/mol, yield: 350 mg (44 %), ¹H-NMR (CDCl₃, 400 MHz): δ / ppm = 7.17 (2H, s, Aryl-H), 3.92 (4H, t, ³J_{H,H} = 6.4 Hz, -OCH₂-), 1.84 – 1.74 (4H, m, -OCH₂CH₂-), 1.55 – 1.46 (4H, m, -OCH₂CH₂CH₂-), 1.35 – 1.19 (68H, m, -CH₂-), 0.88 (18H, t, ³J_{H,H} = 6.8 Hz, -CH₃), 0.54 – 0.44 (16H, m, -SiCH₂-). ²⁹Si-NMR (CDCl₃, 79 MHz): δ / ppm = 2.93 (Si).

1,4-Bis[7-(triheptylsilyl)heptoxy]-2,5-diiodobenzene 4/7: Synthesized from 2,6-diiodohydroquinon (0.5 g, 1.3 mmol), **2/7** (1.4 g, 2.8 mmol), K₂CO₃ (1.8 g, 12.9 mmol), Bu₄NI (0.2 g, 0.7 mmol) in DMF (13 ml); purification by column chromatography (eluent: *n*-hexane); colorless liquid, C₆₂H₁₂₀I₂O₂Si₂ M = 1207.62 g/mol, yield: 650 mg (42 %), ¹H-NMR (CDCl₃, 400 MHz): δ / ppm = 7.17 (2H, s, Aryl-H), 3.92 (4H, t, ³J_{H,H} = 6.4 Hz, -OCH₂-), 1.83 – 1.74 (4H, m, -OCH₂CH₂-), 1.51 – 1.44 (4H, m, -OCH₂CH₂CH₂-), 1.38 – 1.20 (72H, m, -CH₂-), 0.87 (18H, t, ³J_{H,H} = 7.0 Hz, -CH₃), 0.52 – 0.44 (16H, m, -SiCH₂-). ²⁹Si-NMR (CDCl₃, 79 MHz): δ / ppm = 2.91 (Si).

1,4-Bis[8-(triheptylsilyl)octoxy]-2,5-diiodobenzene 4/8: Synthesized from 2,6-diiodohydroquinon (0.6 g, 1.7 mmol), **2/8** (1.9 g, 3.6 mmol), K₂CO₃ (2.3 g, 16.5 mmol), Bu₄NI (0.3 g, 0.8 mmol) in DMF (17 ml); purification by column chromatography (eluent: *n*-hexane); colorless liquid, C₆₄H₁₂₄I₂O₂Si₂ M = 1235.67 g/mol, yield: 440 mg (22 %), ¹H-NMR (CDCl₃, 400 MHz): δ / ppm = 7.18 (2H, s, Aryl-H), 3.93 (4H, t, ³J_{H,H} = 6.4 Hz, -OCH₂-), 1.84 – 1.77 (4H, m, -OCH₂CH₂-), 1.53 – 1.46 (4H, m, -OCH₂CH₂CH₂-), 1.42 – 1.21 (76H, m, -CH₂-), 0.89 (18H, t, ³J_{H,H} = 6.9 Hz, -CH₃), 0.53 – 0.45 (16H, m, -SiCH₂-). ²⁹Si-NMR (CDCl₃, 79 MHz): δ / ppm = 2.92 (Si).

1,4-Bis[9-(triheptylsilyl)nonoxy]-2,5-diiodobenzene 4/9: Synthesized from 2,6-diiodohydroquinon (0.4 g, 1.1 mmol), **2/9** (1.3 g, 2.4 mmol), K₂CO₃ (1.5 g, 11.0 mmol), Bu₄NI (0.2 mg, 0.6 mmol) in DMF (11 ml); purification by column chromatography (eluent: *n*-hexane); colorless liquid, C₆₆H₁₂₈I₂O₂Si₂ M = 1263.73 g/mol, yield: 880 mg (63 %), ¹H-NMR (CDCl₃, 400 MHz): δ / ppm = 7.17 (2H, s, Aryl-H), 3.93 (4H, t, ³J_{H,H} = 6.4 Hz, -OCH₂-), 1.84 – 1.77 (4H, m, -OCH₂CH₂-), 1.53 – 1.46 (4H, m, -OCH₂CH₂CH₂-), 1.40 – 1.21 (80H, m, -CH₂-), 0.89 (18H, t, ³J_{H,H} = 6.9 Hz, -CH₃), 0.53 – 0.44 (16H, m, -SiCH₂-). ²⁹Si-NMR (CDCl₃, 79 MHz): δ / ppm = 2.92 (Si).

1,4-Bis[10-(triheptylsilyl)decoxy]-2,5-diiodobenzene 4/10: Synthesized from 2,6-diiodohydroquinon (0.4 g, 1.0 mmol), **2/10** (1.2 g, 2.2 mmol), K₂CO₃ (1.4 g, 9.9 mmol), Bu₄NI (0.2 g, 0.5 mmol) in DMF (10 ml); purification by column chromatography (eluent: *n*-hexane); colorless liquid, C₆₈H₁₃₂I₂O₂Si₂ M = 1291.78 g/mol, yield: 880 mg (69 %), ¹H-NMR (CDCl₃, 500 MHz): δ / ppm = 7.17 (2H, s, Aryl-H), 3.93 (4H, t, ³J_{H,H} = 6.4 Hz, -OCH₂-), 1.84 – 1.75 (4H, m, -OCH₂CH₂-), 1.53 – 1.45 (4H, m, -OCH₂CH₂CH₂-), 1.40 – 1.19 (84H, m, -CH₂-), 0.89 (18H, t, ³J_{H,H} = 7.0 Hz, -CH₃), 0.53 – 0.44 (16H, m, -SiCH₂-). ²⁹Si-NMR (CDCl₃, 99 MHz): δ / ppm = 2.92 (Si).

1,4-Bis[11-(triheptylsilyl)undecoxy]-2,5-diiodobenzene 4/11: Synthesized from 2,6-diiodohydroquinon (0.3 g, 1.0 mmol), **2/11** (1.2 g, 2.1 mmol), K₂CO₃ (1.3 g, 9.5 mmol), Bu₄NI (0.2 g, 0.5 mmol) in DMF (10 ml); purification by column chromatography (eluent: *n*-hexane); colorless liquid, C₆₀H₁₃₆I₂O₂Si₂ M = 1319.83 g/mol, yield: 500 mg (40 %), ¹H-NMR (CDCl₃, 400 MHz): δ / ppm = 7.17 (2H, s, Aryl-H), 3.92 (4H, t, ³J_{H,H} = 6.4 Hz, -OCH₂-), 1.84 – 1.75 (4H, m, -OCH₂CH₂-), 1.55 – 1.44 (4H, m, -

OCH₂CH₂CH₂-), 1.41 – 1.20 (88H, m, -CH₂), 0.89 (18H, t, ³J_{H,H} = 6.9 Hz, -CH₃), 0.52 – 0.44 (16H, m, -SiCH₂). ²⁹Si-NMR (CDCl₃, 79 MHz): δ / ppm = 2.91 (Si).

1,4-Bis[12-(triheptylsilyl)dodecoxy]-2,5-diiodobenzene 4/12: Synthesized from 2,6-diiodohydroquinon (0.4 g, 1.0 mmol), **2/12** (1.3 g, 2.2 mmol), K₂CO₃ (1.4 g, 10.1 mmol), Bu₄NI (0.2 g, 0.5 mmol) in DMF (10 ml); purification by column chromatography (eluent: *n*-hexane); colorless liquid, C₇₂H₁₄₀I₂O₂Si₂ M = 1347.89 g/mol, yield: 460 mg (33 %), ¹H-NMR (CDCl₃, 500 MHz): δ / ppm = 7.17 (2H, s, Aryl-H), 3.93 (4H, t, ³J_{H,H} = 6.4 Hz, -OCH₂-), 1.80 (4H, p, ³J_{H,H} = 7.1 Hz, -OCH₂CH₂-), 1.53 – 1.46 (4H, m, -OCH₂CH₂CH₂-), 1.41 – 1.21 (92H, m, -CH₂), 0.89 (18H, t, ³J_{H,H} = 7.0 Hz, -CH₃), 0.53 – 0.44 (16H, m, -SiCH₂). ²⁹Si-NMR (CDCl₃, 99 MHz): δ / ppm = 2.92 (Si).

4.2.3 Syntheses of the acetonides HnA and FnA

1,4-Bis[ω-(triheptylsilyl)alkyloxy]-2,5-bis{4-[4-(2,3-isopropylidene-2,3-dihydroxypropyl-1-oxy)phenylethynyl]phenylethynyl}benzenes HnA and 1,4-bis[ω-(triheptylsilyl)alkyloxy]-2,5-bis{4-[2,3,5,6-tetrafluoro-4-(2,3-isopropylidene-2,3-dihydroxypropyl-1-oxy)phenylethynyl]phenylethynyl}benzenes FnA: A mixture of **5/n** (1 equ.) and the appropriate acetylene **5H** or **5F** (2.1 equ.) was dissolved in purified NEt₃ (10 mL/~1 mmol **5/n**). After degassing with argon for 30 min [Pd(PPh₃)₄] (3 mol%) and CuI (3 mol%) were added and the mixture was stirred at 80 °C for 24 h.⁵¹¹ After removing the solvent by evaporation the obtained residue was purified by column chromatography.

1,4-Bis[3-(triheptylsilyl)propoxy]-2,5-bis{4-[4-(2,3-isopropylidene-2,3-dihydroxypropyl-1-oxy)phenylethynyl]phenylethynyl}benzene H3A: Synthesized from **4/3** (150 mg, 0.14 mmol), **5H** (100 mg, 0.30 mmol), [Pd(PPh₃)₄] (4.8 mg, 4.2·10⁻³ mmol), CuI (0.8 mg, 4.2·10⁻³ mmol) in NEt₃ (20 ml); purification by column chromatography (eluent: CHCl₃). Yellow solid, C₉₈H₁₄₂O₈Si₂, M = 1504.38 g/mol, yield: 140 mg (68 %), mp.: 133.3 °C, ¹H-NMR (CDCl₃, 400 MHz): δ / ppm = 7.55 – 7.47 (12H, m, Aryl-H), 7.04 (2H, s, Aryl-H), 6.93 (4H, d, J=8.6 Hz, Aryl-H), 4.52 (2H, p, ³J_{H,H} = 5.9 Hz, -OCH-), 4.21 (2H, dd, ³J_{H,H} = 8.5, ³J_{H,H} = 6.4 Hz, -OCH₂-), 4.11 (2H, dd, ³J_{H,H} = 9.5, ³J_{H,H} = 5.4 Hz, -OCH₂-), 4.07 – 3.98 (6H, m, -OCH₂-), 3.95 (2H, dd, ³J_{H,H} = 8.5, ³J_{H,H} = 5.8 Hz, -OCH₂-), 1.92 – 1.83 (4H, m, -CH₂-), 1.50 (6H, s, -OCH₃), 1.44 (6H, s, -OCH₃), 1.38 – 1.23 (60H, m, -CH₂-), 0.90 (18H, t, ³J_{H,H} = 6.9 Hz, -CH₃), 0.77 – 0.71 (4H, m, -SiCH₂-), 0.60 – 0.52 (12H, m, -SiCH₂-). ²⁹Si-NMR (CDCl₃, 79 MHz): δ / ppm = 3.48 (Si).

1,4-Bis[4-(triheptylsilyl)butoxy]-2,5-bis{4-[4-(2,3-isopropylidene-2,3-dihydroxypropyl-1-oxy)phenylethynyl]phenylethynyl}benzene H4A: Synthesized from **4/4** (275 mg, 0.25 mmol), **5H** (179 mg, 0.54 mmol), [Pd(PPh₃)₄] (8.7 mg, 7.5·10⁻³ mmol), CuI (1.4 mg, 7.5·10⁻³ mmol) in NEt₃ (20 ml); purification by column chromatography (eluent: CHCl₃). Yellow solid, C₁₀₀H₁₄₆O₈Si₂, M = 1532.43 g/mol, yield: 270 mg (72 %), mp.: 89.3 °C, ¹H-NMR (CDCl₃, 400 MHz): δ / ppm = 7.51 – 7.43 (12H, m, Aryl-H), 7.01 (2H, s, Aryl-H), 6.93 – 6.87 (4H, m, Aryl-H), 4.53 – 4.45 (2H, m, -OCH-), 4.18 (2H, dd, ³J_{H,H} = 8.5, ³J_{H,H} = 6.4 Hz, -OCH₂-), 4.11 – 4.03 (6H, m, -OCH₂-), 3.97 (2H, dd, ³J_{H,H} = 9.6, ³J_{H,H} = 5.9 Hz, -OCH₂-), 3.91 (2H, dd, ³J_{H,H} = 8.5, ³J_{H,H} = 5.8 Hz, -OCH₂-), 1.93 – 1.83 (4H, m, -CH₂-), 1.59 – 1.50 (4H, m, -CH₂-), 1.47 (6H, s, -OCH₃), 1.41 (6H, s, -OCH₃), 1.33 – 1.17 (60H, m, -CH₂-), 0.87 (18H, t, ³J_{H,H} = 6.9 Hz, -CH₃), 0.61 – 0.42 (16H, m, -SiCH₂-). ²⁹Si-NMR (CDCl₃, 79 MHz): δ / ppm = 2.99 (Si).

1,4-Bis[5-(triheptylsilyl)pentoxy]-2,5-bis{4-[4-(2,3-isopropylidene-2,3-dihydroxypropyl-1-oxy)phenylethynyl]phenylethynyl}benzene H5A: Synthesized from **4/5** (120 mg, 0.10 mmol), **5H** (76 mg, 0.23 mmol), [Pd(PPh₃)₄] (3.6 mg, 3·10⁻³ mmol), CuI (0.6 mg, 3·10⁻³ mmol) in NEt₃ (20 ml); purification by column chromatography (eluent: CHCl₃). Yellow solid, C₁₀₂H₁₅₀O₈Si₂, M = 1560.48 g/mol, yield: 150 mg (92 %), mp.: 115.8 °C, ¹H-NMR (CDCl₃, 500 MHz): δ / ppm = 7.53 – 7.44 (12H, m, Aryl-H),

7.02 (2H, s, Aryl-H), 6.92 – 6.88 (4H, m, Aryl-H), 4.52 – 4.46 (2H, m, -OCH-), 4.18 (2H, dd, $^3J_{H,H} = 8.5$, $^3J_{H,H} = 6.4$ Hz, -OCH₂-), 4.11 – 4.06 (2H, m, -OCH₂-), 4.04 (4H, t, $^3J_{H,H} = 6.5$ Hz, -OCH₂-), 3.98 (2H, dd, $^3J_{H,H} = 9.5$, $^3J_{H,H} = 5.9$ Hz, -OCH₂-), 3.92 (2H, dd, $^3J_{H,H} = 8.5$, $^3J_{H,H} = 5.8$ Hz, -OCH₂-), 2.06 – 1.92 (4H, m, -CH₂-), 1.62 – 1.53 (4H, m, -CH₂-), 1.47 (6H, s, -OCH₃), 1.42 (6H, s, -OCH₃), 1.40 – 1.20 (64H, m, -CH₂-), 0.87 (18H, t, $^3J_{H,H} = 6.9$ Hz, -CH₃), 0.57 – 0.44 (16H, m, -SiCH₂-). ²⁹Si-NMR (CDCl₃, 99 MHz): δ / ppm = 2.90 (Si).

1,4-Bis[6-(triheptylsilyl)hexoxy]-2,5-bis{4-[4-(2,3-isopropylidene-2,3-dihydroxypropyl-1-oxy)phenylethynyl]phenylethynyl}benzene H6A: Synthesized from **4/6** (175 mg, 0.15 mmol), **5H** (104 mg, 0.31 mmol), [Pd(PPh₃)₄] (5.2 mg, 4.5·10⁻³ mmol), CuI (0.9 mg, 4.5·10⁻³ mmol) in NEt₃ (20 ml); purification by column chromatography (eluent: CHCl₃). Yellow glassy solid, C₁₀₄H₁₅₄O₂Si₂, M = 1588.54 g/mol, yield: 210 mg (89 %), ¹H-NMR (CDCl₃, 400 MHz): δ / ppm = 7.67 – 7.36 (12H, m, Aryl-H), 7.01 (2H, s, Aryl-H), 6.94 – 6.87 (4H, m, Aryl-H), 4.55 – 4.44 (2H, m, -OCH-), 4.18 (2H, dd, $^3J_{H,H} = 8.5$, $^3J_{H,H} = 6.4$ Hz, -OCH₂-), 4.08 (2H, dd, $^3J_{H,H} = 8.7$, $^3J_{H,H} = 5.5$ Hz, -OCH₂-), 4.04 (4H, t, $^3J_{H,H} = 6.5$ Hz, -OCH₂-), 3.97 (2H, dd, $^3J_{H,H} = 9.5$, $^3J_{H,H} = 5.7$ Hz, -OCH₂-), 3.91 (2H, dd, $^3J_{H,H} = 8.5$, $^3J_{H,H} = 5.8$ Hz, -OCH₂-), 1.90 – 1.79 (4H, m, -CH₂-), 1.59 – 1.51 (4H, m, -CH₂-), 1.47 (6H, s, -OCH₃), 1.41 (6H, s, -OCH₃), 1.34 – 1.00 (68H, m, -CH₂-), 0.87 (18H, t, $^3J_{H,H} = 6.5$ Hz, -CH₃), 0.57 – 0.35 (16H, m, -SiCH₂-). ²⁹Si-NMR (CDCl₃, 79 MHz): δ / ppm = 2.94 (Si).

1,4-Bis[7-(triheptylsilyl)heptoxy]-2,5-bis{4-[4-(2,3-isopropylidene-2,3-dihydroxypropyl-1-oxy)phenylethynyl]phenylethynyl}benzene H7A: Synthesized from **4/7** (200 mg, 0.17 mmol), **5H** (121 mg, 0.36 mmol), [Pd(PPh₃)₄] (5.9 mg, 5.1·10⁻³ mmol), CuI (1.0 mg, 5.1·10⁻³ mmol) in NEt₃ (20 ml); purification by column chromatography (eluent: CHCl₃). Yellow solid, C₁₀₆H₁₅₈O₈Si₂, M = 1616.59 g/mol, yield: 260 mg (97 %), mp.: 104.6 °C, ¹H-NMR (CDCl₃, 400 MHz): δ / ppm = 7.52 – 7.43 (12H, m, Aryl-H), 7.01 (2H, s, Aryl-H), 6.94 – 6.85 (4H, m, Aryl-H), 4.48 (2H, p, $^3J_{H,H} = 5.9$ Hz, -OCH-), 4.17 (2H, dd, $^3J_{H,H} = 8.5$, $^3J_{H,H} = 6.4$ Hz, -OCH₂-), 4.11 – 4.00 (6H, m, -OCH₂-), 3.96 (2H, dd, $^3J_{H,H} = 9.6$, $^3J_{H,H} = 5.8$ Hz, -OCH₂-), 3.91 (2H, dd, $^3J_{H,H} = 8.5$, $^3J_{H,H} = 5.8$ Hz, -OCH₂-), 1.91 – 1.80 (4H, m, -CH₂-), 1.58 – 1.49 (4H, m, -CH₂-), 1.47 (6H, s, -OCH₃), 1.41 (6H, s, -OCH₃), 1.40 – 1.19 (72H, m, -CH₂-), 0.87 (18H, t, $^3J_{H,H} = 6.9$ Hz, -CH₃), 0.53 – 0.40 (16H, m, -SiCH₂-). ²⁹Si-NMR (CDCl₃, 79 MHz): δ / ppm = 2.89 (Si).

1,4-Bis[8-(triheptylsilyl)octoxy]-2,5-bis{4-[4-(2,3-isopropylidene-2,3-dihydroxypropyl-1-oxy)phenylethynyl]phenylethynyl}benzene H8A: Synthesized from **4/8** (220 mg, 0.18 mmol), **5H** (130 mg, 0.39 mmol), [Pd(PPh₃)₄] (6.2 mg, 5.4·10⁻³ mmol), CuI (1.0 mg, 5.4·10⁻³ mmol) in NEt₃ (20 ml); purification by column chromatography (eluent: CHCl₃). Yellow solid, C₁₀₈H₁₆₂O₈Si₂, M = 1644.65 g/mol, yield: 180 mg (62 %), mp.: 59.1 °C, ¹H-NMR (CDCl₃, 400 MHz): δ / ppm = 7.51 – 7.44 (12H, m, Aryl-H), 7.01 (2H, s, Aryl-H), 6.90 (4H, d, $^3J_{H,H} = 8.3$ Hz, Aryl-H), 4.52 – 4.45 (2H, m, -OCH-), 4.18 (2H, dd, $^3J_{H,H} = 8.6$, $^3J_{H,H} = 6.4$ Hz, -OCH₂-), 4.08 (2H, dd, $^3J_{H,H} = 9.4$, $^3J_{H,H} = 5.4$ Hz, -OCH₂-), 4.03 (4H, t, $^3J_{H,H} = 6.5$ Hz, -OCH₂-), 3.97 (2H, dd, $^3J_{H,H} = 9.5$, $^3J_{H,H} = 5.9$ Hz, -OCH₂-), 3.91 (2H, dd, $^3J_{H,H} = 8.5$, $^3J_{H,H} = 5.8$ Hz, -OCH₂-), 1.90 – 1.81 (4H, m, -CH₂-), 1.59 – 1.50 (4H, m, -CH₂-), 1.47 (6H, s, -OCH₃), 1.41 (6H, s, -OCH₃), 1.35 – 1.20 (76H, m, -CH₂-), 0.87 (18H, t, $^3J_{H,H} = 6.8$ Hz, -CH₃), 0.51 – 0.43 (16H, m, -SiCH₂-). ²⁹Si-NMR (CDCl₃, 79 MHz): δ / ppm = 2.90 (Si).

1,4-Bis[9-(triheptylsilyl)nonoxy]-2,5-bis{4-[4-(2,3-isopropylidene-2,3-dihydroxypropyl-1-oxy)phenylethynyl]phenylethynyl}benzene H9A: Synthesized from **4/9** (200 mg, 0.16 mmol), **5H** (116 mg, 0.35 mmol), [Pd(PPh₃)₄] (5.6 mg, 4.8·10⁻³ mmol), CuI (0.9 mg, 4.8·10⁻³ mmol) in NEt₃ (20 ml); purification by column chromatography (eluent: CHCl₃). Yellow solid, C₁₁₀H₁₆₆O₈Si₂, M = 1672.70 g/mol, yield: 160 mg (61 %), mp.: 95.8 °C, ¹H-NMR (CDCl₃, 400 MHz): δ / ppm = 7.52 – 7.44 (12H, m, Aryl-H), 7.01 (2H, s, Aryl-H), 6.92 – 6.86 (4H, m, Aryl-H), 4.48 (2H, p, $^3J_{H,H} = 5.9$ Hz, -OCH-), 4.17 (2H, dd, $^3J_{H,H} = 8.5$, $^3J_{H,H} = 6.4$ Hz, -OCH₂-), 4.11 – 4.01 (6H, m, -OCH₂-), 3.96 (2H, dd, $^3J_{H,H} = 9.5$, $^3J_{H,H} = 5.9$ Hz, -OCH₂-), 3.91 (2H, dd, $^3J_{H,H} = 8.5$, $^3J_{H,H} = 5.8$ Hz, -OCH₂-), 1.92 – 1.79 (4H, m, -CH₂-), 1.60 – 1.49 (4H, m, -CH₂-),

1.47 (6H, s, -OCH₃), 1.41 (6H, s, -OCH₃), 1.36 – 1.17 (80H, m, -CH₂-), 0.87 (18H, t, ³J_{H,H} = 6.8 Hz, -CH₃), 0.53 – 0.41 (16H, m, -SiCH₂). ²⁹Si-NMR (CDCl₃, 79 MHz): δ / ppm = 2.90 (Si).

1,4-Bis[10-(triheptylsilyl)decoxy]-2,5-bis{4-[4-(2,3-isopropylidene-2,3-dihydroxypropyl-1-oxy)phenylethynyl]phenylethynyl}benzene H10A: Synthesized from **4/10** (200 mg, 0.16 mmol), **5H** (113 mg, 0.34 mmol), [Pd(PPh₃)₄] (5.6 mg, 4.8·10⁻³ mmol), CuI (0.9 mg, 4.8·10⁻³ mmol) in NEt₃ (20 ml); purification by column chromatography (eluent: CHCl₃). Yellow solid, C₁₁₂H₁₇₀O₈Si₂, M = 1700.75 g/mol, yield: 145 mg (55 %), mp.: 45.2 °C, ¹H-NMR (CDCl₃, 400 MHz): δ / ppm = 7.51 – 7.44 (12H, m, Aryl-H), 7.01 (2H, s, Aryl-H), 6.92 – 6.87 (4H, m, Aryl-H), 4.48 (2H, p, ³J_{H,H} = 6.0 Hz, -OCH-), 4.17 (2H, dd, ³J_{H,H} = 8.5, ³J_{H,H} = 6.4 Hz, -OCH₂-), 4.10 – 4.01 (6H, m, -OCH₂-), 3.96 (2H, dd, ³J_{H,H} = 9.5, ³J_{H,H} = 5.9 Hz, -OCH₂-), 3.91 (2H, dd, ³J_{H,H} = 8.5, ³J_{H,H} = 5.8 Hz, -OCH₂-), 1.89 – 1.81 (4H, m, -CH₂-), 1.58 – 1.49 (4H, m, -CH₂-), 1.47 (6H, s, -OCH₃), 1.41 (6H, s, -OCH₃), 1.39 – 1.19 (84H, m, -CH₂-), 0.87 (18H, t, ³J_{H,H} = 6.9 Hz, -CH₃), 0.50 – 0.43 (16H, m, -SiCH₂). ²⁹Si-NMR (CDCl₃, 79 MHz): δ / ppm = 2.90 (Si).

1,4-Bis[11-(triheptylsilyl)undecoxy]-2,5-bis{4-[4-(2,3-isopropylidene-2,3-dihydroxypropyl-1-oxy)phenylethynyl]phenylethynyl}benzene H11A: Synthesized from **4/11** (250 mg, 0.19 mmol), **5H** (138 mg, 0.42 mmol), [Pd(PPh₃)₄] (6.6 mg, 5.7·10⁻³ mmol), CuI (1.1 mg, 5.7·10⁻³ mmol) in NEt₃ (20 ml); purification by column chromatography (eluent: CHCl₃). Yellow solid, C₁₁₄H₁₇₄O₈Si₂, M = 1728.81 g/mol, yield: 270 mg (82 %), mp. 135.0 °C, ¹H-NMR (CDCl₃, 400 MHz): δ / ppm = 7.53 – 7.42 (12H, m, Aryl-H), 7.01 (2H, s, Aryl-H), 6.92 – 6.87 (4H, m, Aryl-H), 4.53 – 4.44 (2H, m, -OCH-), 4.18 (2H, dd, ³J_{H,H} = 6.7, ³J_{H,H} = 2.3 Hz, -OCH₂-), 4.08 (2H, dd, ³J_{H,H} = 9.5, ³J_{H,H} = 5.4 Hz, -OCH₂-), 4.03 (4H, t, ³J_{H,H} = 6.5 Hz, -OCH₂-), 3.97 (2H, dd, ³J_{H,H} = 9.5, ³J_{H,H} = 5.9 Hz, -OCH₂-), 3.91 (2H, dd, ³J_{H,H} = 8.5, ³J_{H,H} = 5.8 Hz, -OCH₂-), 1.92 – 1.80 (4H, m, -CH₂-), 1.57 – 1.51 (4H, m, -CH₂-), 1.47 (6H, s, -OCH₃), 1.41 (6H, s, -OCH₃), 1.35 – 1.20 (88H, m, -CH₂-), 0.88 (18H, t, ³J_{H,H} = 6.9 Hz, -CH₃), 0.50 – 0.42 (16H, m, -SiCH₂). ²⁹Si-NMR (CDCl₃, 79 MHz): δ / ppm = 2.90 (Si).

1,4-Bis[12-(triheptylsilyl)dodecoxy]-2,5-bis{4-[4-(2,3-isopropylidene-2,3-dihydroxypropyl-1-oxy)phenylethynyl]phenylethynyl}benzene H12A: Synthesized from **4/12** (200 mg, 0.15 mmol), **5H** (109 mg, 0.33 mmol), [Pd(PPh₃)₄] (5.2 mg, 4.5·10⁻³ mmol), CuI (0.9 mg, 4.5·10⁻³ mmol) in NEt₃ (20 ml); purification by column chromatography (eluent: CHCl₃). Yellow solid, C₁₁₆H₁₇₈O₈Si₂, M = 1756.86 g/mol, yield: 140 mg (54 %), mp.: 92.9 °C, ¹H-NMR (CDCl₃, 500 MHz): δ / ppm = 7.50 – 7.45 (12H, m, Aryl-H), 7.01 (2H, s, Aryl-H), 6.92 – 6.89 (4H, m, Aryl-H), 4.49 (2H, p, ³J_{H,H} = 5.9 Hz, -OCH-), 4.18 (2H, dd, ³J_{H,H} = 8.5, ³J_{H,H} = 6.4 Hz, -OCH₂-), 4.08 (2H, dd, ³J_{H,H} = 9.4, ³J_{H,H} = 5.4 Hz, -OCH₂-), 4.04 (4H, t, ³J_{H,H} = 6.5 Hz, -OCH₂-), 3.97 (2H, dd, ³J_{H,H} = 9.5, ³J_{H,H} = 5.9 Hz, -OCH₂-), 3.92 (2H, dd, ³J_{H,H} = 8.5, ³J_{H,H} = 5.8 Hz, -OCH₂-), 1.90 – 1.82 (4H, m, -CH₂-), 1.58 – 1.51 (4H, m, -CH₂-), 1.48 (6H, s, -OCH₃), 1.42 (6H, s, -OCH₃), 1.41 – 1.20 (92H, m, -CH₂-), 0.88 (18H, t, ³J_{H,H} = 6.9 Hz, -CH₃), 0.51 – 0.44 (16H, m, -SiCH₂). ²⁹Si-NMR (CDCl₃, 99 MHz): δ / ppm = 2.91 (Si).

1,4-Bis[3-(triheptylsilyl)propoxy]-2,5-bis{4-[2,3,5,6-tetrafluoro-4-(2,3-isopropylidene-2,3-dihydroxypropyl-1-oxy)phenylethynyl]phenylethynyl}benzene F3A: Synthesized from **4/3** (150 mg, 0.14 mmol), **5F** (122 mg, 0.30 mmol), [Pd(PPh₃)₄] (4.9 mg, 4.2·10⁻³ mmol), CuI (0.8 mg, 4.2·10⁻³ mmol) in NEt₃ (20 ml); purification by column chromatography (eluent: CHCl₃). Yellow solid, C₉₈H₁₃₄F₈O₈Si₂, M = 1648.30 g/mol, yield: 152.5 mg (68%), mp.: 90.4 °C, ¹H-NMR (CDCl₃, 500 MHz): δ / ppm = 7.60 – 7.53 (8H, m, Aryl-H), 7.05 (2H, s, Aryl-H), 4.52 – 4.46 (2H, m, -OCH-), 4.37 (2H, dd, ³J_{H,H} = 10.2, ³J_{H,H} = 5.1 Hz, -OCH₂-), 4.28 (2H, dd, ³J_{H,H} = 8.2, ³J_{H,H} = 5.6 Hz, -OCH₂-), 4.20 (2H, dd, ³J_{H,H} = 8.6, ³J_{H,H} = 6.5 Hz, -OCH₂-), 4.07 – 3.97 (6H, m, -OCH₂-), 1.93 – 1.83 (4H, m, -CH₂-), 1.47 (6H, s, -OCH₃), 1.42 (6H, s, -OCH₃), 1.37 – 1.22 (60H, m, -CH₂-), 0.90 (18H, t, ³J_{H,H} = 6.8 Hz, -CH₃), 0.79 – 0.70 (4H, m, -SiCH₂-), 0.61 – 0.51 (12H, m, -SiCH₂-). ¹⁹F-NMR (CDCl₃, 470 MHz): δ / ppm = -137.35 – -137.64 (m, Aryl-F), -156.72 – -157.07 (m, Aryl-F). ²⁹Si-NMR (CDCl₃, 99 MHz): δ / ppm = 3.48 (Si).

1,4-Bis[4-(triheptylsilyl)butoxy]-2,5-bis{4-[2,3,5,6-tetrafluoro-4-(2,3-isopropylidene-2,3-dihydroxypropyl-1-oxy)phenylethynyl]phenylethynyl}benzene F4A: Synthesized from **4/4** (275 mg, 0.25 mmol), **5F** (218 mg, 0.54 mmol), [Pd(PPh₃)₄] (8.7 mg, 7.5·10⁻³ mmol), CuI (1.4 mg, 7.5·10⁻³ mmol) in NEt₃ (20 ml); purification by column chromatography (eluent: CHCl₃). Yellow glassy solid, C₁₀₀H₁₃₈F₈O₈Si₂, M = 1676.35 g/mol, yield: 390 mg (95 %), ¹H-NMR (CDCl₃, 400 MHz): δ / ppm = 7.57 – 7.49 (8H, m, Aryl-H), 7.02 (2H, s, Aryl-H), 4.49 – 4.42 (2H, m, -OCH-), 4.33 (2H, dd, ³J_{H,H} = 8.1, ³J_{H,H} = 5.6 Hz, -OCH₂-), 4.24 (2H, dd, ³J_{H,H} = 6.8, ³J_{H,H} = 4.5 Hz, -OCH₂-), 4.16 (2H, dd, ³J_{H,H} = 8.1, ³J_{H,H} = 4.4 Hz, -OCH₂-), 4.05 (4H, t, ³J_{H,H} = 7.2 Hz, -OCH₂-), 3.96 (2H, dd, ³J_{H,H} = 8.5, ³J_{H,H} = 5.4 Hz, -OCH₂-), 1.94 – 1.82 (4H, m, -CH₂-), 1.62 – 1.50 (4H, m, -CH₂-), 1.43 (6H, s, -OCH₃), 1.38 (6H, s, -OCH₃), 1.33 – 1.16 (60H, m, -CH₂-), 0.87 (18H, t, ³J_{H,H} = 7.3 Hz, -CH₃), 0.61 – 0.41 (16H, m, -SiCH₂-). ¹⁹F-NMR (CDCl₃, 376 MHz): δ / ppm = -137.37 – -137.65 (m, Aryl-F), -156.79 – -157.08 (m, Aryl-F). ²⁹Si-NMR (CDCl₃, 79 MHz): δ / ppm = 3.00 (Si).

1,4-Bis[5-(triheptylsilyl)pentoxy]-2,5-bis{4-[2,3,5,6-tetrafluoro-4-(2,3-isopropylidene-2,3-dihydroxypropyl-1-oxy)phenylethynyl]phenylethynyl}benzene F5A: Synthesized from **4/5** (100 mg, 0.09 mmol), **5F** (77 mg, 0.19 mmol), [Pd(PPh₃)₄] (3.1 mg, 2.7·10⁻³ mmol), CuI (0.5 mg, 2.7·10⁻³ mmol) in NEt₃ (20 ml); purification by column chromatography (eluent: CHCl₃). Yellow solid, C₁₀₂H₁₄₂F₈O₈Si₂, M = 1704.41 g/mol, yield: 140 mg (94 %), mp.: 46.7 °C, ¹H-NMR (CDCl₃, 400 MHz): δ / ppm = 7.58 – 7.52 (8H, m), 7.02 (2H, s), 4.46 (2H, p, ³J_{H,H} = 5.6 Hz), 4.34 (2H, dd, ³J_{H,H} = 10.2, ³J_{H,H} = 5.1 Hz, -OCH₂-), 4.24 (2H, dd, ³J_{H,H} = 10.2, ³J_{H,H} = 5.6 Hz, -OCH₂-), 4.17 (2H, dd, ³J_{H,H} = 8.6, ³J_{H,H} = 6.4 Hz, -OCH₂-), 4.04 (4H, t, ³J_{H,H} = 6.5 Hz, -OCH₂-), 3.97 (2H, dd, ³J_{H,H} = 8.6, ³J_{H,H} = 5.5 Hz, -OCH₂-), 1.92 – 1.83 (4H, m, -CH₂-), 1.62 – 1.53 (4H, m, -CH₂-), 1.44 (6H, s, -OCH₃), 1.39 (6H, s, -OCH₃), 1.34 – 1.18 (64H, m, -CH₂-), 0.87 (18H, t, ³J_{H,H} = 6.9 Hz, -CH₃), 0.57 – 0.43 (16H, m, -SiCH₂-). ¹⁹F-NMR (CDCl₃, 376 MHz): δ / ppm = -137.40 – -137.64 (m, Aryl-F), -156.83 – -156.98 (m, Aryl-F). ²⁹Si-NMR (CDCl₃, 79 MHz): δ / ppm = 2.90 (Si).

1,4-Bis[6-(triheptylsilyl)hexoxy]-2,5-bis{4-[2,3,5,6-tetrafluoro-4-(2,3-isopropylidene-2,3-dihydroxypropyl-1-oxy)phenylethynyl]phenylethynyl}benzene F6A: Synthesized from **4/6** (175 mg, 0.15 mmol), **5F** (126 mg, 0.31 mmol), [Pd(PPh₃)₄] (5.2 mg, 4.5·10⁻³ mmol), CuI (0.9 mg, 4.5·10⁻³ mmol) in NEt₃ (20 ml); purification by column chromatography (eluent: CHCl₃). Yellow solid, C₁₀₄H₁₄₆F₈O₈Si₂, M = 1732.46 g/mol, yield: 210 mg (82%), mp.: 135.0 °C, ¹H-NMR (CDCl₃, 400 MHz): δ / ppm = 7.57 – 7.50 (8H, m, Aryl-H), 7.02 (2H, s, Aryl-H), 4.49 – 4.42 (2H, m, -OCH-), 4.32 (2H, dd, ³J_{H,H} = 6.6, ³J_{H,H} = 4.4 Hz, -OCH₂-), 4.24 (2H, dd, ³J_{H,H} = 10.1, ³J_{H,H} = 5.6 Hz, -OCH₂-), 4.16 (2H, dd, ³J_{H,H} = 8.6, ³J_{H,H} = 6.4 Hz, -OCH₂-), 4.04 (4H, t, ³J_{H,H} = 6.5 Hz, -OCH₂-), 3.96 (2H, dd, ³J_{H,H} = 8.6, ³J_{H,H} = 5.6 Hz, -OCH₂-), 1.90 – 1.82 (4H, m, -CH₂-), 1.60 – 1.50 (4H, m, -CH₂-), 1.43 (6H, s, -OCH₃), 1.39 (6H, s, -OCH₃), 1.36 – 1.17 (68H, m, -CH₂-), 0.87 (18H, t, ³J_{H,H} = 7.1 Hz, -CH₃), 0.52 – 0.43 (16H, m, -SiCH₂-). ¹⁹F-NMR (CDCl₃, 376 MHz): δ / ppm = -137.00 – -137.63 (m, Aryl-F), -156.80 – -157.50 (m, Aryl-F). ²⁹Si-NMR (CDCl₃, 79 MHz): δ / ppm = 2.89 (Si).

1,4-Bis[7-(triheptylsilyl)heptoxy]-2,5-bis{4-[2,3,5,6-tetrafluoro-4-(2,3-isopropylidene-2,3-dihydroxypropyl-1-oxy)phenylethynyl]phenylethynyl}benzene F7A: Synthesized from **4/7** (200 mg, 0.17 mmol), **5F** (147 mg, 0.37 mmol), [Pd(PPh₃)₄] (5.9 mg, 5.1·10⁻³ mmol), CuI (1.1 mg, 5.1·10⁻³ mmol) in NEt₃ (20 ml); purification by column chromatography (eluent: CHCl₃). Yellow glassy solid, C₁₀₆H₁₅₀F₈O₈Si₂, M = 1760.52 g/mol, yield: 253 mg (87 %), mp.: 57.0 °C, ¹H-NMR (CDCl₃, 400 MHz): δ / ppm = 7.57 – 7.49 (8H, m, Aryl-H), 7.01 (2H, s, Aryl-H), 4.45 (2H, p, ³J_{H,H} = 5.6 Hz, -OCH-), 4.33 (2H, dd, ³J_{H,H} = 10.1, ³J_{H,H} = 5.1 Hz, -OCH₂-), 4.23 (2H, dd, ³J_{H,H} = 10.1, ³J_{H,H} = 5.6 Hz, -OCH₂-), 4.15 (2H, dd, ³J_{H,H} = 9.5, ³J_{H,H} = 6.5 Hz, -OCH₂-), 4.03 (4H, t, ³J_{H,H} = 6.5 Hz, -OCH₂-), 3.96 (2H, dd, ³J_{H,H} = 8.6, ³J_{H,H} = 5.6 Hz, -OCH₂-), 1.91 – 1.81 (4H, m, -CH₂-), 1.59 – 1.49 (4H, m, -CH₂-), 1.43 (6H, s, -OCH₃), 1.38 (6H, s, -OCH₃), 1.33 – 1.17 (72H, m, -CH₂-), 0.87 (18H, t, ³J_{H,H} = 6.9 Hz, -CH₃), 0.53 – 0.40 (16H, m, -SiCH₂-). ¹⁹F-NMR (CDCl₃, 376 MHz): δ / ppm = -137.40 – -137.67 (m, Aryl-F), -156.83 – -157.06 (m, Aryl-F). ²⁹Si-NMR (CDCl₃, 79 MHz): δ / ppm = 2.89 (Si).

1,4-Bis[8-(triheptylsilyl)octoxy]-2,5-bis{4-[2,3,5,6-tetrafluoro-4-(2,3-isopropylidene-2,3-dihydroxypropyl-1-oxy)phenylethynyl]phenylethynyl}benzene F8A: Synthesized from **4/8** (220 mg, 0.18 mmol), **5F** (158 mg, 0.39 mmol), [Pd(PPh₃)₄] (6.2 mg, 5.4·10⁻³ mmol), CuI (1.0 mg, 5.1·10⁻³ mmol) in NEt₃ (20 ml); purification by column chromatography (eluent: CHCl₃). Yellow solid, C₁₀₈H₁₅₄F₈O₈Si₂, M = 1788.57 g/mol, yield: 300 mg (94 %), mp.: 62.0 °C, ¹H-NMR (CDCl₃, 400 MHz): δ / ppm = 7.57 – 7.49 (8H, m, Aryl-H), 7.02 (2H, s, Aryl-H), 4.50 – 4.42 (2H, m, -OCH-), 4.33 (2H, dd, ³J_{H,H} = 10.1, ³J_{H,H} = 5.2 Hz, -OCH₂-), 4.24 (2H, dd, ³J_{H,H} = 10.1, ³J_{H,H} = 5.7 Hz, -OCH₂-), 4.16 (2H, dd, ³J_{H,H} = 7.9, ³J_{H,H} = 4.3 Hz, -OCH₂-), 4.04 (4H, t, ³J_{H,H} = 6.5 Hz, -OCH₂-), 3.96 (2H, dd, ³J_{H,H} = 8.6, ³J_{H,H} = 5.6 Hz, -OCH₂-), 1.92 – 1.80 (4H, m, -CH₂-), 1.60 – 1.50 (4H, m, -CH₂-), 1.43 (6H, s, -OCH₃), 1.38 (6H, s, -OCH₃), 1.34 – 1.18 (76H, m, -CH₂-), 0.87 (18H, t, ³J_{H,H} = 6.9 Hz, -CH₃), 0.51 - 0.41 (16H, m, -SiCH₂-). ¹⁹F-NMR (CDCl₃, 376 MHz): δ / ppm = -137.38 – -137.70 (m, Aryl-F), -156.82 – -157.12 (m, Aryl-F). ²⁹Si-NMR (CDCl₃, 79 MHz): δ / ppm = 2.89 (Si).

1,4-Bis[9-(triheptylsilyl)nonoxy]-2,5-bis{4-[2,3,5,6-tetrafluoro-4-(2,3-isopropylidene-2,3-dihydroxypropyl-1-oxy)phenylethynyl]phenylethynyl}benzene F9A: Synthesized from **4/9** (200 mg, 0.16 mmol), **5F** (141 mg, 0.35 mmol), [Pd(PPh₃)₄] (5.6 mg, 4.8·10⁻³ mmol), CuI (0.9 mg, 4.8·10⁻³ mmol) in NEt₃ (20 ml); purification by column chromatography (eluent: CHCl₃). Yellow solid, C₁₁₀H₁₅₈F₈O₈Si₂, M = 1816.62 g/mol, yield: 250 mg (87 %), mp.: 46.7 °C, ¹H-NMR (CDCl₃, 400 MHz): δ / ppm = 7.57 – 7.50 (8H, m, Aryl-H), 7.01 (2H, s, Aryl-H), 4.45 (2H, p, ³J_{H,H} = 5.6 Hz, -OCH-), 4.33 (2H, dd, ³J_{H,H} = 10.2, ³J_{H,H} = 5.1 Hz, -OCH₂-), 4.23 (2H, dd, ³J_{H,H} = 10.1, ³J_{H,H} = 5.6 Hz, -OCH₂-), 4.16 (2H, dd, ³J_{H,H} = 9.3, ³J_{H,H} = 6.5 Hz, -OCH₂-), 4.03 (4H, t, ³J_{H,H} = 6.5 Hz, -OCH₂-), 3.96 (2H, dd, ³J_{H,H} = 8.6, ³J_{H,H} = 5.6 Hz, -OCH₂-), 1.91 – 1.81 (4H, m, -CH₂-), 1.60 – 1.48 (4H, m, -CH₂-), 1.43 (6H, s, -OCH₃), 1.38 (6H, s, -OCH₃), 1.34 – 1.18 (80H, m, -CH₂-), 0.87 (18H, t, ³J_{H,H} = 6.9 Hz, -CH₃), 0.52 – 0.42 (16H, m, -SiCH₂-). ¹⁹F-NMR (CDCl₃, 376 MHz): δ / ppm = -137.30 – -137.74 (m, Aryl-F), -156.71 – -157.02 (m, Aryl-F). ²⁹Si-NMR (CDCl₃, 79 MHz): δ / ppm = 2.89 (Si).

1,4-Bis[10-(triheptylsilyl)decoxy]-2,5-bis{4-[2,3,5,6-tetrafluoro-4-(2,3-isopropylidene-2,3-dihydroxypropyl-1-oxy)phenylethynyl]phenylethynyl}benzene F10A: Synthesized from **4/10** (200 mg, 0.16 mmol), **5F** (138 mg, 0.34 mmol), [Pd(PPh₃)₄] (5.6 mg, 4.8·10⁻³ mmol), CuI (0.9 mg, 4.8·10⁻³ mmol) in NEt₃ (20 ml); purification by column chromatography (eluent: CHCl₃). Yellow solid, C₁₁₂H₁₆₂F₈O₈Si₂, M = 1844.68 g/mol, yield: 180 mg (63 %), mp.: 45.2 °C, ¹H-NMR (CDCl₃, 400 MHz): δ / ppm = 7.57 – 7.50 (8H, m, Aryl-H), 7.01 (2H, s, Aryl-H), 4.45 (2H, p, ³J_{H,H} = 5.6 Hz, -OCH-), 4.33 (2H, dd, ³J_{H,H} = 10.1, ³J_{H,H} = 5.2 Hz, -OCH₂-), 4.23 (2H, dd, ³J_{H,H} = 10.1, ³J_{H,H} = 5.6 Hz, -OCH₂-), 4.16 (2H, dd, ³J_{H,H} = 9.4, ³J_{H,H} = 6.4 Hz, -OCH₂-), 4.03 (4H, t, ³J_{H,H} = 6.5 Hz, -OCH₂-), 3.97 (2H, dd, ³J_{H,H} = 8.6, ³J_{H,H} = 5.7 Hz, -OCH₂-), 1.90 – 1.81 (4H, m, -CH₂-), 1.58 – 1.49 (4H, m, -CH₂-), 1.43 (6H, s, -OCH₃), 1.38 (6H, s, -OCH₃), 1.34 – 1.18 (84H, m, -CH₂-), 0.87 (18H, t, ³J_{H,H} = 7.2 Hz, -CH₃), 0.50 – 0.42 (16H, m, -SiCH₂-). ¹⁹F-NMR (CDCl₃, 376 MHz): δ / ppm = -137.34 – -137.61 (m, Aryl-F), -156.85 – -156.99 (m, Aryl-F). ²⁹Si-NMR (CDCl₃, 79 MHz): δ / ppm = 2.89 (Si).

1,4-Bis[11-(triheptylsilyl)undecoxy]-2,5-bis{4-[2,3,5,6-tetrafluoro-4-(2,3-isopropylidene-2,3-dihydroxypropyl-1-oxy)phenylethynyl]phenylethynyl}benzene F11A: Synthesized from **4/11** (200 mg, 0.15 mmol), **5F** (134 mg, 0.33 mmol), [Pd(PPh₃)₄] (5.2 mg, 4.5·10⁻³ mmol), CuI (0.9 mg, 4.5·10⁻³ mmol) in NEt₃ (20 ml); purification by column chromatography (eluent: CHCl₃). Yellow solid, C₁₁₄H₁₆₆F₈O₈Si₂, M = 1872.73 g/mol, yield: 270 mg (95 %), mp.: 64.3 °C, ¹H-NMR (CDCl₃, 500 MHz): δ / ppm = 7.58 – 7.51 (8H, m, Aryl-H), 7.02 (2H, s, Aryl-H), 4.51 – 4.43 (2H, m, -OCH-), 4.34 (2H, dd, ³J_{H,H} = 10.1, ³J_{H,H} = 5.1 Hz, -OCH₂-), 4.25 (2H, dd, ³J_{H,H} = 10.1, ³J_{H,H} = 5.6 Hz, -OCH₂-), 4.17 (2H, dd, ³J_{H,H} = 8.7, ³J_{H,H} = 6.4 Hz, -OCH₂-), 4.05 (4H, t, ³J_{H,H} = 6.5 Hz, -OCH₂-), 3.97 (2H, dd, ³J_{H,H} = 8.6, ³J_{H,H} = 5.6 Hz, -OCH₂-), 1.91 – 1.82 (4H, m, -CH₂-), 1.60 – 1.51 (4H, m, -CH₂-), 1.44 (6H, s, -OCH₃), 1.39 (6H, s, -OCH₃), 1.35 – 1.19 (88H, m, -CH₂-), 0.88 (18H, t, ³J_{H,H} = 7.0 Hz, -CH₃), 0.51 – 0.44 (16H, m, -SiCH₂-). ¹⁹F-NMR (CDCl₃, 470 MHz): δ / ppm = -137.39 – -137.63 (m, Aryl-F), -156.78 – -157.02 (m, Aryl-F). ²⁹Si-NMR (CDCl₃, 99 MHz): δ / ppm = 2.90 (Si).

1,4-Bis[12-(triheptylsilyl)dodecoxy]-2,5-bis{4-[2,3,5,6-tetrafluoro-4-(2,3-isopropylidene-2,3-dihydroxypropyl-1-oxy)phenylethynyl]phenylethynyl}benzene F12A: Synthesized from **4/12** (200 mg, 0.15 mmol), **5F** (132 mg, 0.33 mmol), [Pd(PPh₃)₄] (5.2 mg, 4.5·10⁻³ mmol), CuI (0.9 mg, 4.5·10⁻³ mmol) in NEt₃ (20 ml); purification by column chromatography (eluent: CHCl₃), Yellow solid, C₁₁₆H₁₇₈F₈O₈Si₂, M = 1756.86 g/mol, yield: 190 mg (67 %), mp.: 104.4 °C, ¹H-NMR (CDCl₃, 500 MHz): δ / ppm = 7.57 – 7.52 (8H, m, Aryl-H), 7.02 (2H, s, Aryl-H), 4.46 (2H, p, ³J_{H,H} = 5.7 Hz, -OCH-), 4.34 (2H, dd, ³J_{H,H} = 10.1, ³J_{H,H} = 5.1 Hz, -OCH₂-), 4.24 (2H, dd, ³J_{H,H} = 10.1, ³J_{H,H} = 5.6 Hz, -OCH₂-), 4.17 (2H, dd, ³J_{H,H} = 7.3, ³J_{H,H} = 4.5 Hz, -OCH₂-), 4.04 (4H, t, ³J_{H,H} = 6.5 Hz, -OCH₂-), 3.97 (2H, dd, ³J_{H,H} = 8.6, ³J_{H,H} = 5.6 Hz, -OCH₂-), 1.90 – 1.83 (4H, m, -CH₂-), 1.59 – 1.51 (4H, m, -CH₂-), 1.44 (6H, s, -OCH₃), 1.39 (6H, s, -OCH₃), 1.36 – 1.20 (92H, m, -CH₂-), 0.88 (18H, t, ³J_{H,H} = 7.0 Hz, -CH₃), 0.52 – 0.43 (16H, m, -SiCH₂-). ¹⁹F-NMR (CDCl₃, 470 MHz): δ / ppm = -137.36 – -137.68 (m, Aryl-F), -156.84 – -157.02 (m, Aryl-F). ²⁹Si-NMR (CDCl₃, 99 MHz): δ / ppm = 2.90 (Si).

4.3 Syntheses of compounds Hn and Fn

1,4-Bis[ω-(triheptylsilyl)alkyloxy]-2,5-bis{4-[4-(2,3-dihydroxypropyl-1-oxy)phenylethynyl]phenylethynyl}benzenes (Hn) and 1,4-bis[ω-(triheptylsilyl)alkyloxy]-2,5-bis{4-[2,3,5,6-tetrafluoro-4-(2,3-dihydroxypropyl-1-oxy)phenylethynyl]phenylethynyl}benzene (Fn): A mixture of the appropriate isopropylidene acetal **HnA** or **FnA** (1 equ.) and PPTS (2 equ.) was dissolved in THF/MeOH (1:1, 60 ml) and stirred at 50 °C for 24 h.^{S16} After finishing the reaction, the solvent was removed in a rotatory evaporator and the residue dissolved in CH₂Cl₂. The organic layer was washed with NaHCO₃ solution (3 x 50 ml), water, and brine (50 ml each). After drying over Na₂SO₄ the solvent was removed by rotatory evaporation and the residue was purified by column chromatography (eluent: CHCl₃/MeOH = 9:1). The obtained product fractions are combined, evaporated to dryness, and recrystallized in MeOH/THF.

1,4-Bis[3-(triheptylsilyl)propoxy]-2,5-bis{4-[4-(2,3-dihydroxypropyl-1-oxy)phenylethynyl]phenylethynyl}benzene (H3): Synthesized from **H3A** (140 mg, 0.09 mmol), PPTS (47 mg, 0.19 mmol) in MeOH/THF (1:1, 30 ml : 30 ml); purification by column chromatography (eluent: CHCl₃/MeOH = 9:1). Yellowish solid, C₉₂H₁₃₄O₈Si₂, M = 1424.25 g/mol, yield: 94.3 mg (71 %), mp.: 70 °C, ¹H-NMR (500 MHz, Pyridine-d₅): δ / ppm = 7.73 (4H, d, ³J_{H,H} = 8.1 Hz, Aryl-H), 7.67 (4H, d, ³J_{H,H} = 8.0 Hz, Aryl-H), 7.60 (4H, d, ³J_{H,H} = 7.8 Hz, Aryl-H), 7.49 (2H, s, Aryl-H), 7.06 (4H, d, ³J_{H,H} = 8.8 Hz, Aryl-H), 4.56 – 4.49 (2H, m, -OCH-), 4.46 (2H, dd, ³J_{H,H} = 9.6, ³J_{H,H} = 4.3 Hz, -OCH₂-), 4.38 (2H, dd, ³J_{H,H} = 9.6, ³J_{H,H} = 6.3 Hz, -OCH₂-), 4.21 – 4.14 (8H, m, -OCH₂-), 2.05 – 1.95 (4H, m, -CH₂-), 1.49 – 1.19 (60H, m, -CH₂-), 0.98 – 0.91 (4H, m, -SiCH₂-), 0.86 (18H, t, ³J_{H,H} = 6.7 Hz, -CH₃), 0.72 – 0.64 (12H, m, -SiCH₂-). ¹³C-NMR (126 MHz, Pyridine-d₅): δ / ppm = 160.05, 154.07 (C_{Aryl}-O), 133.34, 131.81, 131.71 (C_{Aryl}-H), 124.04, 123.37 (C_{Aryl}-quart), 117.39, 115.16 (C_{Aryl}-H), 114.95, 114.42 (C_{Aryl}-quart), 95.16, 92.42, 88.92, 88.27 (-C≡C-), 72.18, 71.09, 70.84, 64.01 (-OCH-, -OCH₂-), 33.99, 31.92, 29.08, 24.24, 24.11, 22.79 (-CH₂-), 14.08 (-CH₃), 12.60, 8.78 (-SiCH₂-). ²⁹Si-NMR (99 MHz, Pyridine-d₅): δ / ppm = 3.47 (Si). HRMS (m/z): [M]⁺Cl⁻ calcd. For C₉₂H₁₃₄O₈Si₂Cl, 1486.9644; found: 1486.9617.

1,4-Bis[4-(triheptylsilyl)butoxy]-2,5-bis{4-[4-(2,3-dihydroxypropyl-1-oxy)phenylethynyl]phenylethynyl}benzene (H4): Synthesized from **H4A** (270 mg, 0.17 mmol), PPTS (89 mg, 0.35 mmol) in MeOH/THF (1:1, 30 ml : 30 ml); purification by column chromatography (eluent: CHCl₃/MeOH = 9:1). Yellowish solid, C₉₄H₁₃₈O₈Si₂, M = 1452.30 g/mol, yield: 183.7 mg (72 %), mp.: 91 °C, ¹H-NMR (400 MHz, Pyridine-d₅): δ / ppm = 7.76 (4H, d, ³J_{H,H} = 8.4 Hz, Aryl-H), 7.69 (4H, d, ³J_{H,H} = 8.3 Hz, Aryl-H), 7.61 (4H, d, ³J_{H,H} = 8.9 Hz, Aryl-H), 7.48 (2H, s, Aryl-H), 7.08 (4H, d, ³J_{H,H} = 8.6 Hz, Aryl-H), 4.57 – 4.50 (2H, m, -OCH-), 4.48 (2H, dd, ³J_{H,H} = 9.6, ³J_{H,H} = 4.3 Hz, -OCH₂-), 4.39 (2H, dd, ³J_{H,H} = 9.6, ³J_{H,H} = 6.3 Hz, -OCH₂-),

4.24 – 4.17 (8H, m, -OCH₂-), 2.05 – 1.96 (4H, m, -CH₂-), 1.83 – 1.72 (4H, m, -CH₂-), 1.54 – 1.20 (60H, m, -CH₂-), 0.88 (18H, t, ³J_{H,H} = 7.0 Hz, -CH₃), 0.80 – 0.62 (16H, m, -SiCH₂-). ¹³C-NMR (101 MHz, Pyridine-d₅): δ / ppm = 160.06, 154.09 (C_{Aryl}-O), 133.36, 131.84, 131.76 (C_{Aryl}-H), 123.95, 123.35 (C_{Aryl}-quart), 117.14, 115.17 (C_{Aryl}-H), 114.98, 114.29 (C_{Aryl}-quart), 95.21, 92.42, 88.94, 88.32 (-C≡C-), 71.11, 70.86, 68.93, 64.02 (-OCH-, -OCH₂-), 34.01, 33.36, 31.93, 29.12, 24.16, 22.80, 20.65 (-CH₂-), 14.10 (-CH₃), 12.60, 12.30 (-SiCH₂-). ²⁹Si-NMR (79 MHz, Pyridine-d₅): δ / ppm = 3.11 (Si). HRMS (m/z): [M]+Cl⁻ calcd. For C₉₄H₁₃₈O₈Si₂Cl, 1458.9331; found: 1458.9332.

1,4-Bis[5-(triheptylsilyl)pentoxy]-2,5-bis[4-[4-(2,3-dihydroxypropyl-1-oxy)phenylethynyl]phenylethynyl]benzene (H5): Synthesized from H5A (150 mg, 0.10 mmol), PPTS (48 mg, 0.19 mmol) in MeOH/THF (1:1, 30 ml : 30 ml); purification by column chromatography (eluent: CHCl₃/MeOH = 9:1). Yellowish solid, C₉₆H₁₄₂O₈Si₂, M = 1480.35 g/mol, yield: 70.8 mg (50 %), mp.: 50 °C, ¹H-NMR (400 MHz, Pyridine-d₅): δ / ppm = 7.74 (4H, d, ³J_{H,H} = 8.2 Hz, Aryl-H), 7.66 (4H, d, ³J_{H,H} = 8.4 Hz, Aryl-H), 7.61 (4H, d, ³J_{H,H} = 8.6 Hz, Aryl-H), 7.45 (2H, s, Aryl-H), 7.08 (4H, d, ³J_{H,H} = 8.5 Hz, Aryl-H), 4.56 – 4.50 (2H, m, -OCH-), 4.48 (2H, dd, ³J_{H,H} = 9.6, ³J_{H,H} = 4.3 Hz, -OCH₂-), 4.39 (2H, dd, ³J_{H,H} = 9.5, ³J_{H,H} = 6.2 Hz, -OCH₂-), 4.21 – 4.13 (8H, m, -OCH₂-), 2.01 – 1.92 (4H, m, -CH₂-), 1.79 – 1.70 (4H, m, -CH₂-), 1.67 – 1.22 (64H, m, -CH₂-), 0.87 (18H, t, ³J_{H,H} = 7.0 Hz, -CH₃), 0.76 – 0.63 (16H, m, -SiCH₂-). ¹³C-NMR (101 MHz, Pyridine-d₅): δ / ppm = 160.06, 154.15 (C_{Aryl}-O), 133.36, 131.81, 131.73 (C_{Aryl}-H), 123.33, 123.00 (C_{Aryl}-quart), 117.30 (C_{Aryl}-H), 115.16 (C_{Aryl}-quart), 114.98 (C_{Aryl}-H), 114.40 (C_{Aryl}-quart), 95.17, 92.43, 88.94, 88.28 (-C≡C-), 71.10, 70.85, 69.55, 64.02 (-OCH-, -OCH₂-), 33.88, 31.85, 30.24, 28.99, 25.59, 23.93, 22.70, 23.93 (-CH₂-), 14.08 (-CH₃), 12.78, 12.62 (-SiCH₂-). ²⁹Si-NMR (79 MHz, Pyridine-d₅): δ / ppm = 3.00 (Si). HRMS (m/z): [M]+Cl⁻ calcd. For C₉₆H₁₄₂O₈Si₂Cl, 1514.9957; found: 1514.9947.

1,4-Bis[6-(triheptylsilyl)hexoxy]-2,5-bis[4-[4-(2,3-dihydroxypropyl-1-oxy)phenylethynyl]phenylethynyl]benzene (H6): Synthesized from H6A (210 mg, 0.13 mmol), PPTS (66 mg, 0.26 mmol) in MeOH/THF (1:1, 30 ml : 30 ml); purification by column chromatography (eluent: CHCl₃/MeOH = 9:1). Yellowish solid, C₉₈H₁₄₆O₈Si₂, M = 1508.41 g/mol, yield: 139.2 mg (70 %), mp. 54 °C, ¹H-NMR (400 MHz, Pyridine-d₅): δ / ppm = 7.75 (4H, d, ³J_{H,H} = 8.3 Hz, Aryl-H), 7.68 (4H, d, ³J_{H,H} = 8.3 Hz, Aryl-H), 7.62 (4H, d, ³J_{H,H} = 8.9 Hz, Aryl-H), 7.45 (2H, s, Aryl-H), 7.08 (4H, d, ³J_{H,H} = 8.9 Hz, Aryl-H), 4.58 – 4.51 (2H, m, -OCH-), 4.49 (2H, dd, ³J_{H,H} = 9.6, ³J_{H,H} = 4.3 Hz, -OCH₂-), 4.40 (2H, dd, ³J_{H,H} = 9.6, ³J_{H,H} = 6.2 Hz, -OCH₂-), 4.24 – 4.18 (4H, m, -OCH₂-), 4.15 (4H, t, ³J_{H,H} = 6.3 Hz, -OCH₂-), 1.98 – 1.88 (4H, m, -CH₂-), 1.75 – 1.66 (4H, m, -CH₂-), 1.61 – 1.18 (68H, m, -CH₂-), 0.87 (18H, d, ³J_{H,H} = 6.6 Hz, -CH₃), 0.74 – 0.63 (16H, m, -SiCH₂-). ¹³C-NMR (101 MHz, Pyridine-d₅): δ / ppm = 160.07, 154.11 (C_{Aryl}-O), 133.37, 131.82, 131.76 (C_{Aryl}-H), 123.97 (C_{Aryl}-quart), 117.24, 115.18 (C_{Aryl}-H), 115.00, 114.36 (C_{Aryl}-quart), 95.21, 92.45, 88.95, 88.32 (-C≡C-), 71.12, 70.87, 69.54, 64.03 (-OCH-, -OCH₂-), 33.98, 33.75, 31.91, 29.45, 29.10, 25.95, 24.24, 24.15, 22.79 (-CH₂-), 14.08 (-CH₃), 12.63 (-SiCH₂-). ²⁹Si-NMR (79 MHz, Pyridine-d₅): δ / ppm = 3.02 (Si). HRMS (m/z): [M]+Cl⁻ calcd. For C₉₈H₁₄₆O₈Si₂Cl, 1543.0270; found: 1543.0297.

1,4-Bis[7-(triheptylsilyl)hepoxy]-2,5-bis[4-[4-(2,3-dihydroxypropyl-1-oxy)phenylethynyl]phenylethynyl]benzene (H7): Synthesized from H7A (260 mg, 0.16 mmol), PPTS (81 mg, 0.32 mmol) in MeOH/THF (1:1, 30 ml : 30 ml); purification by column chromatography (eluent: CHCl₃/MeOH = 9:1). Yellowish solid, C₁₀₀H₁₅₀O₈Si₂, M = 1536.46 g/mol, yield: 118.7 mg (48 %), mp.: 77 °C, ¹H-NMR (500 MHz, Pyridine-d₅): δ / ppm = 7.78 (4H, d, ³J_{H,H} = 8.0 Hz, Aryl-H), 7.70 (4H, d, ³J_{H,H} = 8.1 Hz, Aryl-H), 7.66 (4H, d, ³J_{H,H} = 8.5 Hz, Aryl-H), 7.48 (2H, s, Aryl-H), 7.12 (4H, d, ³J_{H,H} = 8.4 Hz, Aryl-H), 4.61 – 4.54 (2H, m, -OCH-), 4.52 (2H, dd, ³J_{H,H} = 9.6, ³J_{H,H} = 4.2 Hz, -OCH₂-), 4.43 (2H, dd, ³J_{H,H} = 9.5, ³J_{H,H} = 6.3 Hz, -OCH₂-), 4.27 – 4.19 (4H, m, -OCH₂-), 4.16 (4H, t, ³J_{H,H} = 6.4 Hz, -OCH₂-), 2.00 – 1.90 (4H, m, -CH₂-), 1.74 – 1.64 (4H, m, -CH₂-), 1.58 – 1.27 (72H, m, -CH₂-), 0.91 (18H, t, J = 6.9 Hz, -CH₃), 0.75 – 0.67 (16H, m, -SiCH₂-). ¹³C-NMR (126 MHz, Pyridine-d₅): δ / ppm = 160.31, 154.36 (C_{Aryl}-O), 133.61, 132.06, 132.00 (C_{Aryl}-H), 125.46, 125.04 (C_{Aryl}-quart), 117.51, 115.41 (C_{Aryl}-H), 115.23, 114.60 (C_{Aryl}-quart), 95.44, 92.69, 89.16, 88.55 (-C≡C-), 71.35, 71.10, 69.82, 64.27 (-OCH-, -OCH₂-), 34.34, 34.22, 32.14, 29.73, 29.42, 29.33,

26.51, 24.39, 24.37, 23.03 (-CH₂-), 15.57 (-CH₃), 14.22, 14.16 (-SiCH₂-). ²⁹Si-NMR (99 MHz, Pyridine-d₅): δ / ppm = 2.99 (Si). HRMS (m/z): [M]+Cl⁻ calcd. For C₁₀₂H₁₅₄O₈Si₂Cl, 1571.0583; found: 1571.0620.

1,4-Bis[8-(triheptylsilyloxy)-2,5-bis{4-[4-(2,3-dihydroxypropyl-1-oxy)phenylethynyl]phenylethynyl}benzene (H8): Synthesized from H8A (180 mg, 0.11 mmol), PPTS (55 mg, 0.22 mmol) in MeOH/THF (1:1, 30 ml : 30 ml); purification by column chromatography (eluent: CHCl₃/MeOH = 9:1). Yellow solid, C₁₀₂H₁₅₄O₈Si₂, M = 1564.54 g/mol, yield: 164.5 mg (96 %), mp.: 50 °C, ¹H-NMR (400 MHz, Pyridine-d₅): δ / ppm = 7.76 (4H, d, ³J_{H,H} = 8.3 Hz, Aryl-H), 7.68 (4H, d, ³J_{H,H} = 8.3 Hz, Aryl-H), 7.63 (4H, d, ³J_{H,H} = 8.4 Hz, Aryl-H), 7.46 (2H, s, Aryl-H), 7.09 (4H, d, ³J_{H,H} = 8.4 Hz, Aryl-H), 4.59 – 4.53 (2H, m, -OCH-), 4.49 (2H, dd, ³J_{H,H} = 9.5, ³J_{H,H} = 4.3 Hz, -OCH₂-), 4.40 (2H, dd, ³J_{H,H} = 9.5, ³J_{H,H} = 6.3 Hz, -OCH₂-), 4.23 – 4.19 (4H, m, -OCH₂-), 4.12 (4H, t, ³J_{H,H} = 6.4 Hz, -OCH₂-), 1.96 – 1.84 (4H, m, -CH₂-), 1.70 – 1.59 (4H, m, -CH₂-), 1.54 – 1.19 (76H, m, -CH₂-), 0.94 – 0.84 (18H, m, -CH₃), 0.72 – 0.64 (16H, m, -SiCH₂-). ¹³C-NMR (101 MHz, Pyridine-d₅): δ / ppm = 160.06, 154.08 (C_{Aryl}-O), 133.39, 131.84, 131.76 (C_{Aryl}-H), 123.97 (C_{Aryl}-quart), 117.22, 115.17 (C_{Aryl}-H), 114.94, 114.31 (C_{Aryl}-quart), 95.20, 92.47, 88.94, 88.32 (-C≡C-), 71.12, 70.86, 69.48, 64.04 (-OCH-, -OCH₂-), 33.99, 33.97, 31.90, 29.45, 29.43, 29.10 (4C), 26.26, 24.18, 24.16, 22.80 (-CH₂-), 14.10 (-CH₃), 12.66, 12.63 (-SiCH₂-). ²⁹Si-NMR (79 MHz, Pyridine-d₅): δ / ppm = 3.02 (Si). HRMS (m/z): [M]+Cl⁻ calcd. For C₁₀₂H₁₅₄O₈Si₂Cl, 1599.0896; found: 1599.0886.

1,4-Bis[9-(triheptylsilyloxy)-2,5-bis{4-[4-(2,3-dihydroxypropyl-1-oxy)phenylethynyl]phenylethynyl}benzene (H9): Synthesized from H9A (160 mg, 0.10 mmol), PPTS (48 mg, 0.19 mmol) in MeOH/THF (1:1, 30 ml : 30 ml); purification by column chromatography (eluent: CHCl₃/MeOH = 9:1). Yellow solid, C₁₀₄H₁₅₈O₈Si₂, M = 1592.57 g/mol, yield: 115.5 mg (76 %), mp.: 80 °C, ¹H-NMR (500 MHz, Pyridine-d₅): δ / ppm = 7.72 (4H, d, ³J_{H,H} = 8.3 Hz, Aryl-H), 7.65 (4H, d, ³J_{H,H} = 8.3 Hz, Aryl-H), 7.60 (4H, d, ³J_{H,H} = 8.8 Hz, Aryl-H), 7.43 (2H, s, Aryl-H), 7.06 (4H, d, ³J_{H,H} = 8.9 Hz, Aryl-H), 4.54 – 4.49 (2H, m, -OCH-), 4.46 (2H, dd, ³J_{H,H} = 9.5, ³J_{H,H} = 4.4 Hz, -OCH₂-), 4.37 (2H, dd, ³J_{H,H} = 9.5, ³J_{H,H} = 6.2 Hz, -OCH₂-), 4.18 – 4.16 (4H, m, -OCH₂-), 4.10 (4H, t, ³J_{H,H} = 6.4 Hz, -OCH₂-), 1.92 – 1.82 (4H, m, -CH₂-), 1.64 – 1.56 (4H, m, -CH₂-), 1.50 – 1.20 (80H, m, -CH₂-), 0.85 (18H, t, ³J_{H,H} = 6.8 Hz, -CH₃), 0.70 – 0.62 (16H, m, -SiCH₂-). ¹³C-NMR (126 MHz, Pyridine-d₅): δ / ppm = 160.04, 154.09 (C_{Aryl}-O), 133.35, 131.80, 131.73 (C_{Aryl}-H), 123.95, 123.51 (C_{Aryl}-quart), 117.27, 115.15 (C_{Aryl}-H), 114.97, 114.34 (C_{Aryl}-quart), 95.17, 92.43, 88.89, 88.30 (-C≡C-), 71.09, 70.83, 69.53, 64.01 (-OCH-, -OCH₂-), 34.03, 33.95, 31.87, 29.73, 29.49, 29.42, 29.36, 29.07, 26.21, 24.15, 24.12, 22.76 (-CH₂-), 14.06 (-CH₃), 12.67, 12.64 (-SiCH₂-). ²⁹Si-NMR (99 MHz, Pyridine-d₅): δ / ppm = 3.01 (Si). HRMS (m/z): [M]+Cl⁻ calcd. For C₁₀₄H₁₅₈O₈Si₂Cl, 1627.1209; found: 1627.1231.

1,4-Bis[10-(triheptylsilyloxy)-2,5-bis{4-[4-(2,3-dihydroxypropyl-1-oxy)phenylethynyl]phenylethynyl}benzene (H10): Synthesized from H10A (145 mg, 0.09 mmol), PPTS (43 mg, 0.17 mmol) in MeOH/THF (1:1, 30 ml : 30 ml); purification by column chromatography (eluent: CHCl₃/MeOH = 9:1). Yellow solid, C₁₀₆H₁₆₂O₈Si₂, M = 1620.62 g/mol, yield: 120.6 mg (88 %), mp.: 83 °C, ¹H-NMR (400 MHz, Pyridine-d₅): δ / ppm = 7.74 (4H, d, ³J_{H,H} = 8.2 Hz, Aryl-H), 7.66 (4H, d, ³J_{H,H} = 8.1 Hz, Aryl-H), 7.61 (4H, d, ³J_{H,H} = 9.0 Hz, Aryl-H), 7.45 (2H, s, Aryl-H), 7.08 (4H, d, ³J_{H,H} = 8.9 Hz, Aryl-H), 4.57 – 4.51 (2H, m, -OCH-), 4.48 (2H, dd, ³J_{H,H} = 9.5, ³J_{H,H} = 4.3 Hz, -OCH₂-), 4.39 (2H, dd, ³J_{H,H} = 9.5, ³J_{H,H} = 6.2 Hz, -OCH₂-), 4.21 – 4.17 (4H, m, -OCH₂-), 4.11 (4H, t, ³J_{H,H} = 6.4 Hz, -OCH₂-), 1.94 – 1.83 (4H, m, -CH₂-), 1.67 – 1.54 (4H, m, -CH₂-), 1.52 – 1.22 (84H, m, -CH₂-), 0.87 (18H, t, ³J_{H,H} = 6.2 Hz, -CH₃), 0.74 – 0.63 (16H, m, -SiCH₂-). ¹³C-NMR (101 MHz, Pyridine-d₅): δ / ppm = 160.05, 154.10 (C_{Aryl}-O), 133.37, 131.82, 131.74 (C_{Aryl}-H), 123.96 (C_{Aryl}-quart), 117.28, 115.17 (C_{Aryl}-H), 114.98, 114.35 (C_{Aryl}-quart), 95.19, 92.44, 88.91, 88.31 (-C≡C-), 71.11, 70.85, 69.53, 64.03 (-OCH-, -OCH₂-), 34.03, 33.97, 31.89, 29.81, 29.67, 29.48, 29.46, 29.44, 29.08, 26.20, 24.16, 24.14, 22.78 (-CH₂-), 14.07 (-CH₃), 12.67, 12.65 (-SiCH₂-). ²⁹Si-NMR (79 MHz, Pyridine-d₅): δ / ppm = 3.03 (Si). HRMS (m/z): [M]+Cl⁻ calcd. For C₁₀₆H₁₆₂O₈Si₂Cl, 1655.1522; found: 1655.1536.

1,4-Bis[11-(triheptylsilyl)undecoxy]-2,5-bis{4-[4-(2,3-dihydroxypropyl-1-oxy)phenylethynyl]phenylethynyl}benzene (H11): Synthesized from **H11A** (270 mg, 0.16 mmol), PPTS (79 mg, 0.31 mmol) in MeOH/THF (1:1, 30 ml : 30 ml); purification by column chromatography (eluent: CHCl₃/MeOH = 9:1). Yellow solid, C₁₀₈H₁₆₆O₈Si₂, M = 1648.68 g/mol, yield: 138.5 mg (53 %), mp.: 78.0 °C, ¹H-NMR (400 MHz, Pyridine-d₅): δ / ppm = 7.75 (4H, d, ³J_{H,H} = 8.3 Hz, Aryl-H), 7.67 (4H, d, ³J_{H,H} = 8.2 Hz, Aryl-H), 7.62 (4H, d, ³J_{H,H} = 8.0 Hz, Aryl-H), 7.46 (2H, s, Aryl-H), 7.11 – 7.05 (4H, m, Aryl-H), 4.60 – 4.51 (2H, m, -OCH-), 4.49 (2H, dd, ³J_{H,H} = 9.5, ³J_{H,H} = 4.3 Hz, -OCH₂-), 4.40 (2H, dd, ³J_{H,H} = 9.5, ³J_{H,H} = 6.2 Hz, -OCH₂-), 4.24 – 4.16 (4H, m, -OCH₂-), 4.12 (4H, t, ³J_{H,H} = 6.4 Hz, -OCH₂-), 1.93 – 1.84 (4H, m, -CH₂-), 1.60 (4H, m, -CH₂-), 1.54 – 1.22 (88H, m, -CH₂-), 0.88 (18H, t, ³J_{H,H} = 6.6 Hz, -CH₃), 0.73 – 0.64 (16H, m, -SiCH₂-). ¹³C-NMR (101 MHz, Pyridine-d₅): δ / ppm = 160.07, 154.12 (C_{Aryl}-O), 133.38, 131.83, 131.75 (C_{Aryl}-H), 123.97, (C_{Aryl}-quart), 117.30, 115.18 (C_{Aryl}-H), 114.98, 114.36 (C_{Aryl}-quart), 95.20, 92.45, 88.92, 88.32 (-C≡C-), 71.11, 70.86, 69.55, 64.04 (-OCH-, -OCH₂-), 34.04, 33.97, 31.89, 29.78, 29.75 (4C), 29.46 (4C), 29.44, 29.08, 26.21, 24.17, 24.14, 22.78 (-CH₂-), 14.07 (-CH₃), 12.66, (-SiCH₂-). ²⁹Si-NMR (79 MHz, Pyridine-d₅): δ / ppm = 3.04 (Si). HRMS (m/z): [M]+Cl⁻ calcd. For C₁₀₈H₁₆₆O₈Si₂Cl, 1683.1835; found: 1683.1785.

1,4-Bis[12-(triheptylsilyl)dodecoxy]-2,5-bis{4-[4-(2,3-dihydroxypropyl-1-oxy)phenylethynyl]phenylethynyl}benzene (H12): Synthesized from **H12A** (140 mg, 0.08 mmol), PPTS (40 mg, 0.16 mmol) in MeOH/THF (1:1, 30 ml : 30 ml); purification by column chromatography (eluent: CHCl₃/MeOH = 9:1). Yellow solid, C₁₁₀H₁₇₀O₈Si₂, M = 1685.18 g/mol, yield: 82.6 mg (62 %), mp.: 84 °C, ¹H-NMR (400 MHz, Pyridine-d₅): δ / ppm = 7.78 (4H, d, ³J_{H,H} = 8.2 Hz, Aryl-H), 7.70 (4H, d, ³J_{H,H} = 8.2 Hz, Aryl-H), 7.65 (4H, d, ³J_{H,H} = 8.9 Hz, Aryl-H), 7.49 (2H, s, Aryl-H), 7.11 (4H, d, ³J_{H,H} = 9.9 Hz, Aryl-H), 4.61 – 4.54 (2H, m, -OCH-), 4.52 (2H, dd, ³J_{H,H} = 9.5, ³J_{H,H} = 4.3 Hz, -OCH₂-), 4.43 (2H, dd, ³J_{H,H} = 9.5, ³J_{H,H} = 6.2 Hz, -OCH₂-), 4.25 – 4.21 (2H, m, -OCH₂-), 4.15 (4H, t, ³J_{H,H} = 6.4 Hz, -OCH₂-), 1.98 – 1.86 (4H, m, -CH₂-), 1.69 – 1.58 (4H, m, -CH₂-), 1.57 – 1.25 (92H, m, -CH₂-), 0.91 (18H, t, ³J_{H,H} = 6.7 Hz, -CH₃), 0.77 – 0.67 (16H, m, -SiCH₂-). ¹³C-NMR (101 MHz, Pyridine-d₅): δ / ppm = 160.06, 154.11 (C_{Aryl}-O), 133.37, 131.82, 131.75 (C_{Aryl}-H), 123.97 (C_{Aryl}-quart), 117.29, 115.17 (C_{Aryl}-H), 114.98, 114.35 (C_{Aryl}-quart), 95.20, 92.45, 88.91, 88.31 (-C≡C-), 71.10, 70.85, 69.54, 64.03 (-OCH-, -OCH₂-), 34.03, 33.96, 31.88, 29.84, 29.77, 29.74, 29.72, 29.47 (4C), 29.44, 29.08, 26.20, 24.14 (4C), 22.78 (-CH₂-), 14.07 (-CH₃), 12.65 (-SiCH₂-). ²⁹Si-NMR (79 MHz, Pyridine-d₅): δ / ppm = 3.03 (Si). HRMS (m/z): [M]+Cl⁻ calcd. For C₁₁₀H₁₇₀O₈Si₂Cl, 1711.2148; found: 1711.2149.

1,4-Bis[3-(triheptylsilyl)propoxy]-2,5-bis{4-[2,3,5,6-tetrafluoro-4-(2,3-dihydroxypropyl-1-oxy)phenylethynyl]phenylethynyl}benzene (F3): Synthesized from **F3A** (152.5 mg, 0.09 mmol), PPTS (47 mg, 0.19 mmol) in MeOH/THF (1:1, 30 ml : 30 ml); purification by column chromatography (eluent: CHCl₃/MeOH = 9:1). Yellow solid, C₉₂H₁₂₆F₈O₈Si₂, M = 1568.17 g/mol, yield: 87.9 mg (61 %), mp.: 44 °C, ¹H-NMR (500 MHz, Pyridine-d₅): δ / ppm = 7.75 (4H, d, ³J_{H,H} = 8.3 Hz, Aryl-H), 7.69 (4H, d, ³J_{H,H} = 8.3 Hz, Aryl-H), 7.51 (2H, s, Aryl-H), 4.88 – 4.82 (2H, m, -OCH₂-), 4.79 – 4.72 (2H, m, -OCH₂-), 4.54 – 4.47 (2H, m, -OCH-), 4.21 – 4.15 (8H, m, -OCH₂-), 2.05 – 1.96 (4H, m, -CH₂-), 1.49 – 1.22 (60H, m, -CH₂-), 0.98 – 0.92 (4H, m, -SiCH₂-), 0.87 (18H, t, ³J_{H,H} = 7.6 Hz, -CH₃), 0.72 – 0.65 (12H, m, -SiCH₂-). ¹³C-NMR (126 MHz, Pyridine-d₅): δ / ppm = 154.11 (C_{Aryl}-O), 146.43, 142.14 (m, C_{Aryl}-F), 139.55 (C_{Aryl}-O), 132.09, 131.88 (C_{Aryl}-H), 124.81, 121.85, 117.41, 114.37, 99.94 (C_{Aryl}, -C≡C-), 97.20 (m, C_{Aryl}-quart.), 94.87, 89.64 (-C≡C-), 77.54 (m, C_{Aryl}-O-CH₂-), 76.36 (-C≡C-), 72.18, 71.71, 63.50 (-OCH-, -OCH₂-), 33.99, 31.92, 29.09, 24.22, 24.11, 22.78 (-CH₂-), 14.05 (-CH₃), 12.59, 8.76 (-SiCH₂-). ¹⁹F-NMR (470 MHz, Pyridine-d₅): δ / ppm = -138.57 – -138.93 (m, C_{Aryl}-F), -156.73 – -157.09 (m, C_{Aryl}-F). ²⁹Si-NMR (99 MHz, Pyridine-d₅): δ / ppm = 3.47 (Si). HRMS (m/z): [M]+Cl⁻ calcd. For C₉₂H₁₂₆F₈O₈Si₂Cl, 1602.8577; found: 1062.8609.

1,4-Bis[4-(triheptylsilyl)butoxy]-2,5-bis{4-[2,3,5,6-tetrafluoro-4-(2,3-dihydroxypropyl-1-oxy)phenylethynyl]phenylethynyl}benzene (F4): Synthesized from **F4A** (390 mg, 0.23 mmol), PPTS (117 mg, 0.47 mmol) in MeOH/THF (1:1, 30 ml : 30 ml); purification by column chromatography (eluent:

CHCl₃/MeOH = 9:1). Yellow solid, C₉₄H₁₃₀F₈O₈Si₂, M = 1596.22 g/mol, yield: 235.6 mg (63 %), mp.: 50.3 °C, **¹H-NMR** (400 MHz, Pyridine-d₅): δ / ppm = 7.78 (4H, d, ³J_{H,H} = 8.3 Hz, Aryl-H), 7.72 (4H, d, ³J_{H,H} = 8.3 Hz, Aryl-H), 7.50 (2H, s, Aryl-H), 4.90 – 4.83 (2H, m, -OCH₂-), 4.80 – 4.73 (2H, m, -OCH₂-), 4.57 – 4.48 (2H, m, -OCH-), 4.25 – 4.15 (8H, m, -OCH₂-), 2.08 – 1.96 (4H, m, -CH₂-), 1.85 – 1.72 (4H, m, -CH₂-), 1.54 – 1.22 (60H, m, -CH₂-), 0.90 (18H, t, ³J_{H,H} = 8.0 Hz, -CH₃), 0.80 – 0.60 (16H, m, -SiCH₂-). **¹³C-NMR** (101 MHz, Pyridine-d₅): δ / ppm = 154.15 (C_{Aryl}-O), 146.10, 142.41 (m, C_{Aryl}-F), 132.15, 131.91 (C_{Aryl}-H), 124.87, 121.83, 117.13, 114.23, 99.97, (C_{Aryl}, -C≡C-), 97.23 (m, C_{Aryl}-quart.), 94.94, 89.66 (-C≡C-), 77.56 (C_{Aryl}-O-CH₂-), 76.39 (-C≡C-), 71.72, 68.92, 63.51 (-OCH-, -OCH₂-), 34.01, 33.33, 31.93, 29.12, 24.16, 22.80, 20.64 (-CH₂-), 14.07 (-CH₃), 12.60, 12.29 (-SiCH₂-). **¹⁹F-NMR** (376 MHz, Pyridine-d₅): δ / ppm = -138.50 – -138.86 (m, C_{Aryl}-F), -156.69 – -157.21 (m, C_{Aryl}-F). **²⁹Si-NMR** (79 MHz, Pyridine-d₅): δ / ppm = 3.12 (Si). **HRMS** (m/z): [M]+Cl⁻ calcd. For C₉₄H₁₃₀F₈O₈Si₂Cl, 1630.8890; found: 1630.8900.

1,4-Bis[5-(triheptylsilyl)pentoxy]-2,5-bis[4-[2,3,5,6,-tetrafluoro-4-(2,3-dihydroxypropyl)-1-oxy]phenylethynyl]phenylethynyl]benzene (F5): Synthesized from **F5A** (140 mg, 0.09 mmol), PPTS (44 mg, 0.17 mmol) in MeOH/THF (1:1, 30 ml : 30 ml); purification by column chromatography (eluent: CHCl₃/MeOH = 9:1). Yellow solid, C₉₆H₁₃₄F₈O₈Si₂, M = 1536.46 g/mol, yield: 78.9 mg (59.3 %), mp.: - °C, **¹H-NMR** (400 MHz, Pyridine-d₅): δ / ppm = 7.76 (4H, d, J = 8.4 Hz, Aryl-H), 7.69 (4H, d, J = 8.4 Hz, Aryl-H), 7.47 (2H, s, Aryl-H), 4.86 (2H, dd, J = 10.2, 4.0 Hz, -OCH-), 4.76 (2H, dd, J = 10.2, 6.2 Hz, -OCH₂-), 4.56 – 4.48 (2H, m, -OCH₂-), 4.21 – 4.14 (8H, m, -OCH₂-), 2.03 – 1.93 (4H, m, -CH₂-), 1.82 – 1.71 (4H, m, -CH₂-), 1.62 – 1.52 (4H, m, -CH₂-), 1.51 – 1.23 (64H, m, -CH₂-), 0.90 (18H, t, J = 6.7 Hz, -CH₃), 0.76 – 0.63 (16H, m, -SiCH₂-). **¹³C-NMR** (101 MHz, Pyridine-d₅): δ / ppm = 154.22 (C_{Aryl}-O), 146.10, 142.41 (m, C_{Aryl}-F), 139.97 (C_{Aryl}-O), 132.12, 131.88 (C_{Aryl}-H), 124.84, 121.83, 117.29, 114.35, 99.95, (C_{Aryl}, -C≡C-), 97.25 (m, C_{Aryl}-quart.), 94.90, 89.66 (-C≡C-), 77.58 (d, C_{Aryl}-O-CH₂-), 76.39 (-C≡C-), 71.72, 69.55, 63.51 (-OCH-, -OCH₂-), 33.98, 31.91, 30.47, 29.18, 29.09, 24.14, 23.95, 22.78 (-CH₂-), 14.06 (-CH₃), 12.62, 12.60 (-SiCH₂-). **¹⁹F-NMR** (376 MHz, Pyridine-d₅): δ / ppm = -138.48 – -138.85 (m, C_{Aryl}-F), -156.74 – -157.03 (m, C_{Aryl}-F). **²⁹Si-NMR** (79 MHz, Pyridine-d₅): δ / ppm = 3.00 (Si). **HRMS** (m/z): [M]+Cl⁻ calcd. For C₉₆H₁₃₄F₈O₈Si₂Cl, 1658.9203; found: 1658.9228.

1,4-Bis[6-(triheptylsilyl)hexoxy]-2,5-bis[4-[2,3,5,6,-tetrafluoro-4-(2,3-dihydroxypropyl)-1-oxy]phenylethynyl]phenylethynyl]benzene (F6): Synthesized from **F6A** (210 mg, 0.12 mmol), PPTS (61 mg, 0.24 mmol) in MeOH/THF (1:1, 30 ml : 30 ml); purification by column chromatography (eluent: CHCl₃/MeOH = 9:1). Yellow solid, C₉₈H₁₃₈F₈O₈Si₂, M = 1652.33 g/mol, yield: 113.8 mg (57 %), mp.: < 20 °C, **¹H-NMR** (400 MHz, Pyridine-d₅): δ / ppm = 7.77 (4H, d, ³J_{H,H} = 8.3 Hz, Aryl-H), 7.70 (4H, d, ³J_{H,H} = 8.3 Hz, Aryl-H), 7.47 (2H, s, Aryl-H), 4.90 – 4.84 (2H, m, -OCH₂-), 4.81 – 4.73 (2H, m, -OCH₂-), 4.57 – 4.49 (2H, m, -OCH-), 4.22 – 4.18 (4H, m, -OCH₂-), 4.16 (4H, t, ³J_{H,H} = 6.3 Hz, -OCH₂-), 2.00 – 1.88 (4H, m, -CH₂-), 1.79 – 1.66 (4H, m, -CH₂-), 1.61 – 1.21 (68H, m, -CH₂-), 0.88 (18H, t, ³J_{H,H} = 7.0 Hz, -CH₃), 0.73 – 0.62 (16H, m, -SiCH₂-). **¹³C-NMR** (101 MHz, Pyridine-d₅): δ / ppm = 154.17 (C_{Aryl}-O), 132.15, 131.88 (C_{Aryl}-H), 124.84, 121.84, 117.23, 114.31 (C_{Aryl}), 94.94, 89.67 (-C≡C-), 77.59 (C_{Aryl}-O-CH₂-), 71.73, 69.54, 63.52 (-OCH-, -OCH₂-), 33.98, 33.75, 31.90, 29.44, 29.10, 25.96, 24.25, 24.14, 22.78 (-CH₂-), 14.06 (-CH₃), 12.64, 12.62 (-SiCH₂-). **¹⁹F-NMR** (376 MHz, Pyridine-d₅): δ / ppm = -138.49 – -138.84 (m, C_{Aryl}-F), -156.78 – -157.08 (m, C_{Aryl}-F). **²⁹Si-NMR** (79 MHz, Pyridine-d₅): δ / ppm = 3.01 (Si). **HRMS** (m/z): [M]+Cl⁻ calcd. For C₉₈H₁₃₈F₈O₈Si₂Cl, 1686.9516; found: 1686.9504.

1,4-Bis[7-(triheptylsilyl)heptoxy]-2,5-bis[4-[2,3,5,6,-tetrafluoro-4-(2,3-dihydroxypropyl)-1-oxy]phenylethynyl]phenylethynyl]benzene (F7): Synthesized from **F7A** (253 mg, 0.14 mmol), PPTS (72 mg, 0.29 mmol) in MeOH/THF (1:1, 30 ml : 30 ml); purification by column chromatography (eluent: CHCl₃/MeOH = 9:1). Yellow solid, C₁₀₀H₁₄₂F₈O₈Si₂, M = 1679.01 g/mol, yield: 163.8 mg (69 %), mp.: - °C, **¹H-NMR** (500 MHz, Pyridine-d₅): δ / ppm = 7.74 (4H, d, ³J_{H,H} = 8.2 Hz, Aryl-H), 7.66 (4H, d, ³J_{H,H} = 8.3 Hz, Aryl-H), 7.44 (2H, s, Aryl-H), 4.85 (2H, dd, ³J_{H,H} = 10.1, ³J_{H,H} = 4.0 Hz, -OCH-), 4.75 (2H, dd, ³J_{H,H} = 10.2,

$^3J_{H,H} = 6.3$ Hz, $-OCH_2-$), 4.54 – 4.48 (2H, m, $-OCH_2-$), 4.18 – 4.15 (4H, m, $-OCH_2-$), 4.12 (4H, t, $^3J_{H,H} = 6.3$ Hz, $-OCH_2-$), 1.95 – 1.87 (4H, m, $-CH_2-$), 1.69 – 1.60 (4H, m, $-CH_2-$), 1.50 – 1.22 (72H, m, $-CH_2-$), 0.86 (18H, t, $^3J_{H,H} = 6.7$ Hz, $-CH_3$), 0.69 – 0.61 (16H, m, $-SiCH_2-$). **^{13}C -NMR** (126 MHz, Pyridine- d_5): δ / ppm = 154.16 (C_{Aryl-O}), 146.48, 142.03 (m, C_{Aryl-F}), 140.07 ($C_{ArylF-O}$), 132.12, 131.86 (C_{Aryl-H}), 124.81, 121.81, 117.24, 114.29, 99.95 ($C_{Aryl, -C\equiv C-}$), 97.24 (m, C_{ArylF} -quart.), 94.90, 89.61 ($-C\equiv C-$), 77.56 (m, $C_{ArylF-O-CH_2-}$), 76.37 ($-C\equiv C-$), 71.70, 69.55, 63.50 ($-OCH-$, $-OCH_2-$), 34.08, 33.95, 31.88, 29.46, 29.16, 29.07, 26.25, 24.12 (4C), 22.76 ($-CH_2-$), 14.04 ($-CH_3$), 12.61, 12.59 ($-SiCH_2-$). **^{19}F -NMR** (470 MHz, Pyridine- d_5): δ / ppm = -138.55 – -138.88 (m, C_{Aryl-F}), -156.68 – -157.14 (m, C_{Aryl-F}). **^{29}Si -NMR** (99 MHz, Pyridine- d_5): δ / ppm = 2.99 (Si). **HRMS** (m/z): [M] $^+$ Cl $^-$ calcd. For $C_{100}H_{142}F_8O_8Si_2Cl$, 1714.8929; found: 1714.9887.

1,4-Bis[8-(triheptylsilyl)octoxy]-2,5-bis{4-[2,3,5,6-tetrafluoro-4-(2,3-dihydroxypropyl)-1-oxy]phenylethynyl}phenylethynyl}benzene (F8): Synthesized from **F8A** (300 mg, 0.17 mmol), PPTS (84 mg, 0.34 mmol) in MeOH/THF (1:1, 30 ml : 30 ml); purification by column chromatography (eluent: $CHCl_3/MeOH = 9:1$). Yellow solid, $C_{102}H_{146}F_8O_8Si_2$, M = 1708.44 g/mol, yield: 196.9 mg (69 %), mp.: < 20°C °C, **1H -NMR** (400 MHz, Pyridine- d_5): δ / ppm = 7.77 (4H, d, $^3J_{H,H} = 8.1$ Hz, Aryl-*H*), 7.69 (4H, d, $^3J_{H,H} = 8.1$ Hz, Aryl-*H*), 7.47 (2H, s, Aryl-*H*), 4.91 – 4.85 (2H, m, $-OCH_2-$), 4.81 – 4.74 (2H, m, $-OCH_2-$), 4.57 – 4.50 (2H, m, $-OCH-$), 4.22 – 4.18 (4H, m, $-OCH_2-$), 4.13 (4H, t, $^3J_{H,H} = 6.4$ Hz, $-OCH_2-$), 1.96 – 1.85 (4H, m, $-CH_2-$), 1.70 – 1.60 (4H, m, $-CH_2-$), 1.53 – 1.22 (76H, m, $-CH_2-$), 0.87 (18H, t, $^3J_{H,H} = 7.0$ Hz, $-CH_3$), 0.72 – 0.62 (16H, m, $-SiCH_2-$). **^{13}C -NMR** (101 MHz, Pyridine- d_5): δ / ppm = 154.13 (C_{Aryl-O}), 146.05, 142.28 (m, C_{Aryl-F}), 132.14, 131.89 (C_{Aryl-H}), 124.82, 121.83, 117.20, 114.25, 99.98 ($C_{Aryl, -C\equiv C-}$), 97.25 (m, C_{ArylF} -quart.), 94.93, 89.65 ($-C\equiv C-$), 77.58 ($C_{ArylF-O-CH_2-}$), 76.41 ($-C\equiv C-$), 71.73, 69.46, 63.52 ($-OCH-$, $-OCH_2-$), 33.99 (4C), 31.91, 29.48 (4C), 29.43, 29.11, 26.27, 24.18, 24.15, 22.80 ($-CH_2-$), 14.08 ($-CH_3$), 12.66, 12.61 ($-SiCH_2-$). **^{19}F -NMR** (376 MHz, Pyridine- d_5): δ / ppm = -138.48 – -138.78 (m, C_{Aryl-F}), -156.73 – -157.03 (m, C_{Aryl-F}). **^{29}Si -NMR** (79 MHz, Pyridine- d_5): δ / ppm = 3.01 (Si). **HRMS** (m/z): [M] $^+$ Cl $^-$ calcd. For $C_{102}H_{146}F_8O_8Si_2Cl$, 1743.0142; found: 1743.0115.

1,4-Bis[9-(triheptylsilyl)nonoxy]-2,5-bis{4-[2,3,5,6-tetrafluoro-4-(2,3-dihydroxypropyl)-1-oxy]phenylethynyl}phenylethynyl}benzene (F9): Synthesized from **F9A** (250 mg, 0.14 mmol), PPTS (69 mg, 0.28 mmol) in MeOH/THF (1:1, 30 ml : 30 ml); purification by column chromatography (eluent: $CHCl_3/MeOH = 9:1$). Yellow solid, $C_{104}H_{150}F_8O_8Si_2$, M = 1736.49 g/mol, yield: 180.5 mg (76 %), mp.: - °C, **1H -NMR** (500 MHz, Pyridine- d_5): δ / ppm = 7.74 (4H, d, $^3J_{H,H} = 8.3$ Hz, Aryl-*H*), 7.66 (4H, d, $^3J_{H,H} = 8.3$ Hz, Aryl-*H*), 7.45 (2H, s, Aryl-*H*), 4.85 (2H, dd, $^3J_{H,H} = 10.1$, $^3J_{H,H} = 4.0$ Hz, $-OCH-$), 4.75 (2H, dd, $^3J_{H,H} = 10.2$, $^3J_{H,H} = 6.3$ Hz, $-OCH_2-$), 4.54 – 4.48 (2H, m, $-OCH_2-$), 4.18 – 4.15 (4H, m, $-OCH_2-$), 4.11 (4H, t, $^3J_{H,H} = 6.4$ Hz, $-OCH_2-$), 1.93 – 1.84 (4H, m, $-CH_2-$), 1.65 – 1.57 (4H, m, $-CH_2-$), 1.47 – 1.23 (80H, m, $-CH_2-$), 0.86 (18H, t, $^3J_{H,H} = 6.7$ Hz, $-CH_3$), 0.70 – 0.63 (16H, m, $-SiCH_2-$). **^{13}C -NMR** (101 MHz, Pyridine- d_5): δ / ppm = 154.15 (C_{Aryl-O}), 146.30, 142.03 (m, C_{Aryl-F}), 139.54 ($C_{ArylF-O}$), 132.11, 131.86 (C_{Aryl-H}), 124.80, 121.81, 117.25, 114.29, 99.93 ($C_{Aryl, -C\equiv C-}$), 97.25 (m, C_{ArylF} -quart.), 94.90, 89.60 ($-C\equiv C-$), 77.55 ($C_{ArylF-O-CH_2-}$), 76.37 ($-C\equiv C-$), 71.70, 69.53, 63.50 ($-OCH-$, $-OCH_2-$), 34.04, 33.95, 31.88, 29.75, 29.50, 29.41, 29.38, 29.07, 26.22, 24.15, 24.12, 22.76 ($-CH_2-$), 14.04 ($-CH_3$), 12.65, 12.62 ($-SiCH_2-$). **^{19}F -NMR** (376 MHz, Pyridine- d_5): δ / ppm = -138.51 – -138.86 (m, C_{Aryl-F}), -156.61 – -157.16 (m, C_{Aryl-F}). **^{29}Si -NMR** (99 MHz, Pyridine- d_5): δ / ppm = 3.00 (Si). **HRMS** (m/z): [M] $^+$ Cl $^-$ calcd. For $C_{104}H_{150}F_8O_8Si_2Cl$, 1771.0455; found: 1711.0518.

1,4-Bis[10-(triheptylsilyl)decoxy]-2,5-bis{4-[2,3,5,6-tetrafluoro-4-(2,3-dihydroxypropyl)-1-oxy]phenylethynyl}phenylethynyl}benzene (F10): Synthesized from **F10A** (180 mg, 0.10 mmol), PPTS (49 mg, 0.20 mmol) in MeOH/THF (1:1, 30 ml : 30 ml); purification by column chromatography (eluent: $CHCl_3/MeOH = 9:1$). Yellow solid, $C_{106}H_{154}F_8O_8Si_2$, M = 1764.55 g/mol, yield: 152.9 mg (88 %), mp.: 94 °C, **1H -NMR** (400 MHz, Pyridine- d_5): δ / ppm = 7.75 (4H, d, $^3J_{H,H} = 8.2$ Hz, Aryl-*H*), 7.68 (4H, d, $^3J_{H,H} = 8.2$ Hz, Aryl-*H*), 7.47 (2H, s, Aryl-*H*), 4.86 (2H, dd, $^3J_{H,H} = 10.1$, $^3J_{H,H} = 4.1$ Hz, $-OCH-$), 4.76 (2H, dd, $^3J_{H,H} = 10.1$, $^3J_{H,H} = 6.2$ Hz, $-OCH_2-$), 4.56 – 4.48 (2H, m, $-OCH_2-$), 4.21 – 4.16 (4H, m, $-OCH_2-$), 4.12 (4H, t, $^3J_{H,H} = 6.4$ Hz, $-OCH_2-$), 1.95 – 1.83 (4H, m, $-CH_2-$), 1.67 – 1.57 (4H, m, $-CH_2-$), 1.52 – 1.23 (84H, m, $-CH_2-$), 0.87 (18H,

t, $^3J_{H,H} = 6.9$ Hz, $-CH_3$), 0.74 – 0.62 (16H, m, $-SiCH_2-$). $^{13}C-NMR$ (101 MHz, Pyridine- d_5): δ / ppm = 154.16 (C_{Aryl-O}), 146.08, 142.42 (m, C_{Aryl-F}), 139.97 ($C_{ArylF-O}$), 132.13, 131.87 (C_{Aryl-H}), 124.81, 121.83, 117.27, 114.29, 99.97 ($C_{Aryl, -C\equiv C-}$), 97.26 (m, $C_{ArylF-quart.}$), 94.92, 89.62 ($-C\equiv C-$), 77.57 ($C_{ArylF-O-CH_2-}$), 76.39 ($-C\equiv C-$), 71.71, 69.53, 63.52 ($-OCH-$, $-OCH_2-$), 34.04, 33.97, 31.89, 29.83, 29.69, 29.50, 29.48, 29.43, 29.08, 26.22, 24.16, 24.13, 22.78 ($-CH_2-$), 14.06 ($-CH_3$), 12.66, 12.63 ($-SiCH_2-$). $^{19}F-NMR$ (376 MHz, Pyridine- d_5): δ / ppm = -138.52 – -138.71 (m, C_{Aryl-F}), -156.71 – -157.01 (m, C_{Aryl-F}). $^{29}Si-NMR$ (79 MHz, Pyridine- d_5): δ / ppm = 3.02 (Si). **HRMS** (m/z): $[M]+Cl^-$ calcd. For $C_{106}H_{154}F_8O_8Si_2Cl$, 1799.0738; found: 1799.0736.

1,4-Bis[11-(triheptylsilyl)undecoxy]-2,5-bis{4-[2,3,5,6-tetrafluoro-4-(2,3-dihydroxypropyl-1-oxy)phenylethynyl]phenylethynyl}benzene (F11): Synthesized from **F11A** (270 mg, .014 mmol), PPTS (73 mg, 0.29 mmol) in MeOH/THF (1:1, 30 ml : 30 ml); purification by column chromatography (eluent: $CHCl_3/MeOH = 9:1$). Yellow solid, $C_{108}H_{158}F_8O_8Si_2$, M = 1792.66 g/mol, yield: 176.4 mg (63 %), mp.: 67.0 °C, ^1H-NMR (400 MHz, Pyridine- d_5): δ / ppm = 7.77 (4H, d, $^3J_{H,H} = 8.3$ Hz, Aryl-H), 7.69 (4H, d, $^3J_{H,H} = 8.3$ Hz, Aryl-H), 7.48 (2H, s, Aryl-H), 4.90 – 4.85 (2H, m, $-OCH_2-$), 4.81 – 4.75 (2H, m, $-OCH_2-$), 4.57 – 4.50 (2H, m, $-OCH-$), 4.22 – 4.18 (4H, m, $-OCH_2-$), 4.13 (4H, t, $^3J_{H,H} = 6.4$ Hz, $-OCH_2-$), 1.94 – 1.85 (4H, m, $-CH_2-$), 1.67 – 1.57 (4H, m, $-CH_2-$), 1.52 – 1.23 (88H, m, $-CH_2-$), 0.88 (18H, d, $^3J_{H,H} = 6.6$ Hz, $-CH_3$), 0.74 – 0.64 (16H, m, $-SiCH_2-$). $^{13}C-NMR$ (101 MHz, Pyridine- d_5): 154.17 (C_{Aryl-O}), 132.14, 131.88 (C_{Aryl-H}), 124.82, 121.84, 117.29, 114.31, ($C_{Aryl,}$), 94.93, 89.62 ($-C\equiv C-$), 77.58 ($C_{ArylF-O-CH_2-}$), 71.72, 69.56, 63.52 ($-OCH-$, $-OCH_2-$), 34.04, 33.97, 31.89, 29.76, 29.75, 29.48, 29.42, 29.08, 26.22, 24.17, 24.15, 24.13, 23.57, 22.78 ($-CH_2-$), 14.06 ($-CH_3$), 12.65, 12.63 ($-SiCH_2-$). $^{19}F-NMR$ (376 MHz, Pyridine- d_5): δ / ppm = -138.44 – -138.85 (m, C_{Aryl-F}), -156.73 – -157.07 (m, C_{Aryl-F}). $^{29}Si-NMR$ (79 MHz, Pyridine- d_5): δ / ppm = 3.03 (Si). **HRMS** (m/z): $[M]+Cl^-$ calcd. For $C_{108}H_{158}F_8O_8Si_2Cl$, 1827.1082; found: 1827.1016.

1,4-Bis[12-(triheptylsilyl)dodecoxy]-2,5-bis{4-[2,3,5,6-tetrafluoro-4-(2,3-dihydroxypropyl-1-oxy)phenylethynyl]phenylethynyl}benzene (F12): Synthesized from **F12A** (190 mg, 0.10 mmol), PPTS (50 mg, 0.020 mmol) in MeOH/THF (1:1, 30 ml : 30 ml); purification by column chromatography (eluent: $CHCl_3/MeOH = 9:1$). Yellow solid, $C_{110}H_{162}F_8O_8Si_2$, M = 1820.66 g/mol, yield: 129.6 mg (71 %), mp.: 94 °C, ^1H-NMR (400 MHz, Pyridine- d_5): δ / ppm = 7.79 (4H, d, $^3J_{H,H} = 7.9$ Hz, Aryl-H), 7.72 (4H, d, $^3J_{H,H} = 7.7$ Hz, Aryl-H), 7.51 (2H, s, Aryl-H), 4.91 (2H, dd, $^3J_{H,H} = 10.2$, $^3J_{H,H} = 3.9$ Hz, $-OCH-$), 4.80 (2H, dd, $^3J_{H,H} = 10.0$, $^3J_{H,H} = 6.5$ Hz, $-OCH_2-$), 4.62 – 4.52 (2H, m, $-OCH_2-$), 4.25 – 4.20 (4H, m, $-OCH_2-$), 4.16 (4H, t, $^3J_{H,H} = 6.4$ Hz, $-OCH_2-$), 1.98 – 1.87 (4H, m, $-CH_2-$), 1.69 – 1.59 (4H, m, $-CH_2-$), 1.55 – 1.25 (92H, m, $-CH_2-$), 0.93 (18H, t, $^3J_{H,H} = 7.1$ Hz, $-CH_3$), 0.77 – 0.65 (16H, m, $-SiCH_2-$). $^{13}C-NMR$ (101 MHz, Pyridine- d_5): δ / ppm = 155.67 (C_{Aryl-O}), 133.64, 133.39 (C_{Aryl-H}), 126.31, 123.34, 118.79, 115.81, 101.47 ($C_{Aryl, -C\equiv C-}$), 98.77 (m, $C_{ArylF-quart.}$), 96.43, 91.13 ($-C\equiv C-$), 79.05 (m, $C_{ArylF-O-CH_2-}$), 77.65 ($-C\equiv C-$), 73.23, 71.05, 65.03 ($-OCH-$, $-OCH_2-$), 35.54, 35.47, 33.39, 31.36, 31.29, 31.24, 31.23, 30.99, 30.97, 30.96, 30.58, 27.52, 26.64 (4C), 24.28 ($-CH_2-$), 15.57 ($-CH_3$), 14.15 ($-SiCH_2-$). $^{19}F-NMR$ (376 MHz, Pyridine- d_5): δ / ppm = -136.93 – -137.40 (m, C_{Aryl-F}), -155.21 – -155.67 (m, C_{Aryl-F}). $^{29}Si-NMR$ (79 MHz, Pyridine- d_5): δ / ppm = 3.02 (Si). **HRMS** (m/z): $[M]+Cl^-$ calcd. For $C_{110}H_{162}F_8O_8Si_2Cl$, 1855.1395; found: 1855.1408.

4.4 Representative NMR spectra

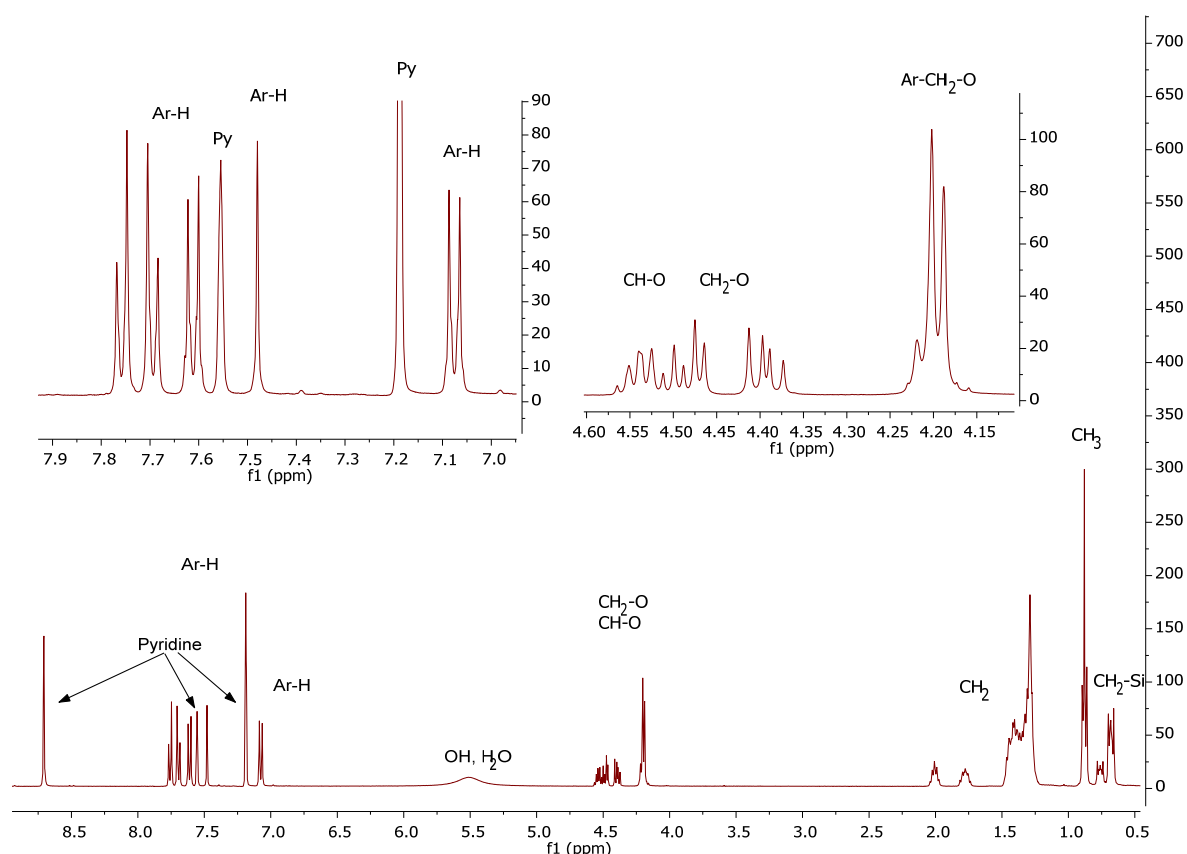


Figure S18. $^1\text{H-NMR}$ of compound **H4** (400 MHz, pyridine- d_5).

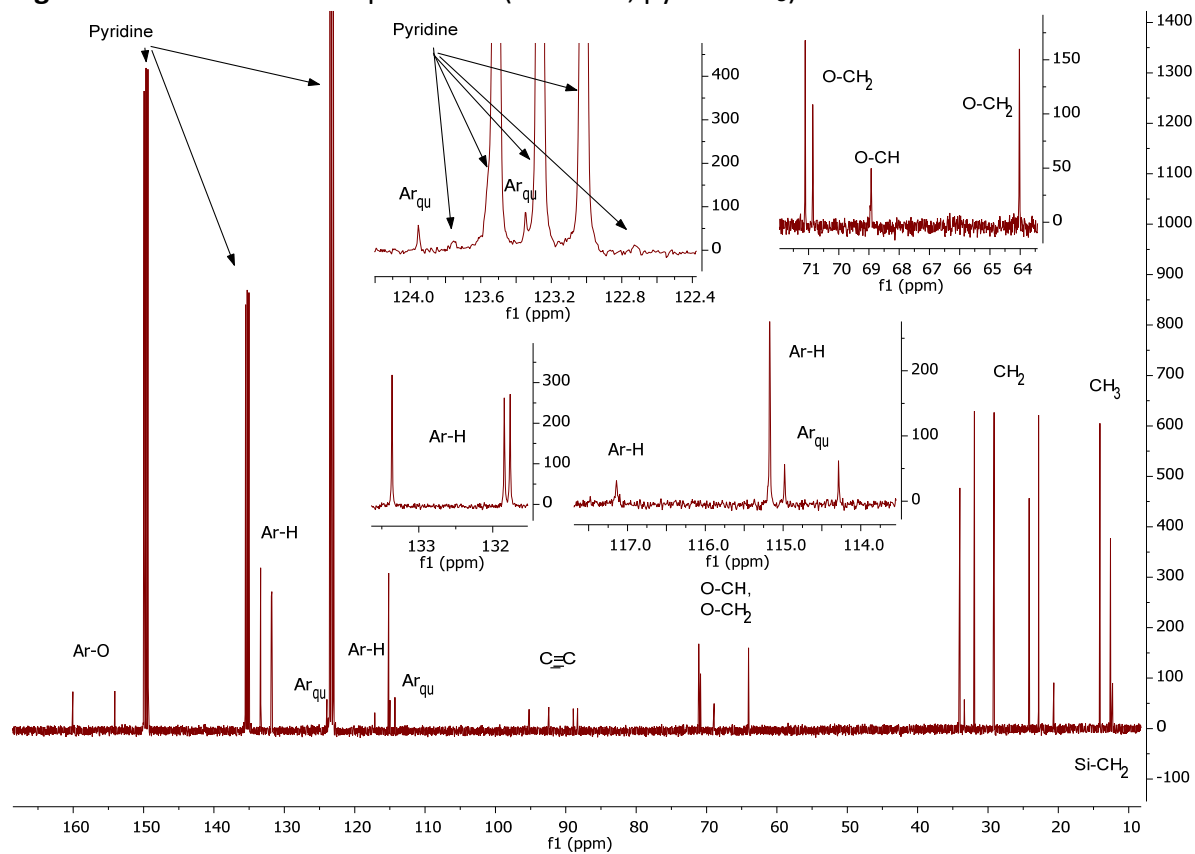


Figure S19. $^{13}\text{C-NMR}$ of compound **H4** (101 MHz, pyridine- d_5).

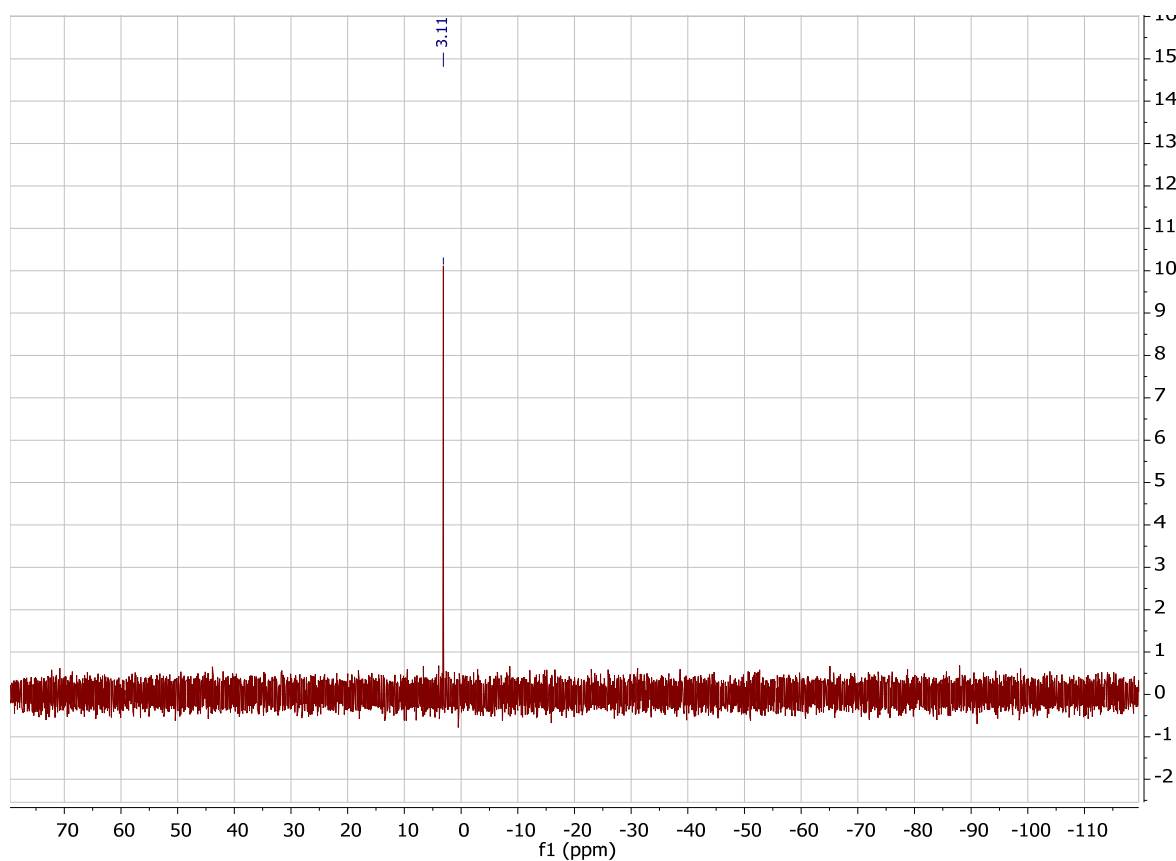


Figure S20. ^{29}Si -NMR of compound H4 (79 MHz, pyridine- d_5).

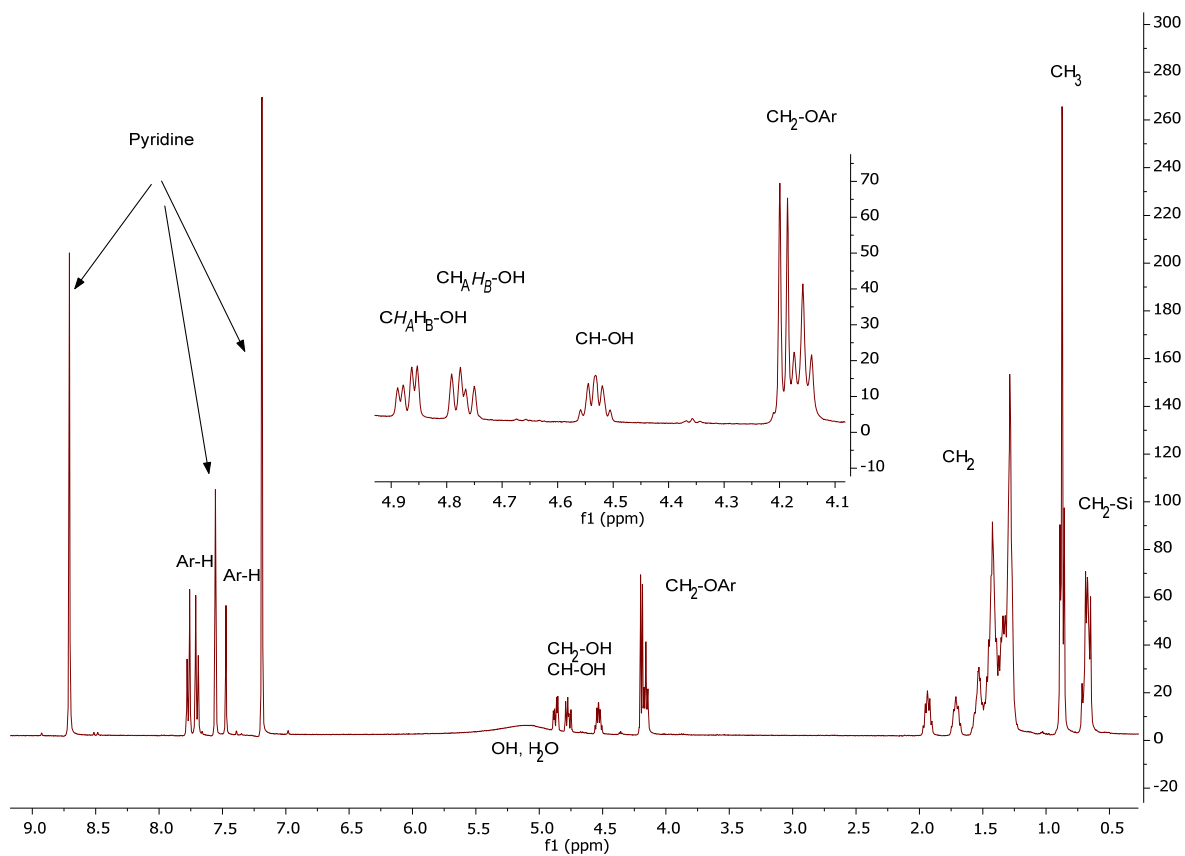


Figure S21. ^1H -NMR of compound F6 (400 MHz, pyridine- d_5).

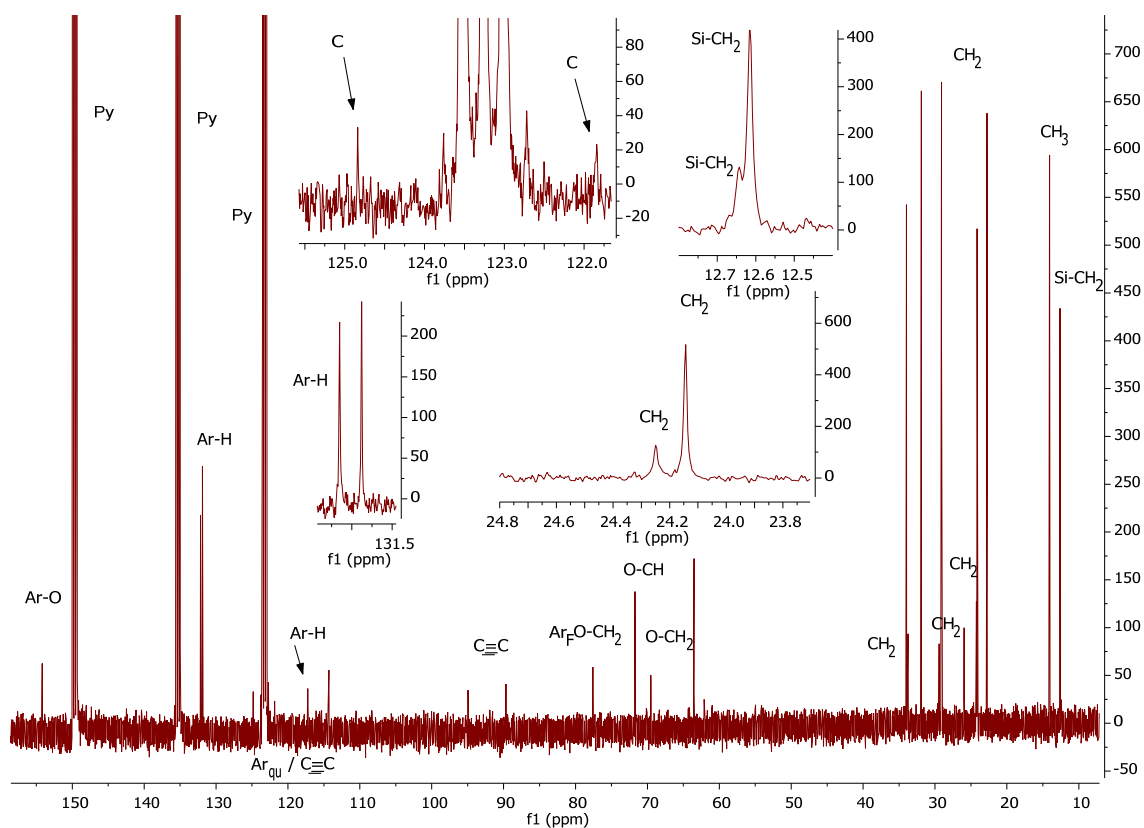


Figure S22. ^{13}C -NMR of compound **F6** (101 MHz, pyridine- d_5); carbons of the fluorinated benzenes and the adjacent acetylene units are invisible due to the coupling with fluorine.

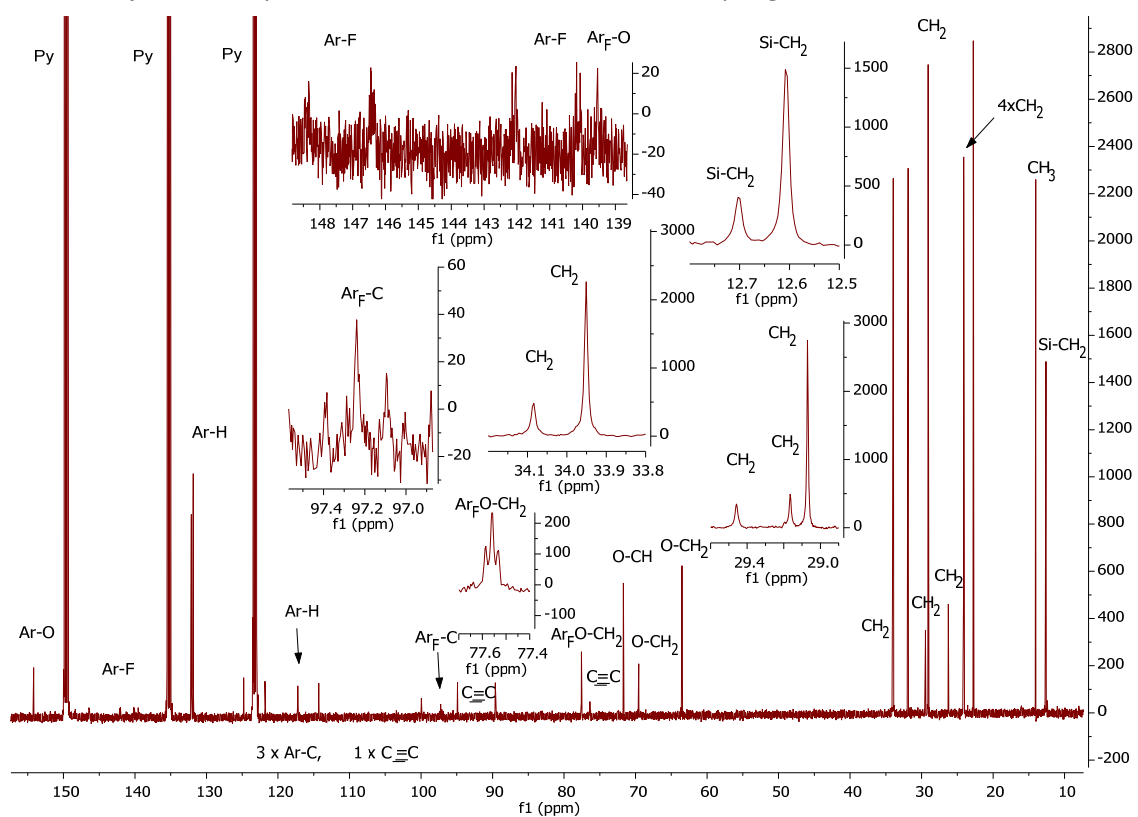


Figure S23. ^{13}C -NMR of compound **F7** (101 MHz, pyridine- d_5) after extra-long exposure time, showing also the carbons of the fluorinated benzenes and the adjacent acetylene units.

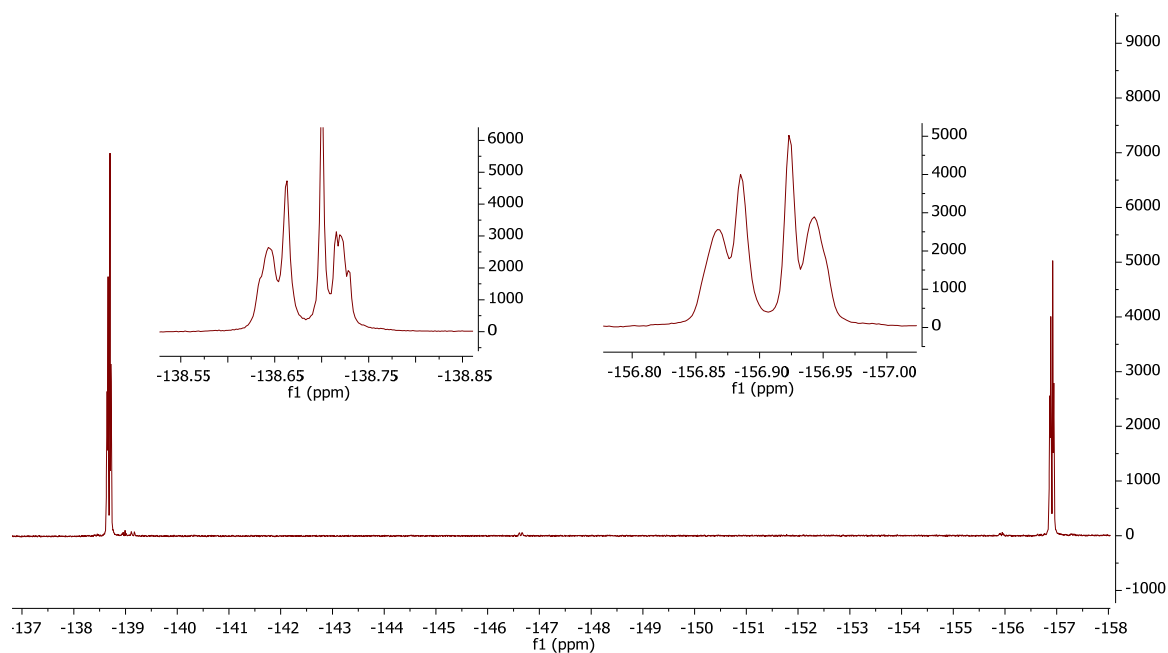


Figure S24. ^{19}F -NMR of compound **F6** (376 MHz, pyridine- d_5).

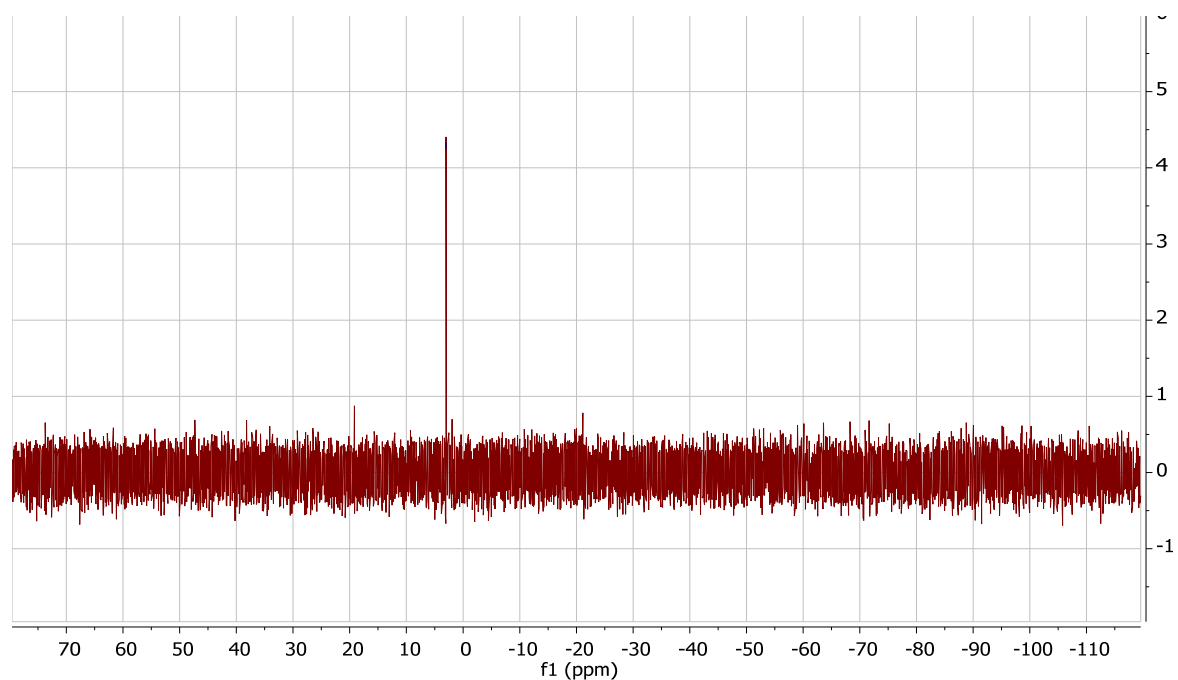


Figure S25. ^{29}Si -NMR of compound **F6** (79 MHz, pyridine- d_5).

5 References

- S1 A. Immirzi and B. Perini, *Acta Cryst. A*, 1977, **33**, 216.
 S2 W. S. Sheldrick, *Acta Cryst. B*, 1980, **36**, 2194.
 S3 J. W. Steed, J. L. Atwood, *Supramolecular Chemistry*, 2nd Ed. Wiley, Chichester, UK, 2009
 S4 a) C. Tschierske, *J. Mater. Chem.* 1998, **8**, 1485; b) C. Tschierske, *J. Mater. Chem.* 2001, **11**, 2647;
 c) C. Tschierske, in *Handbook of Liquid Crystals*, 2nd Ed. (Eds: J.W. Goodby, P. J. Collings, T. Kato, C. Tschierske, H. F. Gleeson, P. Raynes), Vol. 5, Wiley-VCH, Weinheim, 2014, pp 1- 43 and pp. 45-87;

- d) C. Tschierske, G. Ungar in *Handbook of Liquid Crystals*, 2nd Ed. (Eds: J.W. Goodby, P. J. Collings, T. Kato, C. Tschierske, H. F. Gleeson, P. Raynes), Vol. 5, Wiley-VCH, Weinheim, 2014, pp 437-482;
- e) C. Tschierske, *Isr. J. Chem.* **2012**, 52, 835.
- S5 S. Poppe, M. Poppe, H. Ebert, M. Prehm, C. Chen, F. Liu, S. Werner, K. Bacia and C. Tschierske, *Polymers*, 2017, **9**, 471
- S6 A. Saeed, M. Poppe, M. B. Wagner, S. Hauche, C. Anders, Y. Cao, L. Zhang, C. Tschierske and F. Liu, *Chem. Commun.*, 2022, **58**, 7054.
- S7 C. Chen, M. Poppe, S. Poppe, M. Wagner, C. Tschierske, F. Liu, *Angew. Chem. Int. Ed.* 2022, e202203447.
- S8 M. Poppe, C. Chen, F. Liu, M. Prehm, S. Poppe, C. Tschierske, *Soft Matter*, 2017, **13**, 4676.
- S9 Y.-C. Chiang, H.-C. Wu, H.-F. Wen, C.-C. Hung, C.-W. Hong, C.-C. Kuo, T. Higashihara and W.-C. Chen, *Macromolecules*, 2019, **52**, 4396.
- S10 Y. Duan, J.-H. Lin, J.-C. Xiao and Y.-C. Gu, *Org. Chem. Front.*, 2017, **4**, 1917
- S11 K. Sonogashira, Y. Tohda and N. Hagihara, *Tetrahedron Lett*, 1975, **50**, 4467.
- S12 a) S. Werner, H. Ebert, B.-D. Lechner, F. Lange, A. Achilles, R. Bärenwald, S. Poppe, A. Blume, K. Saalwächter, C. Tschierske and K. Bacia, *Chem. Eur. J.*, 2015, **21**, 8840; b) M. Poppe, C. Chen, F. Liu, S. Poppe and C. Tschierske, *Chem. Eur. J.*, 2017, **23**, 7196.
- S13 G. Nagarjuna, A. Kokil, J. Kumar, D. Venkataraman, *J. Mater. Chem.*, 2012, **22**, 16091.
- S14 A. Williamson, *The London, Edinburgh, and Dublin Philosophical Magazine and Journal of Science*, 1850, **37**, 350.
- S15 S. Santra, R. Bean, B. Heckert, Z. Shaw, V. Jain, L. Shrestha, R. Narayanam and Q. Austin, *Polym. Chem.*, 2020, **11**, 3723.
- S16 R. van Rijsbergen, M. J. O. Anteunis and A. De Bruyn, *J. Carbohydr. Chem.*, 1983, **2**, 395.